UNIVERSITY OF NAPLES FEDERICO II

DEPARTMENT OF AGRICULTURAL SCIENCES

Ph.D.

in

Sustainable Agricultural and Forestry System and Food Security

XXXVIII Cycle

USE OF PHOSPHATE-SOLUBILIZING MICROORGANISMS (PSMs) AS BIOFERTILIZERS IN CROP PRODUCTION

Tutor:
Prof Roberta Marra

Candidate:
Sonia Marcone

Co-tutor:
Dr Stefania Lanzuise

PhD Coordinator:
Prof Albino Maggio

A Vincenzo,

che tu possa volare in alto,

non così vicino al sole da sciogliere le tue ali,

ma abbastanza in alto

da capire che nel mondo non esistono i giganti

INDEX

LIST OF ABBREVIATIONS

AMF: Arbuscular Mycorrhizal Fungi

AMY: *Bacillus amyloliquefaciens*

BCAs: Biological Control Agents

ISR: Induced Systemic Resistance

MEGA: *Bacillus megaterium* FBM09

NA: Nutrient Agar

NB: Nutrient Broth

PGPB: Plant Growth-Promoting Bacteria

PGPR: Plant Growth–Promoting Rhizobacteria

PO: *Pseudomonas salmasensis* POE54

PSE: *Pseudomonas putida* RPT12

PSMs: Phosphate Solubilizing Microorganisms

PUMI: *Bacillus pumilus* FBP01

RP: Phosphorite (Rock phosphate)

SUB: *Bacillus subtilis* FBS07

TCP: Tricalcium Phosphate

VOCs: Volatile Organic Compounds

1. INTRODUCTION

Since the second half of the twentieth century, agriculture has undergone profound transformations driven by intensification, which has increased productivity but also led to significant environmental impacts, including biodiversity loss and ecosystem degradation. This has highlighted the need for more sustainable models based on an integrated approach that considers soil health, habitat conservation, and reduced reliance on chemical inputs.

From the 1990s onward, the European Union has promoted agri-environmental policies aimed at sustainability, encouraging practices such as organic farming and biodiversity conservation. This pathway was further strengthened with the European Green Deal (2019), which recognizes agriculture as a key sector for environmental protection and climate change mitigation.

In this context, strategies such as the Biodiversity Strategy, the Soil Strategy, and the Farm to Fork Strategy aim to reduce the use of fertilizers and pesticides, promote resilient agricultural systems, and enhance ecosystem services (Fig. 1.1). Overall, a new agricultural paradigm is emerging, focused on low-impact models capable of combining productivity, sustainability, and adaptation to climate change.

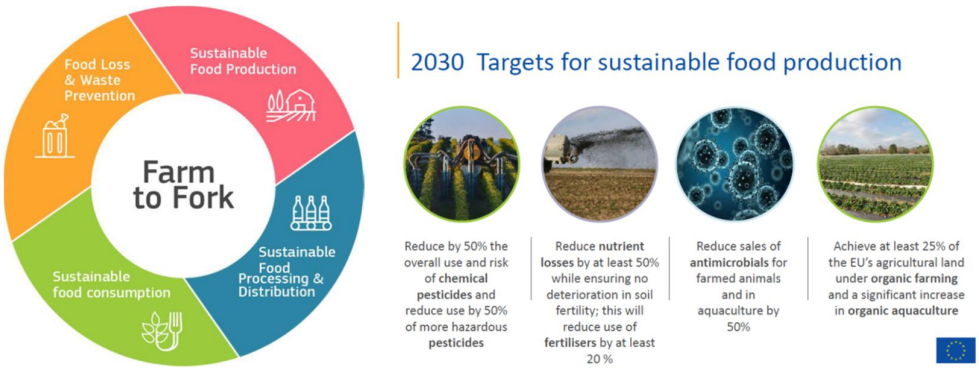

Figure 1.1. Overview of the Farm-to-Fork Strategy and the goals to be achieved by 2030 to ensure sustainable food production (https://ec.europa.eu/food/farm2fork_en).

Therefore, in a rapidly changing landscape characterized by emerging challenges, the agricultural sector, supported by scientific research and guided by policy frameworks, is increasingly focusing on alternative solutions that reduce reliance on synthetic fertilizers. Among these, biofertilizers, including plant growth–promoting rhizobacteria (PGPR) and arbuscular mycorrhizal fungi (AMF), play a pivotal role in enhancing soil fertility and crop productivity. Likewise, in the context of plant protection, biocontrol microorganisms represent a promising alternative to synthetic pesticides, as they can suppress plant

pathogens through effective and selective mechanisms while exerting minimal environmental impact.

In recent decades, the use of microorganisms or their derivatives to improve the sustainability of agricultural production has attracted growing attention not only within the scientific community but also among industry stakeholders and policymakers (Batista and Singh, 2021). The investigation and application of beneficial plant–microbe interactions constitute innovative and environmentally sustainable strategies with significant potential for both conventional and organic agricultural systems worldwide (Berg, 2009).

1.1 Beneficial microorganisms in agriculture: functions and mechanisms of action

Microorganisms are ubiquitous in natural environments, particularly in soils, where they establish complex interactions both among themselves and with plants. The soil region surrounding plant roots, known as the rhizosphere, is especially rich in microbial diversity and activity, representing a hotspot for metabolic exchanges and mutualistic interactions. Root exudates, composed of a wide range of organic compounds released by plants, serve as a key nutrient source for many beneficial microorganisms, which in turn produce metabolites that support plant growth and health (Sellitto, 2002).

Among the key functions performed by beneficial microorganisms are plant growth promotion and biocontrol. Plant development is enhanced by microorganisms such as plant growth–promoting rhizobacteria (PGPR), arbuscular mycorrhizal fungi (AMF), and endophytes, which facilitate nutrient acquisition from the soil. Notable mechanisms include biological nitrogen fixation, phosphate solubilization, thereby increasing its bioavailability, siderophore production for iron acquisition, and the synthesis of phytohormones (Fig. 1.2).

In terms of biocontrol, certain microorganisms act as antagonists of plant pathogens through both direct and indirect mechanisms. Direct interactions involve processes such as parasitism, competition, and antibiosis. Indirect mechanisms, by contrast, operate through the activation of plant defence responses, whereby the biocontrol agent induces systemic resistance. This leads to the accumulation of structural barriers and the activation of a wide range of biochemical and molecular defence pathways in the host plant (Lahlali et al., 2022). In addition, beneficial microorganisms contribute to the mitigation of abiotic stresses and play a crucial role in improving soil quality and structure.

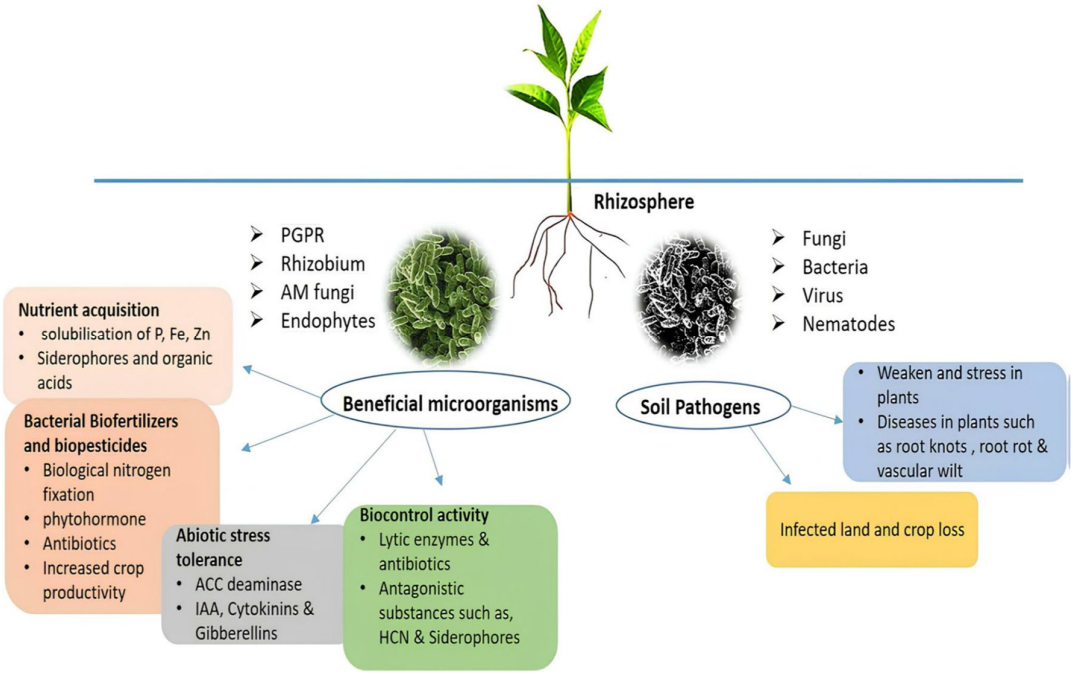

Figure 1.2. Main functions performed by beneficial microorganisms (PGPR, *Rhizobium*, AM fungi, endophytes) and soil-borne pathogens (fungi, bacteria, viruses, nematodes) present in the rhizosphere (from Argentel-Martínez et al., 2025).

1.1.1. Plant Growth Promotion (PGP) activity

Plant growth and development are influenced by multiple factors, including the availability of essential nutrients such as nitrogen (N), phosphorus (P), potassium (K), and iron (Fe). However, these elements are often present in soils in organic or insoluble forms that are not readily accessible to plant roots. To overcome nutrient deficiencies and sustain crop productivity, chemical fertilizers are widely applied; nevertheless, their use entails environmental drawbacks and represents a substantial economic burden for farmers.

Microorganisms offer a sustainable alternative, as they can enhance the availability and uptake of essential nutrients in plants. Attracted by root exudates, these microorganisms colonize the rhizosphere, the rhizoplane (root surface), or even internal root tissues, sometimes establishing specific symbiotic associations with their hosts (Compant et al., 2024). The success of plant–microbe interactions depends on multiple mechanisms, often acting simultaneously, but is largely determined by the ability of microorganisms to efficiently colonize plant niches and establish stable associations (Whipps, 2001; Lugtenberg et al., 2002; Kamilova et al., 2005; Compant et al., 2005).

A well-documented function of both symbiotic and free-living microorganisms is their capacity to increase nitrogen availability. Although atmospheric nitrogen constitutes approximately 78% of the atmosphere, it is not directly accessible to plants (Ahemad et al.,

2024). Certain nitrogen-fixing microorganisms convert atmospheric nitrogen into ammoniacal nitrogen (NH_3) through the nitrogenase enzyme complex, making it available for plant uptake (Das et al., 2022). This process is particularly associated with bacteria such as Azotobacter and Rhizobium spp., which can form symbiotic relationships with plants and significantly improve nitrogen supply (Halbleib et al., 2000).

Another key mechanism of plant growth promotion is phosphorus solubilization; however, this topic will be discussed in greater detail in the following sections.

Beneficial microorganisms can increase potassium (K) availability through mechanisms analogous to those involved in phosphorus solubilization, primarily via the production of organic acids. Potassium plays a crucial role in enzyme activation, photosynthesis, and overall plant metabolism (Das et al., 2022).

The activity of plant-beneficial microorganisms also extends to improving iron availability. Iron is essential for chlorophyll synthesis and cellular respiration but is predominantly present in soils as ferric iron (Fe^{3+}), which is poorly available to plants. Some microorganisms produce siderophores, high-affinity iron-chelating compounds, that facilitate the reduction of Fe^{3+} to the more bioavailable ferrous form (Fe^{2+}), thereby enhancing plant iron uptake (Glick, 2012).

Beyond nutrient mobilization, growth-promoting microorganisms contribute to improved seed germination and reduced dormancy. For instance, certain beneficial fungi colonizing seeds can stimulate germination through the production of volatile organic compounds (VOCs) and the degradation of germination inhibitors (Hossain et al., 2017). Moreover, plant growth promotion is often associated with enhanced photosynthetic performance, resulting from increases in leaf area, leaf number, and chlorophyll content (Hossain and Sultana, 2020).

Finally, close associations between plants and beneficial microorganisms can significantly improve root system architecture, including increased root biomass, diameter, and root hair development. For example, the application of Trichoderma spp. in maize has been shown to enhance root growth and nutrient and water uptake efficiency (Hossain and Sultana, 2020).

1.1.2. Microbial Biological Control Agents (BCAs)

Biological control (or biocontrol) encompasses a range of strategies that exploit direct and indirect interactions among living organisms to suppress populations of harmful species, maintaining them below economic damage thresholds (Viggiani et al., 1994). This approach represents a sustainable alternative to conventional plant protection methods, supporting crop growth while reducing reliance on synthetic agrochemicals. In this context, microorganisms used to decrease the inoculum density or virulence of plant pathogens, whether in active or dormant stages, are defined as biological control agents (BCAs).

Numerous soil-borne fungi and bacteria exhibit biocontrol potential against a wide range of pathogens, limiting their proliferation and pathogenicity and thereby contributing to improved plant health and productivity (El-Saadony et al., 2022). These antagonistic microorganisms act through multiple mechanisms, broadly classified as direct and indirect. Direct mechanisms include competition, antibiosis, and parasitism, whereas indirect mechanisms involve the activation of plant defense responses, enhancing the plant's capacity to resist infections.

- *Competition*

Competition refers to the ability of BCAs to exploit environmental resources more efficiently than competing microorganisms. This includes competition for space (e.g., colonization of roots and soil), nutrients (such as nitrogen, iron, and carbohydrates), and oxygen. By effectively colonizing shared ecological niches and occupying infection sites, BCAs can limit pathogen access to essential resources and entry points into plant tissues (O'Brien, 2017). A notable example is the production of siderophores—iron-chelating compounds that sequester iron in the soil, making it unavailable to pathogens and thereby inhibiting their growth and metabolic activity (Lahlali et al., 2022).

The effectiveness of competition largely depends on the ecological fitness of the antagonist, including its ability to adapt to the host plant and environmental conditions. Rapid and efficient colonization, coupled with the establishment of high population densities, confers a competitive advantage over pathogens, restricting their ability to establish and proliferate (Ghorbanpour et al., 2018).

- *Antibiosis*

Antibiosis involves the production of antibiotic compounds or toxic metabolites by BCAs that inhibit pathogen growth or cause cell death. These substances may include polar or non-polar compounds, low-molecular-weight antibiotics, and both volatile and non-volatile metabolites (Vinale et al., 2008).

Many antagonistic fungi and bacteria can produce bioactive compounds. For instance, *Trichoderma* spp. synthesize metabolites such as harzianopyridone, viridin, and gliotoxin, which are active against fungal pathogens like *Pythium ultimum* and *Rhizoctonia solani*. Additionally, 6-pentyl-α-pyrone (6PP), produced by species such as *T. atroviride* and *T. viride*, exhibits antagonistic activity against *Fusarium moniliforme* and *P. ultimum* (El-Hasan et al., 2007; Vinale et al., 2008).

- *Parasitism*

Parasitism refers to the ability of a microorganism to establish a close association with a pathogen and derive nutrients from it (Bardin and Pugliese, 2020). This interaction typically involves several stages: recognition and localization, direct contact, formation of specialized infection structures, penetration, and colonization of the host, followed by nutrient

acquisition. While rarely observed in bacteria, parasitism is common among antagonistic fungi and is referred to as mycoparasitism when it involves fungal pathogens.

Mycoparasitic interactions may be biotrophic or necrotrophic. In biotrophic parasitism, the antagonist derives nutrients while keeping the host alive; in necrotrophic parasitism, the pathogen is killed through the action of secondary metabolites and lytic enzymes—such as chitinases, glucanases, and proteases—that degrade cell walls (Harman et al., 2021). This mechanism is characteristic of several BCAs, including species of *Trichoderma*, which are effective against pathogens such as *Botrytis cinerea, R. solani, Pythium spp., Sclerotium rolfsii, Sclerotinia sclerotiorum,* and *Fusarium* spp. Other mycoparasitic genera include *Cladosporium* and *Gliocladium* (Verma et al., 2019).

- *Induced Systemic Resistance (ISR)*

Some BCAs enhance plant defense by activating induced systemic resistance (ISR), a mechanism that indirectly suppresses pathogens by strengthening the plant's immune system (Choudhary et al., 2017). Unlike direct antagonism, ISR does not involve direct interaction with the pathogen but instead primes the plant for a faster and more effective defensive response (Fig. 1.3).

Plant defense activation typically involves the recognition of pathogen-associated molecular patterns (PAMPs) and damage-associated molecular patterns (DAMPs) by plant receptors encoded by resistance (R) genes. This recognition triggers local defense responses, including the hypersensitive response (HR), characterized by the accumulation of reactive oxygen species (ROS), antimicrobial compounds, and cell wall–reinforcing structures that limit pathogen spread (Conrath, 2000; Vlot et al., 2008; Gozzo, 2003).

These local responses can lead to systemic signaling throughout the plant, resulting in systemic acquired resistance (SAR), a long-lasting and broad-spectrum defense mechanism mediated by signaling molecules such as salicylic acid, phytoalexins, and pathogenesis-related proteins (Gao et al., 2015).

Similarly, ISR is triggered by beneficial microorganisms through the recognition of microbe-associated molecular patterns (MAMPs). During colonization, BCAs release metabolites that act as elicitors, inducing a primed physiological state in the plant. This priming enables a more rapid and robust activation of defense mechanisms upon pathogen attack (Romera et al., 2019; Vinale et al., 2008).

ISR is primarily regulated by signaling pathways involving jasmonic acid and ethylene, distinguishing it from SAR, which is typically associated with salicylic acid accumulation. Moreover, ISR is induced by beneficial root-colonizing microorganisms rather than pathogens and does not generally involve the accumulation of pathogenesis-related proteins (Harman et al., 2004). This mechanism plays a key role in sustainable plant protection strategies, enhancing plant resilience against a wide range of pathogens (Fig. 1.3).

A variety of microorganisms, particularly species belonging to the genera *Bacillus, Pseudomonas,* and *Trichoderma,* are known to effectively induce ISR (Yu et al., 2022; Van Wees et al., 2008).

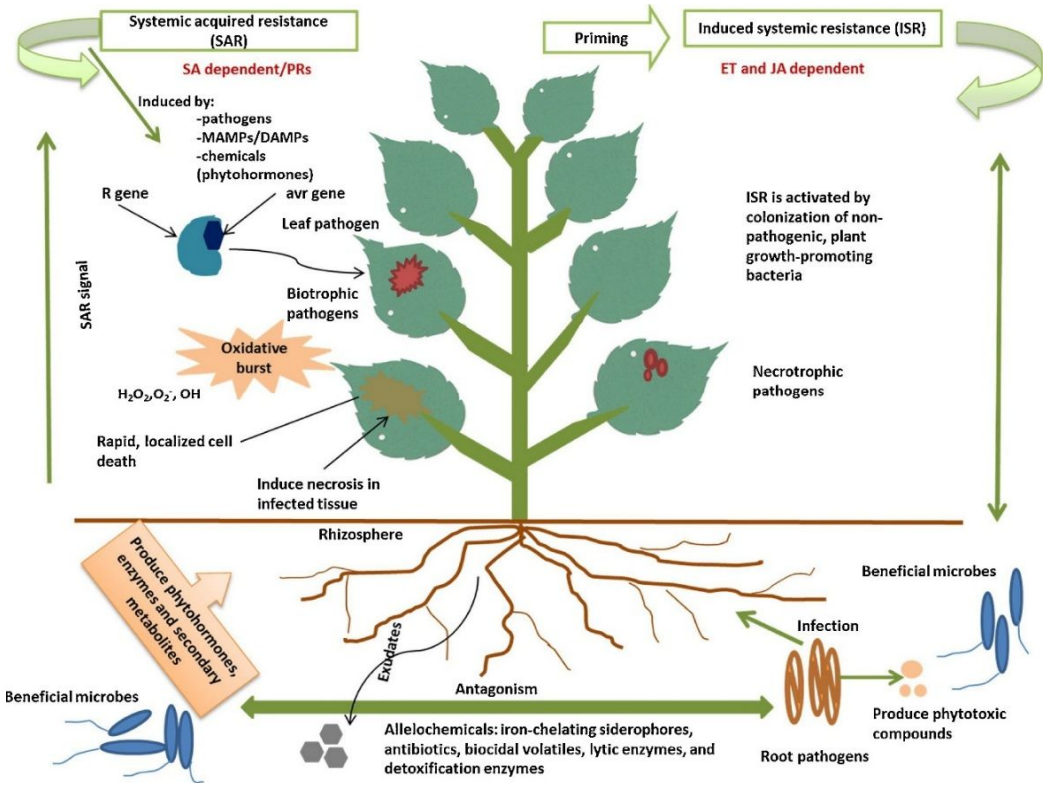

Figure 1.3. A schematic diagram illustrating the activation mechanisms of the two different types of plant resistance: SAR (systemic acquired resistance) and ISR (induced systemic resistance). SAR, which depends on salicylic acid (SA), is triggered by plant-pathogen interactions through the recognition of MAMPs/DAMPs, as well as by foliar treatments with chemicals and phytohormones. ISR is primarily regulated by jasmonic acid (JA) and ethylene (ET) and is triggered by beneficial agent-plant interactions (Ab Rahman et al., 2018).

1.1.3. Mitigation of environmental stresses

Plants are frequently exposed to environmental stresses such as drought, salinity, and extreme temperatures, which can severely constrain their growth and development. To mitigate these adverse effects, plants modulate phytohormone levels, thereby adjusting their physiological responses to cope with unfavorable conditions (Glick, 2012).

Phytohormones, or plant growth regulators, are endogenous signaling molecules that play a central role in regulating plant physiology and enabling adaptation to environmental stresses (Fahad et al., 2015). A substantial body of research has demonstrated that beneficial

rhizosphere microorganisms can synthesize or modulate phytohormone levels, contributing to the maintenance of hormonal homeostasis and enhancing plant tolerance to abiotic stress (Glick, 2012; Fig. 1.4).

The principal classes of phytohormones influenced by microbial activity include auxins, gibberellins, cytokinins, abscisic acid, and ethylene, all of which are involved in key processes of plant growth and development.

Auxins are among the most important phytohormones, as they regulate cell division and differentiation. They play a crucial role in root system architecture by stimulating lateral root formation, thereby enhancing water and nutrient uptake and improving plant tolerance to drought stress (Saeed et al., 2021). The most common naturally occurring auxin is indole-3-acetic acid (IAA), which can be synthesized through multiple biosynthetic pathways. Several microorganisms, including species of *Aspergillus, Trichoderma,* and *Talaromyces*, can produce IAA via diverse metabolic routes (Olanrewaju et al., 2017; Adedayo et al., 2023).

Gibberellins constitute a group of phytohormones involved in numerous physiological and developmental processes, including seed germination, stem elongation, and leaf expansion (Goswami and Suresh, 2020). They also enhance photosynthetic efficiency, leaf area development, and light interception (Fahad et al., 2015). Gibberellins produced by certain bacteria, such as *Pseudomonas* and *Azospirillum*, have been shown to improve plant tolerance to salinity and drought by modulating antioxidant systems (Goswami and Suresh, 2020).

Cytokinins are essential for maintaining meristematic activity and promoting shoot development. They facilitate nutrient mobilization, delay leaf senescence, and contribute to vascular tissue differentiation (Choi et al., 2011). Moreover, cytokinins are involved in plant responses to environmental stress. For example, inoculation with *Bacillus subtilis* has been reported to significantly increase cytokinin levels in shoots under drought conditions (Liu et al., 2013).

Abscisic acid (ABA) plays a pivotal role in stress responses, as well as in seed dormancy and germination inhibition. It also regulates processes such as senescence and organ abscission (Tsukanova et al., 2017). Widely recognized as a “stress hormone,” ABA functions as a key signaling molecule under adverse conditions, including water deficit, salinity, and high temperatures. It contributes to the maintenance of plant water status by inducing stomatal closure and limiting leaf expansion (Cohen et al., 2015).

Ethylene is a gaseous phytohormone produced by most plants and is involved in a wide range of physiological processes (Shaharoona et al., 2011). Like ABA, ethylene is associated with stress responses, and its production increases under conditions such as salinity, drought, and waterlogging, often inhibiting root growth (Saleem et al., 2007). Ethylene biosynthesis involves the precursor 1-aminocyclopropane-1-carboxylate (ACC). Certain beneficial microorganisms produce the enzyme ACC deaminase (ACCD), which degrades ACC into α-ketobutyrate and ammonium, thereby lowering ethylene levels. This regulation is crucial

for maintaining normal plant growth and development under stress conditions (Backer et al., 2018).

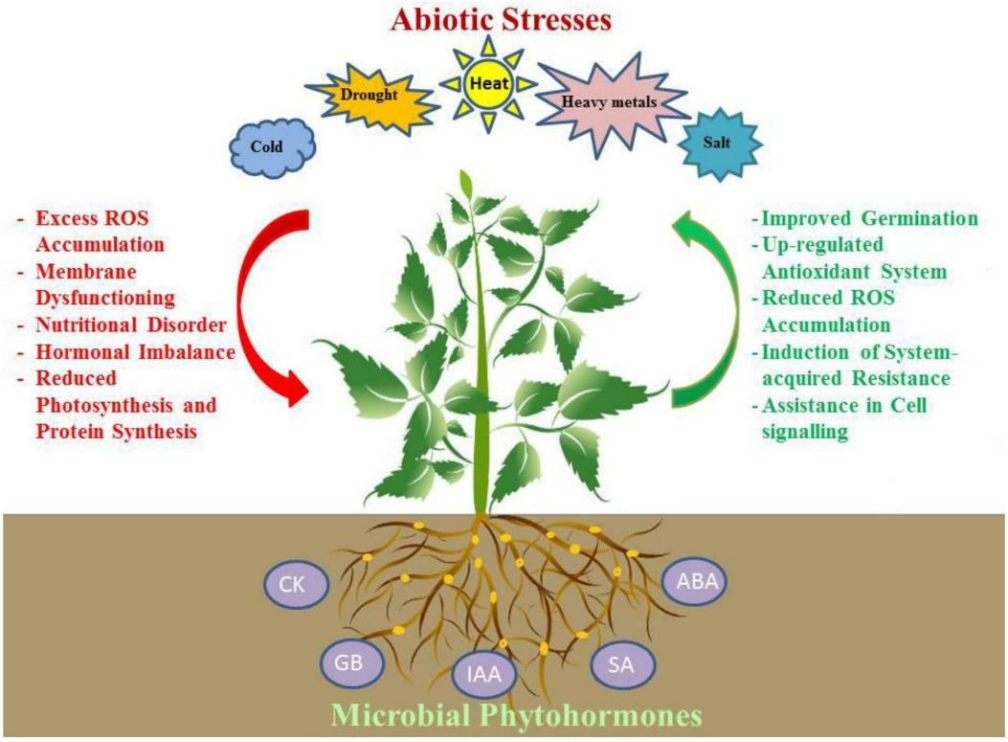

Figure 1.4. Production of phytohormones such as cytokinins (CK), gibberellins (GB), auxins (IAA), abscisic acid (ABA), and ethylene (ET) by beneficial microorganisms. Phytohormones enable plants to tolerate abiotic stress by enhancing antioxidant potential and photosynthetic capacity, and by stimulating root growth and development (from Egamberdieva et al., 2017).

1.2 Plant biostimulants

Plant biostimulants have emerged as a fundamental component of modern plant physiology, acting as complex regulators of metabolic processes rather than mere nutrient sources. Biostimulants exert both direct effects on plant metabolism and indirect effects through improvements in soil fertility and stimulation of beneficial microbial communities, including bacteria, yeasts, and fungi capable of producing growth-promoting metabolites. Their activity involves the soil–plant–microbiome continuum, leading to physiological, hormonal, and metabolic adjustments, as well as modifications in gene expression (Brown et Sa, 2015). In addition, organic fractions provide sources of carbon, nitrogen, and energy that support microbial proliferation in the rhizosphere, promoting organic matter turnover and the production of bioactive compounds. Consequently, modifications in soil microbiome

composition and functionality represent a key mechanism underlying the enhancement of crop productivity (Tejada et al., 2011; Colla et al., 2017).

Within the broader framework of sustainable agriculture, biostimulants are increasingly regarded as strategic tools for reconciling high crop productivity with reduced environmental impact. They are generally defined as substances or microorganisms capable of stimulating natural plant processes when applied to seeds, plants, or the rhizosphere, thereby improving nutrient use efficiency, tolerance to abiotic stresses, and crop quality independently of their nutrient content (Traon et al., 2014; Yakhin et al., 2017). Their strategic relevance has also been recognized internationally, with the FAO highlighting the agronomic potential of algal biomass as both plant growth promoters and organic soil amendments (FAO, 2006).

From a biochemical perspective, plant biostimulants exhibit remarkable compositional complexity, encompassing mineral elements, humic substances, vitamins, amino acids, chitin, chitosan, and diverse polysaccharide fractions (Berlyn and Russo, 1990; Hamza and Suggars, 2001; Kauffman et al., 2007). Unlike conventional fertilizers, their efficacy arises from emergent properties generated by the interaction of multiple constituents, often active at very low concentrations but capable of inducing systemic and synergistic responses (Sharif et al., 2002; Ertani et al., 2011). Among the most extensively studied classes are brown seaweed extracts (e.g., *Ascophyllum nodosum*, *Ecklonia maxima*, and *Laminaria* spp.), which have been shown to improve vegetative vigor, photosynthetic efficiency, and stress tolerance (Norrie and Keathley, 2006; Carvalho et al., 2013). Likewise, humic substances can exert auxin-like effects through modulation of plasma membrane H^+-ATPase activity, thereby stimulating root development and nutrient uptake (Zandonadi et al., 2016; Baldotto and Baldotto, 2013). The effectiveness of products is strongly influenced by plant species, cuticular properties, dosage, timing, and application method (Kunicki et al., 2010; Kolomaznik et al., 2012; Vargas-Hernandez et al., 2017).

To address the intrinsic complexity of these systems, advanced omics approaches such as transcriptomics and microarray analyses are increasingly employed to elucidate the molecular pathways activated by biostimulant application. These methodologies are essential for identifying molecular markers, optimizing raw material selection, and validating novel formulations (Povero et al., 2016). In this perspective, biostimulants are fully integrated into circular bioeconomy strategies and the current European regulatory framework (Regulation EU 2019/1009), representing a critical resource for the development of resilient agricultural systems characterized by improved resource-use efficiency (Nardi et al., 2016; De Pascale et al., 2017; EBIC, 2018).

In the current agro-industrial landscape, the transition from fundamental research to the development of commercial biostimulant formulations has required a deeper understanding of plant growth-promoting (PGP) mechanisms. Commercial products are increasingly designed to target specific physiological processes involved in biomass accumulation and root system architecture (Rouphael and Colla, 2020). For instance, widely used commercial biostimulants include products such as Kelpak®, derived from *Ascophyllum nodosum*, which

has been shown to enhance root growth and improve plant vigor through hormone-like activity (auxins and cytokinins) (Hidangmayum et al., 2017). Similarly, Trainer®, a protein hydrolysate-based biostimulant, promotes nitrogen metabolism and biomass accumulation by stimulating enzymatic activity and gene expression related to nutrient assimilation (Colla et al., 2017). Another example is Humic-based products derived from leonhardite, which are known to enhance root architecture and nutrient uptake through modulation of plasma membrane H^+-ATPase activity (Nardi et al., 2016).

Within this context, microbial biostimulants represent a particularly promising category, as they integrate nutrient mobilization with the regulation of plant physiological processes. Among them, phosphorus-solubilizing microorganisms (PSMs) play a crucial role by addressing one of the main limitations in agricultural systems, namely the low bioavailability of phosphorus in soils. Beyond their capacity to mobilize nutrients, PSMs can produce bioactive compounds such as indole-3-acetic acid (IAA) and siderophores, contributing to root development and improved nutrient acquisition (Vargas-Hernandez et al., 2017; Yakhin et al., 2017).

1.3 Phosphate-Solubilizing Microorganisms (PSMs)

The promotion of plant growth and development by soil microorganisms is closely associated with enhanced nutrient acquisition, particularly of phosphorus (P), which plays a critical role in plant metabolism. Microorganisms are key drivers of the biogeochemical cycling of phosphorus, as they facilitate its transformation from insoluble inorganic and organic forms into plant-available fractions through solubilization and mineralization processes (Rodríguez and Fraga, 1999). In the context of modern agriculture—where the aim is to optimize productivity while minimizing environmental impacts—PSMs have attracted considerable attention as bioinoculants. Their ability to improve nutrient uptake and increase crop yields makes them a promising and sustainable alternative to conventional fertilization strategies (Young, 1994; Goldstein et al., 1999; Fasim et al., 2002).

PSMs represent a diverse group of beneficial organisms, including bacterial genera such as *Bacillus, Pseudomonas,* and *Rhizobium*; fungal taxa such as *Penicillium* and *Aspergillus*; as well as actinomycetes and arbuscular mycorrhizal fungi (AMF; Kalayu, 2019). Although soil constitutes the primary habitat for microbial growth —harboring between 10^1 and 10^{10} bacteria per gram of fertile soil (Khan et al., 2009a)— phosphate-solubilizing bacteria (PSB) typically account for 1–50% of the total microbial population, whereas phosphate-solubilizing fungi (PSF) represent approximately 0.1–0.5% (Walpola and Yoon, 2012; Chen et al., 2006). These microorganisms are particularly active in the rhizosphere, where they are most frequently isolated (Selvi et al., 2017). In addition to the commonly reported genera, symbiotic nitrogen-fixing rhizobia and saprophytic fungi, such as *Arthrobotrys oligospora*, have also demonstrated notable phosphate-solubilizing capabilities (Thakur et al., 2014; Duponnois et al., 2006).

In recent decades, numerous PSB strains have been isolated from diverse environments, including metal-contaminated soils, phosphate mines, composts, and soil macrofauna (Mendoza-Arroyo et al., 2020; Teng et al., 2019; Hamdali et al., 2012). These indigenous microorganisms enhance nutrient mobilization by accelerating biological processes that convert unavailable phosphorus into plant-accessible forms (Alfa et al., 2014). Empirical studies highlight their effectiveness; for example, Rawat et al. (2021) reported that the combined application of PSM and phosphatic fertilizers increased wheat yield by 22% and phosphorus uptake by 26%, while reducing chemical fertilizer inputs by 30%. Similarly, co-inoculation with fungal strains has been shown to mobilize phosphorus bound to soil particles, thereby further improving its availability (Mittal et al., 2008; Jain et al., 2010).

From an applied perspective, particular attention has been given to spore-forming *Bacillus* species, such as *Bacillus amyloliquefaciens*, due to their high formulation stability, extended shelf life, and effective rhizosphere colonization (Qiao et al., 2014). Moreover, Actinobacteria—especially members of the genus *Streptomyces*—are recognized for their strong biocontrol potential against fungal pathogens such as *Fusarium* and *Phytophthora*, primarily through the production of secondary metabolites and hydrolytic enzymes (Sabaratnam and Traquair, 2015).

1.4 Biochemical and molecular mechanisms of phosphorus solubilization by PSMs

Phosphorus solubilization by rhizospheric microorganisms is a complex and multifactorial process governed by the interplay among soil nutrient status, microbial physiology, and the developmental stage of the host plant (Reyes et al., 1999). PSMs employ three main, often synergistic, strategies: microenvironmental acidification, cation chelation, and enzymatic mineralization of organic phosphorus fractions. These mechanisms operate in an integrated manner, representing a coordinated physiological response shaped by phosphorus limitation and selective pressures within the rhizosphere.

At the regulatory level, phosphorus deficiency induces global adaptive responses in microorganisms, activating phosphate acquisition systems and promoting metabolic reprogramming toward the production of organic acids and extracellular enzymes, thereby enhancing phosphorus mobilization under limiting conditions.

1.4.1 Rhizo-acidification and organic acid biosynthesis

The primary mechanism for inorganic phosphorus mobilization involves the reduction of rhizospheric pH through the secretion of low-molecular-weight organic acids or the release of protons (H^+) during ammonium assimilation (Kumar et al., 2018; Satyaprakash et al., 2017; Rodríguez & Fraga, 1999). A strong correlation has been observed between the

solubilization index and the concentration of organic acids produced, which are mainly derived from oxidative or fermentative glucose metabolism (Alam et al., 2002).

Importantly, organic acid production represents not merely a metabolic by-product but an adaptive overflow mechanism that links central carbon metabolism with nutrient acquisition under conditions of imbalance. This metabolic shift enhances carbon flux toward extracellular acidification, thereby increasing the efficiency of mineral phosphate dissolution.

In many Gram-negative bacteria, glucose oxidation occurs via a direct periplasmic pathway mediated by the membrane-bound enzyme glucose dehydrogenase (GDH) and its cofactor pyrroloquinoline quinone (PQQ). This pathway leads to the accumulation of gluconic acid and 2-ketogluconic acid, which are among the most effective agents for solubilizing tricalcium phosphate due to their strong acidifying capacity (Goldstein, 1995; Selvi et al., 2017).

In addition to gluconic acid, PSMs produce a variety of carboxylic acids—such as citric, oxalic, malic, and succinic acids—whose effectiveness depends on their molecular structure, dissociation constants (pKa), and the number of carboxyl functional groups (Ahmed & Shahab, 2019).

1.4.2 Chelation and surface coordination mechanisms

Alongside acidification, organic acids contribute to phosphorus mobilization through chelation and ligand exchange reactions. Their hydroxyl and carboxyl groups form stable coordination complexes with metal cations—primarily Ca^{2+} in alkaline soils and Al^{3+} or Fe^{3+} in acidic soils—that are associated with phosphate compounds (Kpomblekou & Tabatabai, 1994; Kim et al., 1997). This mechanism alters chemical equilibrium, promoting the dissolution of mineral phosphates and preventing phosphorus re-precipitation into insoluble forms.

The chelation-mediated destabilization of mineral surfaces enhances the release of orthophosphate into the soil solution, thereby sustaining phosphorus availability in the rhizosphere. In certain soil conditions, PSMs may also produce inorganic acids that contribute to mineral dissolution, although this pathway is generally less significant than organic acid-mediated processes (Walpola & Yoon, 2012; Khan et al., 2009a).

Additionally, siderophore production—primarily associated with iron acquisition—can indirectly facilitate phosphorus solubilization by chelating Fe^{3+} bound to ferric phosphates, thereby destabilizing these complexes and releasing phosphate ions.

1.4.3 Mineralization of organic phosphorus

While solubilization primarily targets inorganic phosphorus, mineralization is the key biological process responsible for mobilizing phosphorus from organic compounds such as nucleic acids, phospholipids, and phytates (Khan et al., 2009a). This process is mediated by a suite of extracellular enzymes produced by PSMs.

Non-specific acid and alkaline phosphatases catalyze the hydrolysis of phosphomonoesters, releasing inorganic phosphate (Pi) that can be readily absorbed by plants (Tarafdar et al., 2003; Kalayu, 2019). Phytases specifically degrade phytic acid (inositol hexakisphosphate), a major storage form of phosphorus in plant tissues and a recalcitrant compound in soils (Santana et al., 2016; Aseri et al., 2009). Furthermore, phosphodiesterases and phosphonatases catalyze the breakdown of more complex phosphorus-containing compounds, including nucleic acids and C–P bond-containing molecules.

The coordinated activity of these enzymes ensures the continuous regeneration of inorganic phosphate in the soil solution, maintaining nutrient availability even under low-input conditions (Dodor & Tabatabai, 2003; Selvi et al., 2017). From an ecological perspective, this enzymatic network contributes to a dynamic soil–microbe–plant phosphorus cycle, in which microbial metabolism, root exudation, and organic matter turnover are tightly interconnected, ultimately enhancing phosphorus bioavailability and supporting plant growth.

1.5 Soil phosphorus availability

In soil, phosphorus occurs in two main pools: organic phosphorus (P_org) and inorganic phosphorus (P_i). The organic fraction may account for 20–80% of total soil phosphorus and is mainly composed of compounds such as inositol hexakisphosphate (phytic acid), whereas the inorganic fraction is generally associated with calcium, iron, and aluminum minerals (Sanyal and De Datta, 1991; Hinsinger, 2001). In the soil solution, inorganic phosphorus is primarily present as orthophosphate species, mainly $H_2PO_4^-$ and HPO_4^{2-}, whose relative abundance is strongly influenced by soil pH (Furihata et al., 1992; Shen et al., 2011).

Despite its essential role in plant growth, it is often poorly available in soils, as it is rapidly immobilized into insoluble forms, leading to the accumulation of “legacy phosphorus.” As a result, plants rely on complex mechanisms to acquire and utilize P efficiently.

In agriculture, highly soluble fertilizers such as triple superphosphate (TSP) and diammonium phosphate (DAP) are widely used to maintain crop yields; however, their efficiency is low because most of the applied phosphorus becomes unavailable, increasing costs and environmental risks. Rock phosphate (RP) represents a more sustainable alternative, although its effectiveness depends on soil conditions and biological activity. Since phosphorus is a non-renewable resource derived from finite geological reserves, its global supply is limited and unevenly distributed, with a strong geopolitical concentration.

This raises concerns about long-term availability, price volatility, and food security, especially as demand continues to grow. Consequently, improving phosphorus use efficiency and adopting circular management strategies, such as recycling and biological mobilization, are essential for sustainable agriculture.

In Italy, phosphorus is officially recognized as a critical resource. National legislation (Law No. 205/2017) established the Italian Phosphorus Platform to promote sustainable management, recovery, and recycling of phosphorus in alignment with European circular economy policies. At the global level, phosphorus supply represents a strategic concern. Approximately 90% of the phosphate used for fertilizer production in the European Union is imported (European Commission, 2016). Over recent decades, the EU has promoted policies aimed at limiting excessive phosphorus fertilizer use and reducing environmental impacts, particularly regarding water quality and eutrophication (Nesme et al., 2016; Montanarella and Panagos, 2021; Sporchia and Caro, 2023; de Ridder et al., 2012; van Dijk et al., 2016). These policies are designed to enhance nutrient circularity and improve phosphorus use efficiency in agricultural systems (Magaya et al., 2024).

Phosphorus deficiency in soils is mainly due to low bioavailability rather than total content. It is influenced by long-term soil formation processes, chemical fixation with iron, aluminium, or calcium, adsorption to soil particles, low organic matter, and unfavourable physical conditions such as compaction or waterlogging. Additionally, the inefficiency of fertilizers contributes to the buildup of unavailable phosphorus and environmental issues like eutrophication.

1.6 Importance of Phosphorus in biological processes

Phosphorus (P) constitutes approximately 0.2–0.8% of plant dry weight (Sharma et al., 2013) and plays a fundamental role in numerous biological processes essential for plant growth and development. However, as outlined in the previous section, its availability in soils is often severely constrained by geological, chemical, and physical factors, making phosphorus one of the most limiting nutrients in both natural and agricultural systems (Schachtman et al., 1998; Hinsinger, 2001).

At the molecular level, phosphorus is an essential component of nucleic acids, forming part of the sugar–phosphate backbone of DNA and RNA (Marschner, 2012), thereby ensuring the structural stability and transmission of genetic information. It is also central to cellular energy metabolism, as a key constituent of adenosine triphosphate (ATP) and other phosphorylated intermediates, including ADP, AMP, and sugar phosphates (Abel et al., 2002). The hydrolysis of high-energy phosphate bonds in ATP provides the energy required for biosynthesis, active transport, and a wide range of physiological processes.

Phosphorus is deeply integrated into major metabolic pathways, such as glycolysis, the tricarboxylic acid (TCA) cycle, and oxidative phosphorylation. It also plays a regulatory role

through phosphorylation and dephosphorylation reactions, which modulate enzyme activity, substrate affinity, and signal transduction pathways (Marschner, 2012). Furthermore, phosphorus is a structural component of phospholipids, contributing to membrane integrity, fluidity, and functionality, and enabling the selective transport of ions and metabolites across biological membranes (Vance et al., 2003). It is also involved in intracellular signaling, where phosphorylated compounds and protein phosphorylation act as key regulators of gene expression, enzymatic activity, and stress responses (Hinsinger, 2001).

At the whole-plant level, phosphorus is indispensable for growth and development. It plays a central role in root system architecture by promoting root elongation and branching, thereby enhancing the plant's capacity to explore the soil and acquire water and nutrients (López-Bucio et al., 2003; Lynch, 2011). This function is particularly critical under phosphorus-deficient conditions, where efficient root development represents a key adaptive strategy (Marschner, 2012).

Phosphorus is also essential for reproductive development and is therefore a major determinant of crop productivity. Adequate phosphorus availability supports the transition from vegetative to reproductive stages, including flowering, pollination, and fruit set, processes that are highly energy-demanding and dependent on ATP availability. Consequently, phosphorus deficiency often leads to delayed flowering, reduced fruit set, and overall yield decline (Holford, 1997; Grant et al., 2001; Marschner, 2012). In addition, phosphorus contributes to tissue differentiation and structural integrity, indirectly enhancing plant resistance to biotic stresses such as pathogens and pests.

Phosphate uptake by plants is an active, carrier-mediated process that occurs against a concentration gradient, as phosphate levels within root cells and xylem sap are typically 100–1,000 times higher than those in the surrounding soil solution (Violante, 1996). Once absorbed, phosphorus is highly mobile and can be efficiently remobilized from older, senescing tissues to actively growing organs. This internal redistribution is regulated by source–sink relationships, in which mature leaves act as sources and developing tissues function as sinks (Sakano, 1990; Poirier & Bucher, 2002; Versaw and Harrison, 2002; Huang et al., 2011). Such remobilization processes are particularly important under phosphorus-limited conditions, allowing plants to partially compensate for reduced external supply.

From both ecological and agronomic perspectives, the central role of phosphorus in plant metabolism explains why its limited availability directly results in reduced growth, lower biomass accumulation, and decreased crop yields (Schachtman et al., 1998; Elser et al., 2007; Hinsinger, 2001). Consequently, phosphorus availability is a key factor governing ecosystem productivity and agricultural sustainability, underscoring the need for improved strategies to enhance phosphorus use efficiency.

In tomato (*Solanum lycopersicum* L.) plants, phosphorus deficiency induces a range of physiological and morphological alterations. Initial symptoms are generally observed in older leaves, which develop characteristic reddish or purplish coloration due to anthocyanin

accumulation as phosphorus is remobilized toward younger tissues (Fig. 1.5). Under severe deficiency, leaves may become dark, curled, and necrotic, eventually leading to tissue senescence and abscission. Plant growth is typically reduced, with limited root development, delayed shoot formation, and impaired flowering. Seed production and quality may also be negatively affected, representing a critical limitation for seed production systems.

Figure 1.5. Symptoms of phosphorus deficiency on tomato leaves.

At the physiological level, phosphorus deficiency severely impacts central metabolic processes. Plants perceive P limitation when vacuolar phosphorus reserves decline, resulting in reduced phosphorus supply to actively growing tissues. This leads to a decrease in photosynthetic activity, glycolysis, and respiration (Sánchez-Calderón et al., 2010). At the biochemical level, low cytoplasmic phosphorus concentrations inhibit ATP synthesis, thereby limiting energy availability for cellular processes. In addition, phosphorus deficiency reduces the activity of RuBisCO (ribulose-1,5-bisphosphate carboxylase/oxygenase) and causes the accumulation of its substrate, ribulose-1,5-bisphosphate (RuBP), ultimately impairing carbon fixation (De Groot et al., 2003).

The availability of phosphorus in soil is strongly influenced by edaphic factors. In acidic soils (pH < 5.8) or in the presence of high concentrations of iron and zinc, phosphate ions become poorly available due to precipitation and fixation processes. Similarly, clay-rich soils often exhibit reduced phosphorus bioavailability. These conditions highlight the importance of strategies aimed at improving phosphorus use efficiency in agricultural systems.

Overall, phosphorus plays a fundamental role in multiple aspects of plant development, influencing both vegetative growth and reproductive success. Understanding the

mechanisms underlying phosphorus uptake and utilization is therefore essential for optimizing tomato productivity and developing sustainable fertilization strategies.

1.7 Phosphorus uptake and use efficiency in plants

Phosphorus is the third most important nutrient for plants after nitrogen and potassium, and it represents one of the main limiting factors for plant growth and crop productivity. Due to its low mobility and availability in soils, P deficiency constitutes a major constraint for agricultural production, particularly in acidic and alkaline soils, which together account for more than 70% of the world's cultivated land (Schachtman et al., 1998). It has been estimated that limited phosphorus availability can reduce crop yields by up to 30–40% of global arable land (Von Uexkull and Mutert, 1995).

Phosphorus uptake by plants represents the first step in its transfer from soil to plant tissues. This process occurs through specific transporters located in the plasma membrane of root cells and is energy-dependent, as it takes place against a concentration gradient. Once absorbed, phosphate is translocated through root tissues and loaded into the xylem, from where it is transported to the aerial parts of the plant, particularly to actively growing tissues such as young leaves and meristems (Jeschke et al., 1997).

Under conditions of low phosphorus availability, plants have evolved several adaptive strategies to enhance P acquisition. These include the secretion of organic acids and phosphatases by roots and rhizosphere microorganisms, which promote the solubilization of phosphorus bound to soil particles and increase its availability (Comerford, 1998; Hinsinger, 2001; Malhotra et al., 2016). These processes facilitate phosphate diffusion toward the root surface and improve its uptake efficiency.

Despite its importance, the efficiency of phosphorus fertilizers is generally low. It is estimated that only 10–20% of the applied phosphorus is taken up by crops, while the remaining fraction is rapidly immobilized in the soil through fixation and retrogradation processes (Von Uexkull and Mutert, 1995). For this reason, phosphorus fertilization management plays a crucial role in agricultural systems. To ensure adequate phosphorus nutrition and reduce P fixation, it is necessary to adopt appropriate agronomic practices, including maintaining optimal soil structure, regulating soil pH within the range of 5 to 7, applying fertilizers in localized and split applications, preserving high levels of soil organic matter, and promoting soil microbial activity.

An additional concern relates to the quality of phosphate fertilizers, which may contain contaminants such as heavy metals (e.g., cadmium and arsenic) and radionuclides from the uranium and thorium decay series (Anonymous, 1991; Rutherford et al., 1995). In this context, a significant reduction in mineral fertilizer use could be achieved by improving the mobilization of insoluble phosphorus already present in soils. Biological approaches based

on phosphorus-solubilizing microorganisms represent a promising strategy to increase the availability of otherwise inaccessible phosphorus and enhance overall system efficiency (Rodriguez and Fraga, 1999; Vessey, 2003; Thauriae et al., 2004; Islam et al., 2007; Islam and Hossain, 2012; Sarker et al., 2012).

2. AIM OF THE WORK

This work addresses the current challenges associated with the sustainability of agricultural systems, with particular emphasis on reducing reliance on mineral fertilizers and improving nutrient use efficiency under conditions of increasing environmental pressure and ongoing soil fertility decline. Phosphorus (P) represents one of the main limiting factors for agricultural productivity, due to its low bioavailability in soils and the environmental and economic concerns associated with synthetic phosphate fertilizers.

Plant Growth-Promoting Bacteria (PGPB) have emerged as a key resource for the development of innovative agro-biotechnological strategies. However, significant gaps remain in the integrated understanding of the functional mechanisms governing the interaction between PGPB, phosphorus availability, and plant response, as well as in the translation of these findings into real cropping systems.

This study aimed to investigate, through a systemic and multi-level approach, the potential of bacterial strains belonging to the genera *Bacillus* and *Pseudomonas* as bioinoculants specifically capable of improving phosphorus nutrition and plant growth.

Specifically, this research is aimed at:

(I) Comprehensively characterize the bacterial strains through an integrated approach combining phenotypic and physiological analyses, defining their functional profile under abiotic stress conditions and their ability to produce key metabolites such as siderophores.

(II) Evaluate the antagonistic potential against agriculturally relevant phytopathogens through *in vitro* dual-culture assays, as a complementary screening to verify the multifunctional versatility of the strains.

(III) Investigate the mechanisms of phosphorus solubilization from insoluble sources (e.g., tricalcium phosphate and rock phosphate), employing quantitative analytical approaches to correlate microbial activity with the production of organic acids and other specific metabolites identified by advanced GC–MS techniques.

An additional objective is to assess, through *in vivo* experiments on model crops such as wheat (*Triticum aestivum* L.) and tomato (*Solanum lycopersicum* L.), the effectiveness of these strains in modulating phosphorus uptake, physiological plant responses, and crop productivity under different nutrient availability conditions.

The working hypothesis is that specific bacterial strains characterized by high phosphorus-solubilizing capacity and the production of bioactive metabolites can significantly enhance P availability in soil, representing a sustainable alternative to conventional fertilization.

Overall, this thesis aims to bridge the gap between functional characterization and agronomic application, providing new insights into the mechanisms governing phosphorus mobilization under realistic conditions. The expected results are intended to support the development of sustainable fertilization strategies based on microbial inoculants.

3. MATERIALS AND METHODS

3.1. Bacteria and Culture Media

In this study, four bacterial strains belonging to the genus *Bacillus (B. megaterium* FBM09, *B. pumilus* FBP01, *B. amyloliquefaciens*, *B. subtilis* FBS07*)* and two bacterial strains belonging to the genus *Pseudomonas (P. putida* RPT12, *P. salmasensis* POE54) were used. *Bacillus* strains and *P. putida* RPT12 were obtained from Fertilidea Srl (Pompei, NA, Italy; www.fertilidea.it), while *P. salmasensis* POE54 was obtained from the collection available at the Plant Pathology Laboratories of the Department of Agriculture, Food, and Environment at the University of Catania (Italy) and has been previously characterized for its genomic and biocontrol traits (Nicotra et al., 2024) . Molecular identification of the bacterial strains was carried out through partial 16S rRNA gene amplification, using the universal primer pairs V3-16S and 341F-805R (Klindworth et al., 2013; Herlemann et al., 2011). All bacterial strains were stored in 30% (v/v) glycerol at −20 °C. For routine use, strains were cultured on Nutrient Agar (NA; HiMedia Laboratories GmbH, Modautal, Germany) and incubated at 30 ± 2 °C for 24 h. Working stocks were maintained at 4 °C and subcultured weekly to ensure viability and purity.

3.2 Phenotypic characterization of bacterial isolates

3.2.1 Salt tolerance

Salt tolerance of the selected bacteria was evaluated *in vitro* by inoculating the isolates into 250 mL Erlenmeyer flasks containing 100 mL of nutrient broth (NB) supplemented with NaCl at final concentrations of 0.5, 1.0, and 1.5 M. NB without NaCl supplementation was used as control (Singh, 2021). All strains were tested in three independent replicates. Pre-inoculum was prepared by transferring a single colony from a nutrient agar (NA) plate into NB medium and incubating at 30 ± 2 °C under agitation (180 rpm) until reaching an optical density of 0.7 at 600 nm (OD_{600}), corresponding to approximately 1×10^7 CFU mL^{-1}. Subsequently, 1 mL of the pre-inoculum was used to inoculate each experimental flask. Cultures were incubated at 30 ± 2 °C under agitation (180 rpm), and bacterial growth was monitored over time by measuring OD_{600} and by determining colony-forming units (CFU mL^{-1}). Measurements were performed at four time points: immediately after inoculation (0 h), and after 24, 48, and 60 h of incubation.

3.2.2 In vitro *dual culture assay against phytopathogenic fungi*

The antimicrobial activity of the selected bacterial strains was evaluated against three phytopathogenic fungi, *Alternaria alternata*, *Fusarium oxysporum* and *Botrytis cinerea*, using an *in vitro* dual-culture assay. Fungal isolates were routinely maintained on Potato Dextrose Agar (PDA, Hi-Media) and subcultured prior to the experiments to ensure active and uniform growth. All assays were conducted on diluted PDA (1:5), to slow down the fungal growth and enhance the detection of antagonistic interactions. Fungal pathogens were inoculated at the center of each plate using a 5 mm diameter mycelial plug excised from the actively growing margin of a fresh culture. To account for differences in intrinsic growth rates among fungal species, inoculation timing was adjusted to ensure comparable colony development prior to bacterial application. Plates were incubated at 22–25 °C for 4 - 7 days, depending on the fungal species, before bacterial inoculation.

Bacterial strains were grown overnight (approximately 16 hours) in NB under agitation at their optimal growth temperature. Subsequently, 20 µL of each bacterial culture (OD_{600} = 0.7) were spotted onto the agar surface at approximately about 2 cm from the edge of the plate of the fungal colony.

Each fungal–bacterial interaction was tested in triplicate. Control treatments included plates inoculated with the fungal pathogen alone (fungal control) and plates inoculated with bacterial strain alone (bacterial control). After bacterial inoculation, plates were further incubated at 25 ± 2 °C and monitored daily. Antagonistic activity was assessed both qualitatively, by observing inhibition zones or morphological alterations of the fungal mycelium, and quantitatively by measuring radial fungal growth. The percentage of radial growth inhibition (PRGI) was calculated according to the following formula (Khamsuk et al., 2024):

$$\text{PRGI}\,(\%) = \frac{R_c - R_t}{R_c} \times 100$$

Where R_c represents the mean radial growth of the fungal colony in the control plates and R_t represents the mean radial growth in the presence of the bacterial strain.

3.2.3 Phenotypic characterization and metabolic profiling

The metabolic profiling and phenotypic characterization of the selected bacterial strains were performed using the Biolog GEN III MicroPlate system (Biolog Inc., Hayward, CA, USA). This system allows simultaneous evaluation of carbon source utilization and sensitivity to a range of chemical and environmental stressors, providing a comprehensive phenotypic fingerprint for microbial identification and functional characterization. Approximately 24

hours prior to the assay, each bacterial strain was streaked onto Nutrient Agar (NA) plates and incubated for 24 h at 28 °C to obtain fresh and actively growing colonies. A single well-isolated colony was then suspended in Biolog inoculating fluid (IF-A) and adjusted to the recommended cell density according to the manufacturer's instructions. An aliquot of 110 µL of the standardized cell suspension was inoculated into each well of the GEN III MicroPlate. The plate contains 94 phenotypic tests, including 71 carbon source utilization assays and 23 chemical sensitivity assays, designed to assess tolerance to factors such as pH, salt, and inhibitory compounds.

The system is based on a redox reaction in which cellular respiration leads to the reduction of tetrazolium dye, resulting in a color change from colorless to purple in metabolically active wells. Well A1, containing no carbon source, served as a negative control, while specific wells included internal controls for chemical sensitivity. Following inoculation, plates were incubated at 28 °C for 24–48 h. The results were recorded using the Biolog MicroStation™ system (Biolog Inc.), which analyzes the pattern of color development to generate a metabolic profile for each strain. The obtained profiles were used for both strain identification and comparative assessment of metabolic capabilities.

GEN III MicroPlate

A1 Negative Control	A2 Dextrin	A3 D-Maltose	A4 D-Trehalose	A5 D-Cellobiose	A6 Gentiobiose	A7 Sucrose	A8 D-Turanose	A9 Stachyose	A10 Positive Control	A11 pH 6	A12 pH 5
B1 D-Raffinose	B2 α-D-Lactose	B3 D-Melibiose	B4 β-Methyl-D-Glucoside	B5 D-Salicin	B6 N-Acetyl-D-Glucosamine	B7 N-Acetyl-β-D-Mannosamine	B8 N-Acetyl-D-Galactosamine	B9 N-Acetyl Neuraminic Acid	B10 1% NaCl	B11 4% NaCl	B12 8% NaCl
C1 α-D-Glucose	C2 D-Mannose	C3 D-Fructose	C4 D-Galactose	C5 3-Methyl Glucose	C6 D-Fucose	C7 L-Fucose	C8 L-Rhamnose	C9 Inosine	C10 1% Sodium Lactate	C11 Fusidic Acid	C12 D-Serine
D1 D-Sorbitol	D2 D-Mannitol	D3 D-Arabitol	D4 myo-Inositol	D5 Glycerol	D6 D-Glucose-6-PO4	D7 D-Fructose-6-PO4	D8 D-Aspartic Acid	D9 D-Serine	D10 Troleandomycin	D11 Rifamycin SV	D12 Minocycline
E1 Gelatin	E2 Glycyl-L-Proline	E3 L-Alanine	E4 L-Arginine	E5 L-Aspartic Acid	E6 L-Glutamic Acid	E7 L-Histidine	E8 L-Pyroglutamic Acid	E9 L-Serine	E10 Lincomycin	E11 Guanidine HCl	E12 Niaproof 4
F1 Pectin	F2 D-Galacturonic Acid	F3 L-Galactonic Acid Lactone	F4 D-Gluconic Acid	F5 D-Glucuronic Acid	F6 Glucuronamide	F7 Mucic Acid	F8 Quinic Acid	F9 D-Saccharic Acid	F10 Vancomycin	F11 Tetrazolium Violet	F12 Tetrazolium Blue
G1 p-Hydroxy-Phenylacetic Acid	G2 Methyl Pyruvate	G3 D-Lactic Acid Methyl Ester	G4 L-Lactic Acid	G5 Citric Acid	G6 α-Keto-Glutaric Acid	G7 D-Malic Acid	G8 L-Malic Acid	G9 Bromo-Succinic Acid	G10 Nalidixic Acid	G11 Lithium Chloride	G12 Potassium Tellurite
H1 Tween 40	H2 γ-Amino-Butyric Acid	H3 α-Hydroxy-Butyric Acid	H4 β-Hydroxy-D,L-Butyric Acid	H5 α-Keto-Butyric Acid	H6 Acetoacetic Acid	H7 Propionic Acid	H8 Acetic Acid	H9 Formic Acid	H10 Aztreonam	H11 Sodium Butyrate	H12 Sodium Bromate

Figure 3.1. Layout of assays in the Biolog GEN III MicroPlate.

3.2.4 Siderophore production

The production of iron-chelating compounds produced by bacteria under iron-limiting conditions was assessed both qualitatively and quantitatively using the Chrome Azurol S (CAS) assay. The CAS assay is based on a competitive reaction for iron between siderophores and a ferric–dye complex. Specifically, siderophores remove iron from the blue CAS–Fe^{3+} complex due to their higher affinity, resulting in a color change from blue to orange, which indicates siderophore production (Schwyn and Neilands, 1987). CAS solution was prepared according to the protocol described by Louden et al. (2011). Bacterial inoculum was prepared by growing cultures in NB to an optical density of approximately 0.7 at 600 nm (OD_{600}). Aliquots of 20 µL of each bacterial culture were spotted onto NA plates. After inoculation, the CAS solution was overlaid onto the plates. Plates were then incubated at 28–30 °C and monitored for the development of orange halos surrounding the colonies, indicating siderophore production due to the removal of iron from the CAS complex.

For quantitative evaluation of siderophore production, bacterial strains were cultured in liquid medium for 48 h at 30 ± 2 °C under agitation (180 rpm). Cultures were then centrifuged at 10,000 × g for 10 min, and the cell-free supernatants were collected. For the quantitative assay, aliquots of bacterial supernatant were mixed with an equal volume of CAS reagent in a microplate format. After 20 min of incubation at room temperature, absorbance was measured at 630 nm using a microplate reader. Siderophore production was expressed as percent siderophore units (PSU) according to the following formula (Schwyn and Neilands, 1987):

$$\text{Siderophore production (PSU)} = \frac{A_r - A_s}{A_r} \times 100$$

where A_r is the absorbance of the reference (CAS solution mixed with uninoculated medium) and A_s is the absorbance of the sample (CAS solution mixed with bacterial supernatant).

3.2.5 Phosphate solubilization

The phosphate-solubilizing ability of the bacterial cultures was evaluated on solid media according to the methods described by Pikovskaya (1948) and Nautiyal (1999), using Pikovskaya's (PVK) and National Botanical Research Institute's phosphate (NBRIP) agar media, respectively. In both media, tricalcium phosphate (TCP, $Ca_3(PO_4)_2$), was used as insoluble inorganic phosphorus source. PVK medium was prepared according to Pikovskaya (1948; pH 7.0) and contained per liter: glucose (10 g), $Ca_3(PO_4)_2$ (5 g), $(NH_4)_2SO_4$ (0.5 g), NaCl (0.2 g), $MgSO_4 \cdot 7H_2O$ (0.1 g), KCl (0.2 g), yeast extract (0.5 g), $MnSO_4 \cdot H_2O$ (0.002 g), and $FeSO_4 \cdot 7H_2O$ (0.002 g). NBRIP medium (Nautiyal, 1999) contained, per liter: glucose

(10 g), $Ca_3(PO_4)_2$ (5 g), $MgCl_2 \cdot 6H_2O$ (5 g), $MgSO_4 \cdot 7H_2O$ (0.25 g), KCl (0.2 g), and $(NH_4)_2SO_4$ (0.1 g). Both media were supplemented with 1.5% (w/v) agar.

Starter cultures were prepared by inoculating single colonies into 20 mL of NB broth and incubating at 28 °C and 180 rpm until reaching an OD_{600} of approximately 0.7 (corresponding to ≈1 × 10^8 CFU/mL). A 10 µL aliquot of each culture was spot inoculated onto PVK and NBRIP agar plates. For each strain, three biological replicates were prepared per medium. Plates were incubated at 28 °C for 7 days and examined daily. Phosphate solubilization was considered positive upon the formation of a clear halo surrounding the bacterial colony, indicating the solubilization of tricalcium phosphate ($Ca_3(PO_4)_2$).

The solubilization index (SI) was calculated according to Edi-Premono et al. (1996) as the ratio between the total diameter (colony + halo zone) and the colony diameter, using the following formula:

$$SI = \frac{\text{Colony diameter} + \text{Halo zone diameter}}{\text{Colony diameter}}$$

In addition, solubilization efficiency (SE) was calculated as described by Nautiyal (1999) and expressed as a percentage by dividing the halo zone diameter (total diameter minus colony diameter) by the colony diameter, according to the following equation:

$$SE(\%) = \frac{\text{Halo zone diameter}}{\text{Colony diameter}} \times 100$$

Measurements were performed daily up to the seventh day, until no further expansion of the halo was observed. This assay allowed a comparative and semi-quantitative evaluation of the phosphate-solubilizing efficiency of the bacterial strains under different nutrient conditions.

Bacterial growth was also evaluated in liquid Pikovskaya medium (PVK) to assess adaptation to rock phosphate as an insoluble phosphorus source. Two variants of PVK medium were used: a standard formulation containing $Ca_3(PO_4)_2$ and a modified formulation in which $Ca_3(PO_4)_2$ was replaced with rock phosphate (RP) as the sole insoluble phosphorus source.

For each strain, bacterial suspensions were obtained from overnight cultures in nutrient broth. Subsequently, 1 mL of each starter culture was used to inoculate 250 mL Erlenmeyer flasks containing 100 mL PVK. Each bacterial strain was inoculated in triplicate in both PVK (standard and modified formulation). Cultures were adjusted to an initial inoculum concentration of approximately 1 × 10^7 CFU mL^{-1}.The flasks were incubated at 30 ± 2 °C and180 rpm. Bacterial growth was monitored for 48 h by measuring the OD_{600} at 4 h intervals using a Jasco V-730 UV-Vis Spectrophotometer (JASCO Corp., Japan). Viable cell counts

were determined using the plate count method. Aliquots from each culture were serially diluted and plated on NA. Plates were incubated at 30 ± 2 °C for 24 h, and the bacterial population was expressed as colony-forming units per milliliter (CFU mL^{-1}). The final CFU mL^{-1} was calculated as the mean of three replicate plates using the following formula:

$$N\left(\frac{\text{Number of colonies}}{\text{mL}}\right) = \frac{\frac{n\ (\text{Number of colonies in the plates considered})}{p\ (\text{Number of plates considered})}}{V\ (\text{Volume of inoculum in mL}) \times d\ (\text{Dilution factor considered})}$$

3.3 Quantitative estimation of phosphate solubilization

The phosphate-solubilizing capacity of the bacterial strains was quantitatively evaluated in liquid culture using modified NBRIP medium in which the standard tricalcium phosphate ($Ca_3(PO_4)_2$) was replaced with rock phosphate (1 g L^{-1}) as the insoluble phosphorus source. Sterile 250 mL Erlenmeyer flasks containing 100 mL of medium were inoculated with 1% (v/v) of standardized bacterial starter cultures ($OD_{600} \approx 0.7$, corresponding to approximately 10^7 CFU mL^{-1}). Cultures were incubated at 30 ± 2 °C on a rotary shaker at 180 rpm for 7 days. Non-inoculated flasks were included as negative controls (Maharana and Dhal, 2022). All experiments were performed in biological triplicates.

At the end of the incubation period, cultures were centrifuged at 10,000 rpm for 10 min to obtain cell-free supernatants The resulting supernatants were collected and used for the determination of soluble phosphorus. The concentration of soluble phosphorus released into the culture medium was quantified using the vanadate–molybdate colorimetric method, in which orthophosphate reacts with ammonium molybdate and ammonium vanadate to form a yellow phospho-vanado-molybdate complex (Sarikhani et al., 2016; Nobahar et al., 2017). Absorbance was measured spectrophotometrically at 720 nm (Perkin-Elmer Instrument, Lambda 25, UV-VIS Spectrometer), and soluble phosphorus concentration was calculated using a calibration curve prepared with known phosphate standards. Finally, the pH of each culture was recorded using a digital pH meter (Hanna Instruments, HI5222, USA).

3.4 Metabolite analysis

Bacterial strains showing phosphorus-solubilizing activity were cultured in liquid NBRIP containing tricalcium phosphate or rock phosphate as P source. For each strain and condition, three independent biological replicates were used. Cultures were inoculated as described

above and incubated at 30 °C under agitation (180 rpm) for 7 days. Then, culture filtrates were collected and subjected to metabolite extraction and GC–MS analysis.

3.4.1 Metabolites extraction

Culture filtrates (50 mL) were extensively extracted with ethyl acetate (EtOAc; Carlo Erba, Cornaredo, Milan, Italy) three times, and the combined organic fractions were dried with anhydrous sodium sulfate (Na_2SO_4, Carlo Erba) and evaporated under vacuum at 40 °C in a rotary evaporator (RV 10, IKA®-Werke GmbH & Co. KG, Staufen, Germany). The crude extracts were resuspended in ethyl acetate at a concentration of 1 mg/mL.

3.4.2 GC–MS analysis

Aliquots of EtOAc extracts were subjected to a derivatization procedure prior to GC-MS analysis. Briefly, fractions resuspended in EtOAc were derivatized with N,O-bis(trimethylsilyl)-trifluoroacetamide (BSTFA) (Fluka, Buchs, Switzerland) for 30 min in an ultrasonic bath (Sonorex, Bandelin electronic GmbH & Co., Berlin, Germany). The derivatized samples were analyzed using an Agilent 5977B MSD mass spectrometer coupled to an Agilent 8890 GC (Agilent Technologies, Santa Clara, USA). Chromatographic and spectrometric parameters were set using MassHunter Workstation software version 10.1.49 (Agilent Technologies), according to the method described by Vinale et al. (2020). The identification of metabolites was achieved by comparing the deconvoluted mass spectra with known compounds, whose spectra are collected in the NIST (National Institute of Standards and Technology) library 20 (NIST 20).

3.5 Effects of PSMs on plant growth and productivity

3.5.1 In vitro *phytotoxicity of rock phosphate*

Preliminary evaluation of potential phytotoxic effects of rock phosphate (RP) was performed according to the protocol described by Daohui (2007). The assay was carried out in sterile Petri dishes (Ø 20 cm) containing nutrient broth supplemented with 0.7% (w/v) agar and finely ground rock phosphate at 1, 2, 4, or 6 % (w/v). Medium prepared without rock phosphate were used as control. Wheat (*Triticum aestivum* L.) seeds were surface sterilized by immersion in 10% (v/v) sodium hypochlorite for 10 min, thoroughly rinsed with sterile distilled water, and air-dried under sterile conditions for 24 h. Ten seeds were evenly distributed in each Petri dish and incubated at 25 °C under controlled light and humidity conditions. Seed germination was recorded daily and expressed as a percentage of germinated seeds, considering radicle emergence as the criterion for germination After 7 days of incubation, radicle length was measured to assess potential phytotoxic effects of rock phosphate on early root development. Each treatment was prepared in three independent biological replicates.

3.5.2 In vivo *assay on wheat (*Triticum aestivum *L.) plants*

A pot experiment was conducted to evaluate the effects of three phosphate-solubilizing bacterial strains (*Pseudomonas putida* RPT12 - PSE; *Bacillus megaterium* FBM09- MEGA; *Bacillus pumilus* FBP01 - PUMI) on the growth of wheat (*Triticum aestivum* L.) and their ability to enhance phosphorus availability from different phosphorus sources.

Each bacterial strain was left to grow in flasks for 72 hours at 30 °C and 150 rpm ($OD_{600} \approx 0.7$, corresponding to approximately 10^7 CFU mL^{-1}). Culture broths were centrifuged at 10.000 g for 10 min and the pellets were resuspended in sterile saline solution (0.9% NaCl). Wheat seeds, surface-sterilized with 1% sodium hypochlorite, were submerged in 20 mL of the cell suspension. The seeds were incubated for 2 h on a rotary shaker (80 rpm, 25 °C) to allow bacterial adhesion to the seed surface. Following incubation, the excessive bacterial inoculum was removed using sterile filter paper, and the seeds were immediately sown in Ø 16 cm pots containing sterile vermiculite that were arranged in a completely randomized block design (Correa et al., 2009). Insoluble rock phosphate (RP) or soluble KH_2PO_4 were supplemented to the substrate at commonly recommended agronomic rates (Table 3.1).

Plants were irrigated every ten days with 20 mL of a modified Hoagland nutrient solution (Hoagland and Arnon, 1950), where RP (1% w/V) or KH_2PO_4 (1M) were added as the only phosphorus source. Bacterial suspensions (20 mL $plant^{-1}$) were applied every 15 days. Control treatments received the same nutrient solution without bacterial inoculation.

Plants were grown in a controlled growth chamber with a photoperiod of 16 h light and 8 h dark and a temperature regime ranging from 15 °C (night) to 25 °C (day). The experiment consisted of a total of eight treatments Uninoculated plants irrigated with either RP or KH_2PO_4 served as controls (Table 3.1). Each treatment consisted of nine independent biological replicates.

Table 3.1. List of the experimental conditions applied to the wheat (*Triticum aestivum* L.) plants grown in vermiculite.

N.	Condition	Bacterial strain	Phosphorus source	P form	P Dose
1	RP	-	Rock phosphate	Insoluble	1% (w/v)
2	K	-	KH_2PO_4	Soluble	1 M
3	PSE+RP	*P. putida* RPT12	Rock phosphate	Insoluble	1% (w/v)
4	PSE+K	*P. putida* RPT12	KH_2PO_4	Soluble	1 M
5	MEGA+RP	*B. megaterium* FBM09	Rock phosphate	Insoluble	1% (w/v)
6	MEGA+K	*B. megaterium* FBM09	KH_2PO_4	Soluble	1 M
7	PUMI+RP	*B. pumilus* FBP01	Rock phosphate	Insoluble	1% (w/v)
8	PUMI+K	*B. pumilus* FBP01	KH_2PO_4	Soluble	1 M

Germination was evaluated five days after sowing, and plants were harvested 30 days after emergence. The following growth parameters were recorded: shoot length, root length, shoot and root fresh weights. For dry weight determination, the samples were dried in an oven at 50 °C for 72 hours.

The chlorophyll content of wheat leaves was estimated by the average of nine readings per plant using a chlorophyll meter (SPAD-502Plus, Konica Minolta Sensing Europe B.V., Nieuwegein, The Netherlands). The results were expressed as absolute values in a range from 0 to 99.

3.5.3 In vivo *assay on tomato (*Solanum lycopersicum *L.) plants – Experiment I*

3.5.3.1 Plant material and bacterial inoculations

In this experiment, tomato seeds (*Solanum lycopersicum* cv. Tydona) were treated with cell suspensions of *B. megaterium* FBM09, *B. pumilus* FBP01, *P. putida* RPT12 or *P. salmasensis* POE54, prepared as described above. Specifically, seeds were submerged in 20 mL of each cell suspension (approximately 10^7 CFU mL^{-1}). Water-treated seeds were used as controls. The seeds were incubated for 2 h on a rotary shaker (80 rpm, 25 °C) to allow bacterial adhesion to the seed surface. Following incubation, the excessive bacterial inoculum was removed using sterile filter paper, and the seeds were immediately sown in plastic pots (Ø 16 cm), each containing a 1:1 (v/v) mixture of soil and sand to reduce the

naturally occurring phosphorus content. The final concentration of available phosphorus in the soil was 50 ppm as determined using the Olsen method (Olsen et al, 1954).

3.5.3.2 Experimental design

The experiment was conducted under greenhouse conditions from June to July 2024 and included a total of 15 conditions, as shown in Table 3.2. Inoculated seeds were grown: i) without any P supplementation; ii) with P supplementation as insoluble rock phosphate (RP); iii) with P supplementation as soluble KH_2PO_4 (K). Uninoculated controls were also included (CTRL; Table 3.2). Each treatment included 8 independent biological replicates. Bacterial suspensions were applied to the soil every 10-14 days at 10^6 CFU/mL for a total of 4 applications (Table 3.3). Hoagland solution was applied to the soil every 7-10 days (Table 3.3). Foliar applications of Ca and Mg were carried out twice (July 4 and 12) during the experiment.

The pots were setup in a completely randomized design, and the plants were grown under greenhouse conditions (day/night temperature 28 °C/18 °C; humidity 50−60%; day length 14 h) for 60 days and watered when necessary.

Table 3.2. List of experimental conditions applied to tomato plants grown in pots under greenhouse conditions (Experiment I).

Condition	Bacterial strain	Inoculation	Phosphorus source	P form	P Dose
CTRL	None	–	None	–	–
RP	None	–	Rock phosphate	Insoluble	34–68 mg /pot
K	None	–	KH_2PO_4	Soluble	1 M
PSE	*P. putida* RPT12	+	None	–	–
PSE+RP	*P. putida* RPT12	+	Rock phosphate	Insoluble	34–68 mg /pot
PSE+K	*P. putida* RPT12	+	KH_2PO_4	Soluble	1 M
MEGA	*B. megaterium* FBM09	+	None	–	–
MEGA+RP	*B. megaterium* FBM09	+	Rock phosphate	Insoluble	34–68 mg /pot
MEGA+K	*B. megaterium* FBM09	+	KH_2PO_4	Soluble	1 M
PUMI	*B. pumilus* FBP01	+	None	–	–
PUMI+RP	*B. pumilus* FBP01	+	Rock phosphate	Insoluble	34–68 mg /pot
PUMI+K	*B. pumilus* FBP01	+	KH_2PO_4	Soluble	1 M
PO	*P. salmasensis* POE54	+	None	–	–
PO+RP	*P. salmasensis* POE54	+	Rock phosphate	Insoluble	34–68 mg /pot
PO+K	*P. salmasensis* POE54	+	KH_2PO_4	Soluble	1 M

Table 3.3. List of treatments applied to tomato plants grown in pots under greenhouse conditions (Experiment I).

Date	Hoagland solution	Bacterial suspension (10^6 CFU/mL)
June 4	20 ml/plant	20 ml/plant
June 12	50 ml/plant	
June 24	50 ml/plant	50 ml/plant
July 2	100 ml/plant	100 ml/plant
July 8	100 ml/plant	
July 16	100 ml/plant	100 ml/plant

The Hoagland solution was prepared as follows (Hoagland and Arnon, 1938):

- 1 M KH_2PO_4: 1.0 mL/L; when rock phosphate was used as P source (Conditions N. 2, 5, 8, 11, 14; Table 3.2) or P was not supplemented to the soil (conditions N. 1, 4, 7, 10, 13; Table 3.2), KH_2PO_4 was not included in the solution.
- 1 M KNO_3: 5.0 mL/L.
- 1 M $Ca(NO_3)_2 \cdot 4H_2O$: 5.0 mL/L.
- 1 M $MgSO_4 \cdot 7H_2O$: 2.0 mL/L.

In the treatments with insoluble P, granular rock phosphate was applied to the soil together with the Hoagland solution. During the first month, 34 mg of rock phosphate per pot were applied; thereafter, the dose increased to 68 mg per pot. The amount of rock phosphate was calculated to provide the same total phosphorus input as KH_2PO_4. KH_2PO_4 contains 22.76% P, whereas rock phosphate contains 22% P_2O_5, corresponding to an effective phosphorus content of 9.6%. Accordingly, 34 mg of rock phosphate supplied an amount of phosphorus equivalent to that provided by 50 mL of Hoagland solution containing 1 mL/L KH_2PO_4. Each pot contained approximately 5 kg of soil, allowing the estimation of phosphorus input on a soil weight basis.

3.5.3.3 Sample Collection and Analysis

After two months, plants were harvested. Roots were carefully washed to remove soil particles, and air dried. The following biometric parameters were measured: plant height, fresh weight of the root system and shoot, number of leaves, and stem diameter. Plant material was then oven-dried at 50 °C until constant weight was reached.

Then, samples were finely ground using a laboratory mixer and passed through a sieve. Total phosphorus content was determined on three plants per condition. For each sample, 300 mg of dry material were weighed and transferred into Teflon digestion vessels. Subsequently, 3 mL of 67% nitric acid were added. The vessels were hermetically sealed and placed in a microwave digestion system (TANK eco Microwave Digestion/Extraction System, Sineo Microwave Chemistry Technology Co., Ltd.), using the following program: (I) initial ramp to 120 °C for 5 min; (II) ramp from 120 to 200 °C for 10 min; (III) hold at 200 °C for 15 min. After digestion, samples were allowed to cool for approximately 1 hour, then transferred under a fume hood to evaporate excess acid. Finally, the solutions were brought to a final volume of 25 mL, transferred into appropriate containers, and stored at 4 °C.

An aliquot (1.0 mL) of the mineralized sample was transferred into a 50 mL volumetric flask containing 10 mL of deionized water. Two drops of phenolphthalein indicator were added (colorless under acidic conditions). The solution was neutralized by adding sodium hydroxide (NaOH) dropwise until the appearance of a faint, persistent pink coloration. In cases of over-neutralization, the pH was carefully adjusted by dropwise addition of sulfuric acid (H_2SO_4). Subsequently, 10 mL of the colorimetric reagent were added, and ultrapure

water was used to bring the volume to approximately 45 mL. After allowing the reaction to proceed for 2 h at room temperature, the solution was diluted to the final volume (50 mL) with ultrapure water and thoroughly mixed. Phosphate concentration was determined spectrophotometrically using a modified molybdenum blue method based on Murphy and Riley (1962) and adapted from Hurtado et al. (2008). Absorbance was measured at 720 nm using a UV–Vis spectrophotometer.

3.5.4 In vivo *assay on tomato (*Solanum lycopersicum *L.) plants – Experiment II*

3.5.4.1 Plant material and experimental conditions

A second experiment was conducted on tomato plants (*Solanum lycopersicum* L., hybrid cv. Tydona) that were grown in a tunnel greenhouse for 90 days from May to August 2024. Seedlings were treated with the same bacterial cell suspensions as described in Experiment I. Three-week-old seedlings were transplanted into plastic pots (Ø 28 cm), each containing the same soil-sand mixture described in Experiment 1. The experimental design included 15 conditions, as reported previously in Table 3.2. For each condition, eight biological replicates were included. The pots were arranged randomly in a tunnel greenhouse and watered when necessary.

Prior to transplant, seedlings were inoculated with bacterial cell suspensions (10^6 CFU mL^{-1}) by root dipping. Water-treated seedlings served as controls. After approximately 30 minutes, seedlings were transplanted into pots. Subsequently, plants were subjected to the treatments, as described in Table 3.4. Foliar applications of Ca and Mg were carried out twice (July 4 and 12) during the experiment.

Table 3.4. List of treatments applied to tomato plants grown in a tunnel greenhouse for 90 days (Experiment II).

Date	Hoagland solution	Bacterial suspension (10^6 CFU/mL)
June 4	50 ml/plant	50 ml/plant
June 12	50 ml/plant	
June 24	100 ml/plant	50 ml/plant
July 2	100 ml/plant 2X*	100 ml/plant
July 8	100 ml/plant 2X*	
July 16	100 ml/plant 2X*	200 ml/plant
July 25	100 ml/plant 2X*	
August 1	100 ml/plant 2X*	200 ml/plant

*A double-strength formulation was used, corresponding to a two-fold increase in nutrient concentration compared to the initial solution.

The Hoagland nutrient solution was prepared as described in the previous section. As in the greenhouse trial, in treatments receiving insoluble phosphorus, 33 mg of granular rock phosphate per pot were applied to the soil together with the Hoagland solution during the first 30 days; thereafter, the dose was increased to 68 mg per pot. Each pot contained approximately 12 kg of soil, allowing the estimation of phosphorus input on a soil weight basis.

3.5.4.2 Sample collection and analysis

Approximately three months after transplantation, tomato fruits were harvested in stages starting from July 19 to August 27, for a total of 4 harvests. At each harvest, the entire fruit cluster of each plant was collected. For each cluster, the following parameters were recorded: number of fruits (green and red fruits), total fresh weight, and vertical and horizontal diameters of two representative fruits per plant. In addition, further qualitative parameters were determined on fruits collected from the second cluster only. For each plant, three representative fruits were selected to determine pH using a pH meter (Hanna Instruments HI5222, USA), fresh and dry weight, and soluble solids content (°Brix), measured using a portable refractometer.

3.5.5 In vivo *assay on tomato (*Solanum lycopersicum *L.) plants – Experiment III*

3.5.5.1 Plant material and experimental conditions

In this experiment, tomato plants (*Solanum lycopersicum* cv. ciliegino) were inoculated with the bacterial strains *B. megaterium* FBM09, *B. pumilus* FBP01, *P. putida* RPT12 and *P. salmasensis* POE54 to evaluate their efficacy in promoting plant growth and phosphate solubilization in P-deficient conditions. Bacterial cell suspensions (approximately 10^6 CFU mL^{-1}) were prepared as described above. Three weeks old seedlings were transplanted into 28 cm diameter pots, each containing 12 kg of a 1:1 (v/v) mixture of soil and sand to reduce the naturally occurring phosphorus content. Specifically, the final concentration of available phosphorus in the soil was 10 ppm as determined using the Olsen method (Olsen et al, 1954).

The experiment was conducted in a tunnel greenhouse during the period May–July 2025 and included a total of 10 conditions, as shown in Table 3.5. Plants were grown: i) without any P supplementation, or ii) with P supplementation as insoluble rock phosphate (RP). Uninoculated controls included plants supplemented with KH_2PO_4 (CTRL; Table 3.5) and those supplemented with rock phosphate (RP; Table 3.5). Each treatment included 15 independent biological replicates. Pots were arranged according to a randomized complete block design with three blocks days and watered when necessary.

Table 3.5. List of experimental conditions applied to tomato plants grown in pots under greenhouse conditions (Experiment III).

N.	Treatment	Bacterial strain	Inoculation	Phosphorus source	P form	P Dose
1	CTRL	None	–	KH_2PO_4	–	–
2	RP	None	–	Rock phosphate	Insoluble	1% (w/v)
3	PSE	*P. putida* RPT12	+	None	–	–
4	PSE+RP	*P. putida* RPT12	+	Rock phosphate	Insoluble	1% (w/v)
5	MEGA	*B. megaterium* FBM09	+	None	–	–
6	MEGA+RP	*B. megaterium* FBM09	+	Rock phosphate	Insoluble	1% (w/v)
7	PUMI	*B. pumilus* FBP01	+	None	–	–
8	PUMI+RP	*B. pumilus* FBP01	+	Rock phosphate	Insoluble	1% (w/v)
9	PO	*P. salmasensis* POE54	+	None	–	–
10	PO+RP	*P. salmasensis* POE54	+	Rock phosphate	Insoluble	1% (w/v)

Prior to transplant, seedlings were inoculated with bacterial cell suspensions (10^6 CFU mL^{-1}) by root dipping. Water-treated seedlings served as controls.

Three applications of macronutrients (nitrogen, potassium, and two different forms of phosphorus) were carried out. The first application was performed two days after transplantation, while the remaining two were applied during fruit development, approximately 30 and 60 days after transplantation.

The nitrogen supply was calculated based on the amount of soil per plant. In summary, nutrients (NPK) were applied at rates of:

- 120 mg N kg^{-1} soil,
- 160 mg K kg^{-1} soil,
- 100 mg P kg^{-1} soil.

Phosphorus was applied in two different forms: rock phosphate or a soluble phosphorus source, with each treatment receiving only one phosphorus source, according to the experimental design.

After transplant, plants were subjected to the treatments, as described in Table 3.6. Foliar applications of Ca and Mg were carried out twice (July 2 and 22) during the experiment.

Table 3.6. List of treatments applied to tomato plants grown in a tunnel greenhouse in P-deficient soil (Experiment III).

Date	NPK	Bacterial suspension (10^6 CFU/mL)
May 9	X	
May 12		50 ml/plant
May 26		50 ml/plant
June 5	X	
June 9		50 ml/plant
June 23		100 ml/plant
July 7		100 ml/plant
July 10	X	
July 15		200 ml/plant
July 30		200 ml/plant

3.5.5.2 Sample collection and analysis

Approximately three months after transplantation, tomato fruits were harvested in stages starting from July 07 to August 7, for a total of 4 harvests. At each harvest, the entire fruit cluster of each plant was collected. Sample collection and analyses were carried out as described for Experiment II.

In addition, after the third harvest, four fully expanded true leaves were selected and collected from three plants per condition. Leaf samples were placed in a drying oven until a constant weight was reached. The dried samples were then finely ground and sieved to obtain a homogeneous powder suitable for subsequent analyses. P content was determined spectrophotometrically as described previously (Par. 3.5.3.3).

3.6 Statistical analysis

Data were presented as mean ± standard deviation (SD) of three replicates. Results were analyzed by one-way analysis of variance (ANOVA) using SigmaPlot software (Systat Software Inc., San Jose, CA, USA). Mean comparisons were performed using Bonferroni's post-hoc test. Differences were considered statistically significant at $p \leq 0.05$.

4. RESULTS

4.1 Phenotyping of bacterial species

The selected bacterial isolates were subjected to a comprehensive phenotypic characterization to evaluate their physiological traits and functional potential related to plant growth promotion and phosphorus solubilization. *In vitro* assays were performed to assess their tolerance to abiotic stress, antimicrobial activity against phytopathogens, metabolic versatility, and the production of key functional metabolites such as siderophores.

Salt tolerance was investigated to determine the adaptability of the strains to osmotic stress conditions, while dual culture assays were conducted to evaluate their potential biocontrol activity against major phytopathogenic fungi. Furthermore, metabolic profiling using the BIOLOG™ GEN III system provided insights into substrate utilization patterns and physiological robustness. Functional traits directly associated with plant growth promotion, including siderophore production and phosphate solubilization capacity, were also assessed.

All *Bacillus* strains were Gram-positive rods, while *Pseudomonas* strains were Gram-negative rods, consistent with their taxonomic classification. Colonies showed typical morphology for each genus when grown on nutrient agar.

4.1.1. Salt tolerance

The halotolerance of the bacterial species was evaluated in Nutrient Broth supplemented with increasing NaCl concentrations (0.5, 1, and 1.5 M), using salt-free medium as control. Growth responses at 24 h revealed strain-specific tolerance patterns under osmotic stress.
Bacterial growth was assessed by colony-forming unit (CFU) counts, and the results were expressed using a semi-quantitative scale: (+++) indicating growth comparable to the control, (++) indicating moderate growth reduction, and (+) indicating limited bacterial growth (Table 4.1).
At 24 h, *P. putida* RPT12 showed a slight but significant reduction in cell density with increasing salt concentration, although the growth remained high across all treatments, indicating good tolerance up to 1.5 M NaCl. *B. megaterium* FBM09 exhibited a clear salt-dependent inhibition, with reduced growth starting from 0.5 M NaCl.
In contrast, *B. pumilus* FBP01, *B. subtilis* FBS07, and *B. amyloliquefaciens* FBA21 maintained growth levels comparable to the control even at the highest NaCl concentration tested, confirming strong halotolerance (Table 4.1). Conversely, *P. salmasensis* POE54 was the most sensitive strain, showing a marked and dose-dependent reduction in growth under saline conditions.

Overall, the results indicate a high level of salt tolerance in most of the *Bacillus* species used in this work.

Table 4.1. Evaluation of salt tolerance of *B. amyloliquefaciens* FBA21(AMY), *B. subtilis* FBS07 (SUB), *B. megaterium* FBM09 (MEGA), *B. pumilus* FBP01 (PUMI), *P. putida* RPT12 (PSE), *P. salmasensis* POE54 (PO), grown in nutrient broth (NB) supplemented with 0.5 M, 1 M or 1.5 M NaCl. CTRL= salt-free NB. +++ = high; ++ = moderate; + = limited salt tolerance compared to CTRL.

	AMY	**SUB**	**MEGA**	**PUMI**	**PSE**	**PO**
CTRL	+ + +	+ + +	+ + +	+ + +	+ + +	+ + +
NaCl O.5 M	+ + +	+ + +	+ +	+ + +	+ +	++
NaCl 1 M	+ + +	+ + +	+	+ + +	+	+
NaCl 1.5 M	+ + +	+ + +	+	+ + +	+	+

4.1.2 In vitro *antimicrobial activity against phytopathogenic fungi*

The biocontrol potential of the selected bacterial strains was evaluated *in vitro* by dual culture assays against three major phytopathogenic fungi: *Fusarium oxysporum*, *Alternaria alternata* and *Botrytis cinerea*. The antimicrobial activity was expressed as percentage of radial growth inhibition (PRGI) in presence of the bacterial strain, compared to the mean radial growth of the fungal colony in the control plates (Khamsuk et al., 2024).

The inhibition of *B. cinerea* varied significantly among treatments (Fig. 4.1). The highest PRGI was observed in the *B. amyloliquefaciens* FBA21 treatment (approximately 58%), which was statistically different from all other treatments. *B. subtilis FBS07* also showed a relatively high inhibition (around 55%), although significantly lower than *B. amyloliquefaciens*.

Intermediate inhibition levels were recorded for *B. pumilus* FBP01, *P. salmasensis* POE54 and *P. putida* RPT12 treatments, with values ranging between approximately 44% and 46%. These treatments were not significantly different from each other and were grouped in the same statistical category. The lowest inhibition was observed in the *B. megaterium* FBM09 treatment (approximately 33%), which was significantly lower than all other treatments.

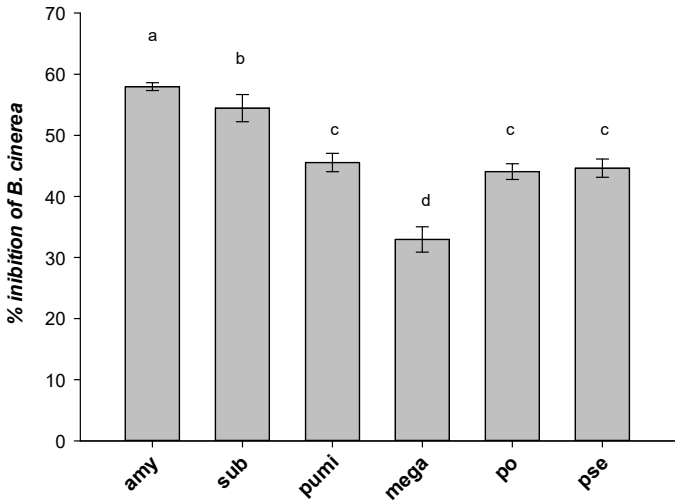

Figure 4.1. Percentage of *B. cinerea* radial growth inhibition (PRGI) observed *in vitro* in presence of different bacterial strains: *B. amyloliquefaciens* FBA21 (amy), *B. subtilis* FBS07 (sub), *B. pumilus* FBP01 (pumi), *B. megaterium* FBM09 (mega), *P. salmasensis* POE54 (po), *P. putida* RPT12 (pse). Different letters indicate statistically significant differences (one-way ANOVA at the 0.05 level of significance).

The growth of *F. oxysporum* was also differently affected by the presence of the bacterial species (Fig. 4.2). The highest inhibition percentages were observed for *Bacillus*

amyloliquefaciens FBA21 and *B. pumilus* FBP01 both showing values of approximately 34–35% and belonging to the same statistical group.

B. subtilis FBS07 exhibited a moderate inhibition effect (around 23%), which was significantly lower than *B. amyloliquefaciens* FBA21 and *B. pumilus* FBP01. In contrast, *Bacillus megaterium* FBM09, *P. salmasensis* POE54, and *P. putida* RPT12 showed very low inhibition percentages (< 5%; fig. 4.2) and were not significantly different from each other.

Overall, the results indicate that *B. amyloliquefaciens* FBA21 and *B. pumilus* FBP01 were the most effective in inhibiting *F. oxysporum*, whereas the other strains exhibited limited or negligible antifungal activity.

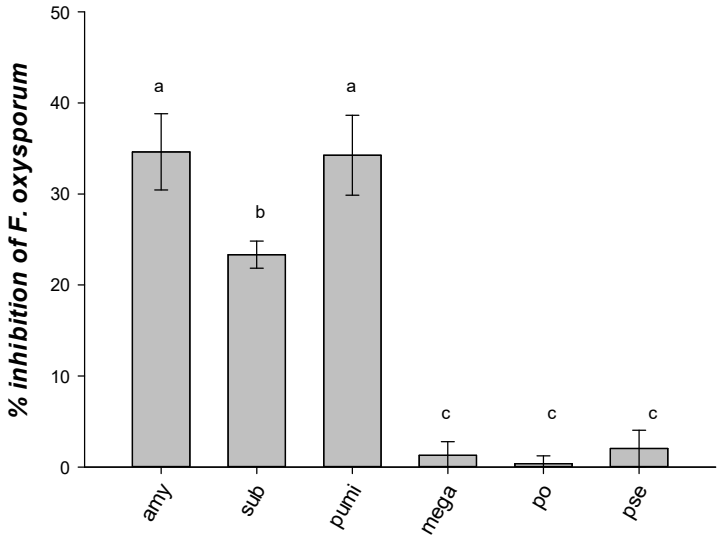

Figure 4.2. Percentage of *F. oxysporum* radial growth inhibition (PRGI) observed *in vitro* in presence of different bacterial strains: *B. amyloliquefaciens* FBA21(amy), *B. subtilis* FBS07 (sub), *B. pumilus* FBP01 (pumi), *B. megaterium* FBM09 (mega), *P. salmasensis* POE54 (po), *P. putida* RPT12 (pse). Different letters indicate statistically significant differences (one-way ANOVA at the 0.05 level of significance).

Similarly, in the case of *A. alternata* the pathogen growth was significantly reduced by the *Bacillus* species (Fig. 4.3). The highest PRGI was observed for *Bacillus amyloliquefaciens*, reaching approximately 54%, and forming a distinct statistical group. *Bacillus subtilis* FBS07 showed a lower but still substantial inhibition (around 45%), significantly different from *B. amyloliquefaciens*. *B. pumilus* FBP01 exhibited intermediate inhibition levels (approximately 40%), forming a separate statistical group. The other bacterial species (*B. megaterium* FBM09*, P. salmasensis* POE54 and *P. putida* RPT12*)* showed limited or no antifungal effect.

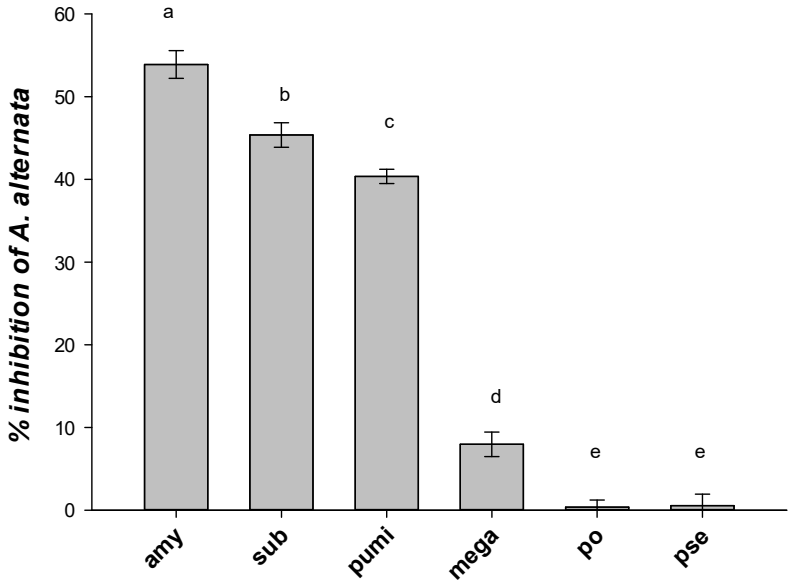

Figure 4.3. Percentage of *A. alternata* radial growth inhibition (PRGI) observed *in vitro* in presence of different bacterial strains: *B. amyloliquefaciens* FBA21(amy), *B. subtilis* FBS07 (sub), *B. pumilus* FBP01 (pumi), *B. megaterium* FBM09 (mega), *P. salmasensis* POE54 (po), *P. putida* RPT12 (pse). Different letters indicate statistically significant differences (one-way ANOVA at the 0.05 level of significance).

4.1.3 Functional characterization of bacterial species

The application of a semi-automated phenotypic/physiological BIOLOG™ system allows the metabolic and physiological characterization of bacterial isolates, ensuring preliminary classification of bacteria into the genus and even to the species level (Wòzniak et al., 2019). After incubation of the GEN III MicroPlates at 33°C, readings were performed at 24 hours. Results were interpreted based on the development of purple coloration in the wells, indicating reduction of tetrazolium dye and therefore metabolic activity of the tested strains.

At 24 hours, purple coloration was already visible in several carbon source wells for all tested isolates. The negative control well (A1) remained colorless, confirming the absence of false-positive reactions.

The results allowed the phenotypic characterization and metabolic profiling of the following bacterial species.

- ***B. amyloliquefaciens***

The isolate exhibited a broad metabolic spectrum, showing positive oxidation (indicated by the development of a purple formazan dye) for a wide range of substrates after 24/48 hours of incubation (Fig. 4.4).

Carbohydrates: The strain showed a high preference for hexoses, pentoses, and disaccharides (Rows A-C), including key sugars such as glucose, fructose, and maltose. This intense metabolic activity suggests efficient enzymatic machinery for complex carbohydrate degradation.

Organic Acids: Positive reactions were recorded for various carboxylic acids and amino acids (Rows E-H). The utilization of substrates like L-alanine (E-3), L-glutamic acid (E-6), and Citric Acid (G-5) highlights the strain's ability to thrive on common root exudates.

Chemical Sensitivity and Stress Tolerance: The profiling confirmed the strain's robustness, showing active growth under acidic conditions pH 6.0 (A-11) and tolerance to salinity (NaCl 1% to 8%, B10-B12).

	1	2	3	4	5	6	7	8	9	10	11	12
A	Negative Control	Dextrin	D-Maltose	D-Trehalose	D-Cellobiose	Gentiobiose	Sucrose	D-Turanose	Stachyose	Positive control	pH 6	pH 5
	-	+	+	+	+	+	+	NB	-	+	+	NB
B	D-Raffinose	α-D-Lactose	D-Melibiose	β-Methyl-D-Glucoside	D-Salicin	N-Acetyl-D-Glucosamine	N-Acetyl-β-D-Mannosamine	N-Acetyl-D-Galactosamine	N-Acetyl Neuraminic Acid	NaCl 1%	NaCl 4%	NaCl 8%
	NB	-	NB	+	+	+	NB	-	-	+	+	+
C	D-Glucose	D-Mannose	D-Fructose	D-Galactose	3 Metil-glucosio	D-Fructose	L-Fucose	L-Rhamnose	Inosine	1% Sodium Lactate	Fusidic Acid	D-Serine
	+	+	+	-	-	NB	NB	NB	-	+	-	-
D	D-Sorbitol	D-Mannitol	D-Arabitol	Myo-Inositol	Glycerol	D-Glucose-6-PO_4	D-Fructose-6-PO_4	D-Aspartic Acid	D-Serine	Troleandomycin	Rifamycin SV	Minocycline
	+	+	-	+	+	NB	NB	+	-	-	-	-
E	Gelatin	Glycyl-L-Proline	L-Alanine	L-Arginine	L-Aspartic Acid	L-Glutamic Acid	L-Histidine	L-Pyroglutamic Acid	L-Serine	Lincomycin	Guanidine HCl	Niaproof 4
	+	+	+	+	+	+	+	NB	NB	-	+	-
F	Pectin	D-Galacturonic Acid	L-Galactonic Acid Lactone	D-Gluconic Acid	D-Glucuronic Acid	Glucuronamide	Mucic Acid	Quinic Acid	D-Saccharic Acid	Vancomycin	Tetrazolium Violet	Tetrazolium Blue
	+	+	+	+	NB	NB	-	+	NB	-	NB	-
G	p-Hydroxyphenylacetic Acid	Methyl Pyruvate	D-Lactic Acid Methyl Ester	L-Lactic Acid	Citric Acid	α-Ketoglutaric Acid	D-Malic Acid	L-Malic Acid	Bromo-succinic Acid	Nalidixic Acid	Lithium Chloride	Potassium Tellurite
	-	+	-	+	+	NB	-	+	+	-	+	+
H	Tween 80	γ-Amino-Butyric Acid	α-Hydroxybutyric Acid	β-Hydroxy-D,L-Butyric Acid	α-Keto-Butyric Acid	Acetoacetic Acid	Propionic Acid	Acetic Acid	Formic Acid	Aztreonam	Sodium Butyrate	Sodium Bromate
	-	NB	-	NB	-	+	-	+	+	NB	+	NB

Figure 4.4. Phenotypic metabolic fingerprint of *B. amyloliquefaciens* FBA21 using the Biolog GEN III MicroPlate system. Legend: + : positive result; - : negative result; NB: weak reaction.

- ***B. pumilus* FBP01**

The metabolic fingerprinting shows a distinct pattern of substrate utilization compared to other isolates (Fig. 4.5).

Metabolic Breadth and Activity: The isolate demonstrated a strong and rapid oxidative response towards a wide array of carbon sources. A dense cluster of positive reactions was observed in columns 2 through 5, indicating an exceptional ability to metabolize various carbohydrates (such as D-Melibiose B-3 and D- Salicin B-5) and amino acids (L-aspartic acid E-5, D-Glucuronic Acid F-5 and Citric Acid G-5).

Chemical Sensitivity: The physiological profile confirmed the strain's resilience to environmental stressors. *B. pumilus* FBP01 exhibited robust growth at acidic pH (6.0) and maintained metabolic activity across a gradient of salinity, 1% NaCl (B-10), 4% NaCl(B-11) and 8% Nacl (B-12). Regarding chemical sensitivity (columns 11-12), the isolate remained sensitive to several inhibitory agents, including Sodium Bromate (H-12), as evidenced by the lack of color development in the respective wells.

	1	2	3	4	5	6	7	8	9	10	11	12
A	Negative Control	Dextrin	D-Maltose	D-Trehalose	D-Cellobiose	Gentiobiose	Sucrose	D-Turanose	Stachyose	Positive control	pH 6	pH 5
	-	+	+	+	+	+	+	+	NB	+	+	NB
B	D-Raffinose	α-D-Lactose	D-Melibiose	β-Methyl-D-Glucoside	D-Salicin	N-Acetyl-D-Glucosamine	N-Acetyl-β-D-Mannosamine	N-Acetyl-D-Galactosamine	N-Acetyl Neuraminic Acid	NaCl 1%	NaCl 4%	NaCl 8%
	NB	NB	+	+	+	+	NB	NB	NB	+	+	+
C	D-Glucose	D-Mannose	D-Fructose	D-Galactose	3 Metil-glucosio	D-Fructose	L-Fucose	L-Rhamnose	Inosine	1% Sodium Lactate	Fusidic Acid	D-Serine
	+	+	+	+	NB	NB	+	+	+	+	-	-
D	D-Sorbitol	D-Mannitol	D-Arabitol	Myo-Inositol	Glycerol	D-Glucose-6-PO_4	D-Fructose-6-PO_4	D-Aspartic Acid	D-Serine	Troleandomycin	Rifamycin SV	Minocycline
	NB	+	NB	NB	+	+	+	+	-	-	-	-
E	Gelatin	Glycyl-L-Proline	L-Alanine	L-Arginine	L-Aspartic Acid	L-Glutamic Acid	L-Histidine	L-Pyroglutamic Acid	L-Serine	Lincomycin	Guanidine HCl	Niaproof 4
	+	NB	+	+	+	+	+	+	NB	NB	+	-
F	Pectin	D-Galacturonic Acid	L-Galactonic Acid Lactone	D-Gluconic Acid	D-Glucuronic Acid	Glucuronamide	Mucic Acid	Quinic Acid	D-Saccharic Acid	Vancomycin	Tetrazolium Violet	Tetrazolium Blue
	+	+	+	+	+	NB	NB	+	NB	-	-	+
G	p-Hydroxyphenylacetic Acid	Methyl Pyruvate	D-Lactic Acid Methyl Ester	L-Lactic Acid	Citric Acid	α-Ketoglutaric Acid	D-Malic Acid	L-Malic Acid	Bromo-succinic Acid	Nalidixic Acid	Lithium Chloride	Potassium Tellurite
	+	+	NB	+	+	+	NB	+	+	-	+	+
H	Tween 80	γ-Amino-Butyric Acid	α-Hydroxybutyric Acid	β-Hydroxy-D,L-Butyric Acid	α-Keto-Butyric Acid	Acetoacetic Acid	Propionic Acid	Acetic Acid	Formic Acid	Aztreonam	Sodium Butyrate	Sodium Bromate
	+	+	-	NB	NB	+	NB	+	-	+	+	-

Figure 4.5. Phenotypic metabolic fingerprint of *B. pumilus* FBP01 using the Biolog GEN III MicroPlate system. Legend: +: positive result; -: negative result; NB: weak reaction.

- ***B. subtilis* FBS07**

The metabolic fingerprinting of *B. subtilis* FBS07 (Figure 4.6) reveals a highly dynamic and selective substrate utilization pattern, clearly distinguishing it from other isolates:

Metabolic Breadth and Activity: The isolate demonstrates a strong oxidative response toward complex sugars and polymers, with robust positive reactions for Dextrin (A-2), D-Maltose (A-3), and Gentiobiose (A-6). However, compared to other strains, it exhibits more pronounced selectivity regarding hexoses: while it readily metabolizes D-Glucose (C-1) and D-Fructose (C-3), it shows negative or negligible responses toward D-Galactose (C-4) and L-Fucose (C-7). Its metabolic efficiency is further highlighted by the strong utilization of amino acids, particularly L-Alanine (E-3), L-Arginine (E-4), and L-Glutamic Acid (E-6).

Chemical Sensitivity and Stress Tolerance: The physiological profile underlines significant environmental robustness. *B. subtilis* FBS07 exhibits exceptional salinity tolerance, maintaining vigorous growth not only at 1% (B-10) and 4% (B-11) but also at 8% NaCl (B-12), suggesting superior osmotic adaptation.

Regarding chemical sensitivity (columns 10-12), the isolate shows marked resistance to Lithium Chloride (G-11) and Sodium Butyrate (H-11), while remaining sensitive to inhibitory agents such as Fusidic Acid (C-11) and Minocycline (D-12), as evidenced by the lack of color development.

	1	2	3	4	5	6	7	8	9	10	11	12
A	Negative Control	Dextrin	D-Maltose	D-Trehalose	D-Cellobiose	Gentiobiose	Sucrose	D-Turanose	Stachyose	Positive control	pH 6	pH 5
	-	+	+	+	+	+	+	+	NB	+	+	NB
B	D-Raffinose	α-D-Lactose	D-Melibiose	β-Methyl-D-Glucoside	D-Salicin	N-Acetyl-D-Glucosamine	N-Acetyl-β-D-Mannosamine	N-Acetyl-D-Galactosamine	N-Acetyl Neuraminic Acid	NaCl 1%	NaCl 4%	NaCl 8%
	+	+	NB	+	+	+	NB	-	-	+	+	+
C	D-Glucose	D-Mannose	D-Fructose	D-Galactose	3 Metil-glucosio	D-Fructose	L-Fucose	L-Rhamnose	Inosine	1% Sodium Lactate	Fusidic Acid	D-Serine
	+	+	+	-	-	-	-	-	NB	+	-	-
D	D-Sorbitol	D-Mannitol	D-Arabitol	Myo-Inositol	Glycerol	D-Glucose-6-PO_4	D-Fructose-6-PO_4	D-Aspartic Acid	D-Serine	Troleandomycin	Rifamycin SV	Minocycline
	+	+	NB	+	-	NB	NB	+	-	-	-	-
E	Gelatin	Glycyl-L-Proline	L-Alanine	L-Arginine	L-Aspartic Acid	L-Glutamic Acid	L-Histidine	L-Pyroglutamic Acid	L-Serine	Lincomycin	Guanidine HCl	Niaproof 4
	NB	+	+	+	+	+	+	+	NB	-	+	-
F	Pectin	D-Galacturonic Acid	L-Galactonic Acid Lactone	D-Gluconic Acid	D-Glucuronic Acid	Glucuronamide	Mucic Acid	Quinic Acid	D-Saccharic Acid	Vancomycin	Tetrazolium Violet	Tetrazolium Blue
	+	+	+	+	NB	-	NB	+	NB	-	-	-
G	p-Hydroxyphenylacetic Acid	Methyl Pyruvate	D-Lactic Acid Methyl Ester	L-Lactic Acid	Citric Acid	α-Ketoglutaric Acid	D-Malic Acid	L-Malic Acid	Bromo-succinic Acid	Nalidixic Acid	Lithium Chloride	Potassium Tellurite
	-	+	NB	+	+	NB	-	+	+	-	+	+
H	Tween 80	γ-Amino-Butyric Acid	α-Hydroxybutyric Acid	β-Hydroxy-D,L-Butyric Acid	α-Keto-Butyric Acid	Acetoacetic Acid	Propionic Acid	Acetic Acid	Formic Acid	Aztreonam	Sodium Butyrate	Sodium Bromate
	+	NB	-	+	-	+	-	+	+	-	+	NB

Figure 4.6. Phenotypic metabolic fingerprint of *B. subtilis* FBS07 using the Biolog GEN III MicroPlate system. Legend: + : positive result; - : negative result; NB: weak reaction.

- ***B. megaterium* FBM09**

The phenotypic profile of *B. megaterium* FBM09 reflects its reputation as a "giant" of the *Bacillus* genus, not just in size but in its versatile metabolic capabilities, particularly regarding sugar alcohols and organic acids (Fig. 4.7).

Metabolic Breadth and Activity: *B. megaterium* FBM09 shows a very broad carbohydrate utilization range. Strong positive reactions are seen for Dextrin (A-2), D-Maltose (A-3), and Sucrose (A-7). A defining characteristic in this specific profile is its ability to utilize Myo-Inositol (D-4).

This isolate shows a preference for certain sugar alcohols and exhibits metabolic activity in the amino acid sector, specifically L-Alanine (E-3).

Chemical Sensitivity and Resilience: Regarding environmental stress, the strain demonstrated an adaptive capacity to moderately acidic conditions at pH 6 (A-11) and pH 5 (A-12). A similar pattern was observed in response to osmotic stress, where the isolate showed significant resistance to high salt concentrations, managing to proliferate in the presence of 8% NaCl (B-12). These findings delineate a physiological profile characterized by a specific window of environmental tolerance of acidity and salinity.

	1	2	3	4	5	6	7	8	9	10	11	12
A	Negative Control	Dextrin	D-Maltose	D-Trehalose	D-Cellobiose	Gentiobiose	Sucrose	D-Turanose	Stachyose	Positive control	pH 6	pH 5
	-	+	+	+	+	+	+	+	+	+	+	+
B	D-Raffinose	α-D-Lactose	D-Melibiose	β-Methyl-D-Glucoside	D-Salicin	N-Acetyl-D-Glucosamine	N-Acetyl-β-D-Mannosamine	N-Acetyl-D-Galactosamine	N-Acetyl Neuraminic Acid	NaCl 1%	NaCl 4%	NaCl 8%
	+	+	+	+	NB	+	-	-	-	+	+	+
C	D-Glucose	D-Mannose	D-Fructose	D-Galactose	3 Metil-glucosio	D-Fructose	L-Fucose	L-Rhamnose	Inosine	1% Sodium Lactate	Fusidic Acid	D-Serine
	+	-	+	+	-	-	-	-	NB	+	NB	NB
D	D-Sorbitol	D-Mannitol	D-Arabitol	Myo-Inositol	Glycerol	D-Glucose-6-PO_4	D-Fructose-6-PO_4	D-Aspartic Acid	D-Serine	Troleandomycin	Rifamycin SV	Minocycline
	-	+	-	-	+	-	-	-	-	NB	NB	NB
E	Gelatin	Glycyl-L-Proline	L-Alanine	L-Arginine	L-Aspartic Acid	L-Glutamic Acid	L-Histidine	L-Pyroglutamic Acid	L-Serine	Lincomycin	Guanidine HCl	Niaproof 4
	NB	-	+	NB	+	NB	NB	NB	NB	+	NB	NB
F	Pectin	D-Galacturonic Acid	L-Galactonic Acid Lactone	D-Gluconic Acid	D-Glucuronic Acid	Glucuronamide	Mucic Acid	Quinic Acid	D-Saccharic Acid	Vancomycin	Tetrazolium Violet	Tetrazolium Blue
	NB	-	-	+	-	-	-	+	NB	-	NB	NB
G	p-Hydroxyphenylacetic Acid	Methyl Pyruvate	D-Lactic Acid Methyl Ester	L-Lactic Acid	Citric Acid	α-Ketoglutaric Acid	D-Malic Acid	L-Malic Acid	Bromo-succinic Acid	Nalidixic Acid	Lithium Chloride	Potassium Tellurite
	-	+	NB	NB	NB	-	-	NB	NB	NB	+	+
H	Tween 80	γ-Amino-Butyric Acid	α-Hydroxybutyric Acid	β-Hydroxy-D,L-Butyric Acid	α-Keto-Butyric Acid	Acetoacetic Acid	Propionic Acid	Acetic Acid	Formic Acid	Aztreonam	Sodium Butyrate	Sodium Bromate
	+	+	NB	+	NB	-	NB	NB	NB	NB	+	+

Figure 4.7. Phenotypic metabolic fingerprint of *B. megaterium* FBM09 using the Biolog GEN III MicroPlate system. Legend: + : positive result; - : negative result; NB: weak reaction.

- ***Pseudomonas salmasensis* POE54**

The Biolog GEN III microplate analysis for the isolate showed a different metabolic spectrum, compared to the *Bacillus* species analysed in the present work (Fig. 4.8).

Metabolic Breadth and Substrate Preference: Unlike the *Bacillus* isolates, *P. salmasensis* POE54 exhibited a more selective carbon source utilization. A significant number of negative reactions (colorless wells) were observed in the carbohydrate and hexose sectors (Rows A-B). In contrast, the strain showed strong metabolic activity (intense purple coloration) for organic acids and amino acids (Rows C-H). Specifically, the rapid oxidation of substrates such as Citric Acid (G-5), L-Lactic Acid (G-4) and D-Glucuronic Acid (F-5) suggests a metabolism highly optimized for the Krebs cycle intermediates typically found in plant root environments.

Chemical Sensitivity: Despite a broad metabolic potential, the isolate exhibited low tolerance to salinity. This was evidenced by absent coloration in wells C-10 (4% NaCl), and D-10 (8% NaCl). Based on the Biolog GEN III map, the strain remained active in the presence of Rifamycin SV (D-11), Lincomycin (E-10) and Vancomycin (F-10). The isolation also showed resistance to selective agents such as Potassium Tellurite (G-12).

	1	2	3	4	5	6	7	8	9	10	11	12
A	Negative Control	Dextrin	D-Maltose	D-Trehalose	D-Cellobiose	Gentiobiose	Sucrose	D-Turanose	Stachyose	Positive control	pH 6	pH 5
	-	-	-	NB	-	-	-	-	-	+	+	+
B	D-Raffinose	α-D-Lactose	D-Melibiose	β-Methyl-D-Glucoside	D-Salicin	N-Acetyl-D-Glucosamine	N-Acetyl-β-D-Mannosamine	N-Acetyl-D-Galactosamine	N-Acetyl Neuraminic Acid	NaCl 1%	NaCl 4%	NaCl 8%
	-	-	-	-	-	-	-	-	-	+	-	-
C	D-Glucose	D-Mannose	D-Fructose	D-Galactose	3 Metil-glucosio	D-Fructose	L-Fucose	L-Rhamnose	Inosine	1% Sodium Lactate	Fusidic Acid	D-Serine
	+	+	NB	+	-	NB	NB	NB	+	+	-	-
D	D-Sorbitol	D-Mannitol	D-Arabitol	Myo-Inositol	Glycerol	D-Glucose-6-PO_4	D-Fructose-6-PO_4	D-Aspartic Acid	D-Serine	Troleandomycin	Rifamycin SV	Minocycline
	NB	NB	NB	+	NB	-	NB	-	NB	+	+	-
E	Gelatin	Glycyl-L-Proline	L-Alanine	L-Arginine	L-Aspartic Acid	L-Glutamic Acid	L-Histidine	L-Pyroglutamic Acid	L-Serine	Lincomycin	Guanidine HCl	Niaproof 4
	-	-	+	+	NB	+	+	+	+	+	NB	+
F	Pectin	D-Galacturonic Acid	L-Galactonic Acid Lactone	D-Gluconic Acid	D-Glucuronic Acid	Glucuronamide	Mucic Acid	Quinic Acid	D-Saccharic Acid	Vancomycin	Tetrazolium Violet	Tetrazolium Blue
	-	+	+	+	+	+	+	+	+	+	+	+
G	p-Hydroxyphenylacetic Acid	Methyl Pyruvate	D-Lactic Acid Methyl Ester	L-Lactic Acid	Citric Acid	α-Ketoglutaric Acid	D-Malic Acid	L-Malic Acid	Bromo-succinic Acid	Nalidixic Acid	Lithium Chloride	Potassium Tellurite
	+	NB	-	+	+	NB	-	+	NB	-	-	+
H	Tween 80	γ-Amino-Butyric Acid	α-Hydroxybutyric Acid	β-Hydroxy-D,L-Butyric Acid	α-Keto-Butyric Acid	Acetoacetic Acid	Propionic Acid	Acetic Acid	Formic Acid	Aztreonam	Sodium Butyrate	Sodium Bromate
	-	NB	-	+	-	-	+	+	-	-	-	-

Figure 4.8. Phenotypic metabolic fingerprint of *P. salmasensis* POE54 using the Biolog GEN III MicroPlate system. Legend: +: positive result; -: negative result; NB: weak reaction

- ***Pseudomonas putida* RPT12**

Finally, Fig. 4.9 shows the phenotypic metabolic fingerprint of *P. putida RPT12*.

Metabolic Breadth and Activity: The metabolic fingerprint of *P. putida* RPT12 reveals a highly specialized substrate utilization pattern, primarily oriented toward organic acids and amino acids rather than complex carbohydrates. The isolate exhibited an oxidative preference for various carboxylic acids, such as D-Gluconic Acid (C-1), Citric Acid (G-5), and L-Malic Acid (G-7), as well as a broad spectrum of amino acids including L-Alanine (E-3), L-Arginine (E-4), and L-Histidine (E-7). Conversely, carbohydrate metabolism was notably restricted; while the isolate successfully metabolized D-Glucose, it showed no metabolic activity toward most sugars, including D-Maltose (A-3), and Sucrose (A-7), which is consistent with the non-fermentative nature of the genus *Pseudomonas.*

Chemical Sensitivity and Physiological Resilience: The isolate demonstrated a unique chemical sensitivity profile characterized by resilience to several inhibitory agents. *P. putida* RPT12 showed metabolic activity in the presence of Vancomycin (F-10), Troleandomycin (D-10), and Guanidine HCl (E-11), indicating intrinsic resistance to these compounds. Regarding environmental stress, the strain exhibited significant resilience to acidic conditions, maintaining growth at both pH 6 (A-11) and pH 5 (A-12).

	1	2	3	4	5	6	7	8	9	10	11	12
A	Negative Control	Dextrin	D-Maltose	D-Trehalose	D-Cellobiose	Gentiobiose	Sucrose	D-Turanose	Stachyose	Positive control	pH 6	pH 5
	-	NB	-	-	-	-	-	-	-	+	+	+
B	D-Raffinose	α-D-Lactose	D-Melibiose	β-Methyl-D-Glucoside	D-Salicin	N-Acetyl-D-Glucosamine	N-Acetyl-β-D-Mannosamine	N-Acetyl-D-Galactosamine	N-Acetyl Neuraminic Acid	NaCl 1%	NaCl 4%	NaCl 8%
	-	-	-	-	-	-	-	-	-	+	NB	NB
C	D-Glucose	D-Mannose	D-Fructose	D-Galactose	3 Metil-glucosio	D-Fructose	L-Fucose	L-Rhamnose	Inosine	1% Sodium Lactate	Fusidic Acid	D-Serine
	+	-	NB	-	-	NB	NB	-	-	+	NB	+
D	D-Sorbitol	D-Mannitol	D-Arabitol	Myo-Inositol	Glycerol	D-Glucose-6-PO_4	D-Fructose-6-PO_4	D-Aspartic Acid	D-Serine	Troleandomycin	Rifamycin SV	Minocycline
	-	-	-	-	NB	-	NB	-	+	+	+	-
E	Gelatin	Glycyl-L-Proline	L-Alanine	L-Arginine	L-Aspartic Acid	L-Glutamic Acid	L-Histidine	L-Pyroglutamic Acid	L-Serine	Lincomycin	Guanidine HCl	Niaproof 4
	-	-	+	+	+	+	+	-	+	+	+	NB
F	Pectin	D-Galacturonic Acid	L-Galactonic Acid Lactone	D-Gluconic Acid	D-Glucuronic Acid	Glucuronamide	Mucic Acid	Quinic Acid	D-Saccharic Acid	Vancomycin	Tetrazolium Violet	Tetrazolium Blue
	-	+	+	NB	+	+	+	+	+	+	+	+
G	p-Hydroxyphenylacetic Acid	Methyl Pyruvate	D-Lactic Acid Methyl Ester	L-Lactic Acid	Citric Acid	α-Ketoglutaric Acid	D-Malic Acid	L-Malic Acid	Bromo-succinic Acid	Nalidixic Acid	Lithium Chloride	Potassium Tellurite
	NB	NB	-	+	+	NB	+	+	NB	-	NB	-
H	Tween 80	γ-Amino-Butyric Acid	α-Hydroxybutyric Acid	β-Hydroxy-D,L-Butyric Acid	α-Keto-Butyric Acid	Acetoacetic Acid	Propionic Acid	Acetic Acid	Formic Acid	Aztreonam	Sodium Butyrate	Sodium Bromate
	NB	+	-	NB	-	-	-	NB	NB	-	-	-

Figure 4.9. Phenotypic metabolic fingerprint of *P. putida* RPT12 using the Biolog GEN III MicroPlate system. Legend: +: positive result; -: negative result; NB: weak reaction.

4.1.4 Production of iron-chelating compounds

The screening for siderophore production revealed a high frequency of producers among the tested isolates, with varying degrees of efficiency. The qualitative CAS-agar assay (Tab. 4.2) provided an initial assessment of the iron-chelating capacity based on the formation of orange-yellow halos.

P. putida RPT12 and *P. salmasensis* POE54 showed the highest qualitative activity, producing wide and bright halos. Conversely, the *Bacillus* species (*B. subtilis* FBS07*, B. amyloliquefaciens, B. pumilus* FBP01) yielded only weak reactions (Score 1), and no halo was detected for *B. megaterium* FBM09.

Table 4.2. Qualitative assessment of siderophore production on CAS-agar plates. The iron-chelating activity was evaluated based on the diameter and intensity of the color change (from blue to orange/yellow) around the bacterial colonies. The scoring system is defined as follows: (0) Negative, no halo; (1) Weak; (2) Moderate; (3) Strong. Results represent the average of three independent replicates.

Bacterial species	**Siderophore production (Score)**
B. amyloliquefaciens	1
***B. subtilis* FBS07**	1
***B. pumilus* FBP01**	1
***B. megaterium* FBM09**	0
***P. putida* RPT12**	3
***P. salmasensis* POE54**	3

The quantitative analysis through the CAS-shuttle assay provided a precise measurement of the iron-sequestering efficiency in liquid culture supernatants. The results, expressed as a percentage of Siderophore Units (SU%), are detailed in Table 4.3.

While *P. putida* RPT12 showed the highest production (32.7%), *B. subtilis* FBS07 and *B. pumilus* FBP01 showed surprisingly high quantitative values (>30%), in contrast with their weak performance on solid agar. Conversely, *P. salmasensis* POE54, despite its strong qualitative halo, yielded the lowest quantitative percentage (11.6%).

Table 4.3. Quantitative estimation of siderophores in cell-free supernatants using the CAS-shuttle assay. Data represents the mean standard deviation of three independent biological replicates (n=3). Different lowercase letters indicate statistically significant differences between the isolates according to Bonferroni test ($p < 0.05$).

Bacterial species	Siderophore Units (%)
P. putida **RPT12**	32.7 ± 1.2 a
B. subtilis **FBS07**	31.7 ± 1.5 a
B. pumilus **FBP01**	30.5 ± 1.1 a
B. amyloliquefaciens **FBA21**	21.1 ± 1.2 b
B. megaterium **FBM09**	19.6 ± 1.3 b
P. salmasensis **POE54**	11.6 ± 0.6 c

4.1.5 In vitro *phosphate-solubilizing ability*

Phosphate solubilization was evaluated on two solid media, PVK and NBRIP, both containing with $Ca_3(PO_4)_2$ as the sole inorganic phosphorus source. From 3 to 9 days of incubation, halo formation was observed exclusively in *Pseudomonas salmasensis* POE54, *Bacillus pumilus* FBP01 and *Pseudomonas putida* RPT12, indicating their ability to solubilize tricalcium phosphate (Fig. 4.10). No detectable halo was observed for *Bacillus megaterium* FBM09, *Bacillus subtilis* FBS07, or *Bacillus amyloliquefaciens* FBA21 on either medium.

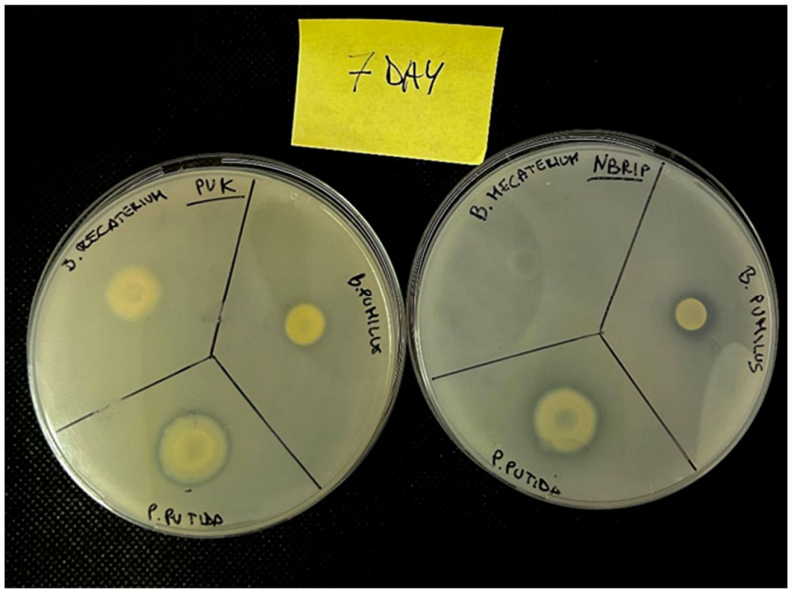

Figure 4.10. Phosphate solubilization on solid media inoculated with *B. megaterium* FBM09*, B. pumilus* FBP01 and *P. putida* RPT12, after 7 days of incubation. Left: Pikovskaya's (PVK) agar medium. Right: National Botanical Research Institute's phosphate growth medium (NBRIP).

For the strains exhibiting phosphate solubilization, the Solubilization Index (SI) and Solubilization Efficiency (SE) were calculated for both growth media. The Solubilization Index (SI) considers both the colony diameter and the diameter of the surrounding halo, thereby reflecting the overall phosphate-solubilizing capacity. In contrast, the Solubilization Efficiency (SE) represents the ratio between the halo diameter and the colony diameter, providing a measure of the relative effectiveness of phosphate solubilization in relation to bacterial growth.

Among the tested strains, *Pseudomonas salmasensis* POE54*, Bacillus pumilus* FBP01, and *Pseudomonas putida* RPT12 produced visible halo zones surrounding the colonies, indicating their ability to solubilize tricalcium phosphate. Both parameters increased progressively over the incubation period for the three solubilizing strains. Across all time points, SI values were significantly higher in NBRIP medium compared to PVK (Fig. 4.11 A). At the end of incubation, the highest SI values were recorded in NBRIP for all three strains, with *Pseudomonas salmasensis* POE54 (1.95) showing the greatest solubilization index, followed by *Bacillus pumilus* FBP01 (1.9) and *Pseudomonas putida* RPT12 (1.4).

A similar trend was observed for SE (Fig. 4.11 B). Solubilization efficiency was consistently higher in NBRIP than in PVK, with statistically significant differences detected up to day 3-9. The greatest SE values were observed in *Pseudomonas salmasensis* POE54, whereas

Bacillus pumilus FBP01 and *Pseudomonas putida* RPT12 exhibited comparatively lower, yet measurable, efficiencies.

Overall, NBRIP medium promoted greater halo formation and higher SI and SE values compared to PVK.

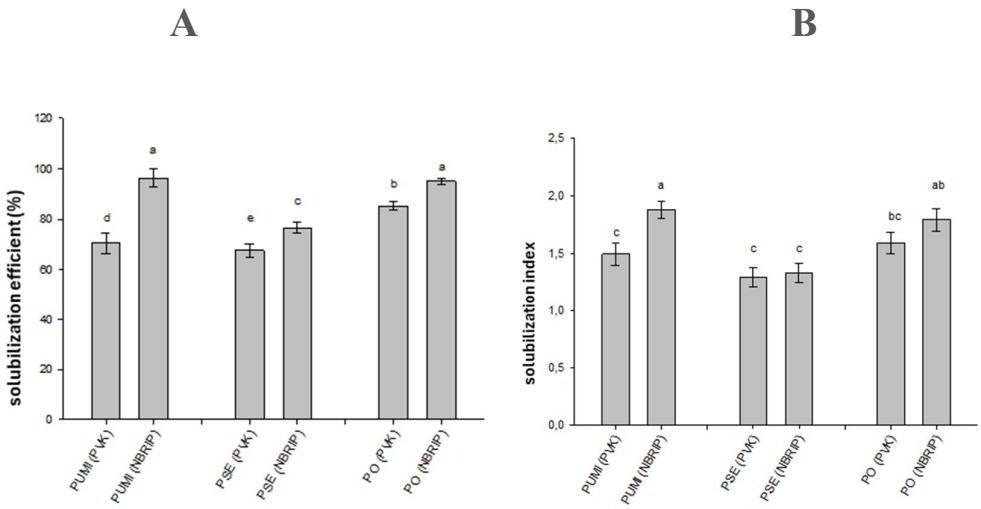

Figure 4.11. (A) Solubilization Efficient (SI) and (B) Solubilization Index (SE) of *Bacillus pumilus* FBP01 (PUMI), *Pseudomonas putida* RPT12 (PSE), and *P. salmasensis POE54* (PO) grown on Pikovskaya's (PVK) agar medium and National Botanical Research Institute's phosphate growth medium (NBRIP), containing calcium phosphate ($Ca_3(PO_4)_2$) as insoluble inorganic phosphorus source.

4.1.6 Bacterial growth in presence of Rock Phosphate (RP)

The growth of bacterial species was monitored for 48h in both standard PVK (containing KH_2PO_4 as P source) and a modified PVK medium (containing phosphorite or rock phosphate as P source). Bacterial growth was quantified as log CFU mL^{-1} (Fig. 4.12).

In both conditions, strains *P. salmasensis* POE54 and *P. putida* RPT12 exhibited the highest growth rates, reaching the stationary phase between 16 and 19 hours and achieving maximum cell densities of approximately 9.5 log CFU/mL. *B. pumilus* FBP01 showed a strong performance in standard PVK, reaching its peak growth after 24 hours before experiencing a slight decline after 48 hours of incubation; however, in PVK+RP medium, it demonstrated a more stable and sustained growth profile.

A notable divergence was observed in the performance of *B. megaterium* FBM09: in standard PVK, it showed a steady and gradual increase, whereas in PVK+RP, it underwent a significant lag or deceleration between 12 and 19 hours before exhibiting a sharp exponential surge to surpass 8.5 log CFU/mL by the 24-hour mark, suggesting a specific metabolic adaptation to the added phosphorus. *B. amyloliquefaciens* FBA21 and *B. subtilis* FBS07 displayed the most stable and reproducible kinetics, maintaining a consistent plateau near 8 log CFU/mL regardless of the medium composition.

Overall, these results indicate that while *P. salmasensis* POE54 and *P. putida* RPT12 are the most robust candidates for biomass production, the phosphorus-enriched medium significantly improves the stability of strains like *B. pumilus* FBP01 and modulates the adaptive responses of others like *B. megaterium* FBM09 (Fig. 4.12). Statistical analysis revealed no significant differences in growth between PVK complete medium (with soluble phosphorus) and PVK substituted with phosphorite for any of the tested strains. The only exception was *Bacillus pumilus* FBP01, which exhibited a significantly higher cell density in PVK+RP after 19 h of incubation (Fig. 4.12).

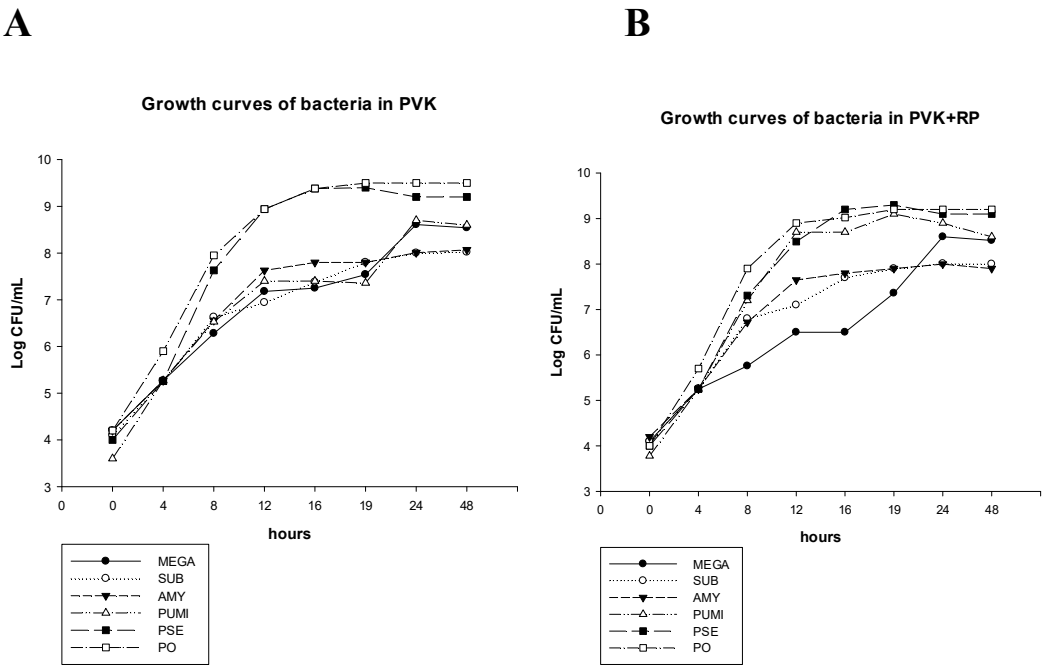

Figure 4.12. Growth curves of bacteria *B. megaterium* FBM09 (MEGA). *B. subtilis* FBS07 (SUB), *B. amyloliquefaciens* FBA21(AMY), *B. pumilus* FBP01 (PUMI), *P. putida* RPT12 (PSE), *P. salmasensis* POE54 (PO) in PVK medium (A) and PVK modified by the addiction of rock phosphate, RP (B), from 0 to 48 hours.

4.2 Determination of bacterial P-solubilizing ability

In presence of rock phosphate as insoluble inorganic phosphorus (P) source, the highest soluble P concentrations were obtained with the same three strains that had previously induced a marked decrease in pH, namely *P. putida* RPT12, *B, pumilus* FBP01, and *B. megaterium* FBM09. The P concentrations (mg L^{-1}) measured in the culture supernatants were 11.56, 10.02, and 8.12, respectively (Table 4.4).

In contrast, the uninoculated control containing phosphorite alone showed only 0.02 mg L^{-1} of soluble phosphorus, indicating minimal abiotic solubilization. Compared with this control, the presence of *P. putida* RPT12, *B. pumilus* FBP01, and *B. megaterium* FBM09 resulted in an approximately 578-fold, 501-fold, and 406-fold increase in soluble phosphorus concentration, respectively, clearly demonstrating their strong phosphorite-solubilizing capacity.

All the other tested strains also showed phosphorus concentrations higher than the abiotic control, indicating some degree of phosphorite solubilization; however, the increases were minimal compared to those observed for the three most effective strains.

Table 4.4. Evaluation of rock phosphate (RP) solubilization after 7 days of incubation of bacterial strains in NBRIP medium containing 1% RP (w/v) as the sole phosphorus source. The control represents the uninoculated medium. Different letters indicate values that are significantly different according to one-way ANOVA followed by Bonferroni multiple comparison test ($p < 0.05$).

Conditions	Phosphorus Concentration (mg/L)
***P. putida* RPT12**	11.56 ± 0.35 a
***B. pumilus* FBP01**	10.02 ± 0.27 b
***B. megaterium* FBM09**	8.12 ± 0.29 b
***B. subtilis* FBS07**	0.39 ± 0.08 c
***B. amyloliquefaciens* FBA21**	0.39 ± 0.09 c
Uninoculated control	0.029 ± 0.0005 c

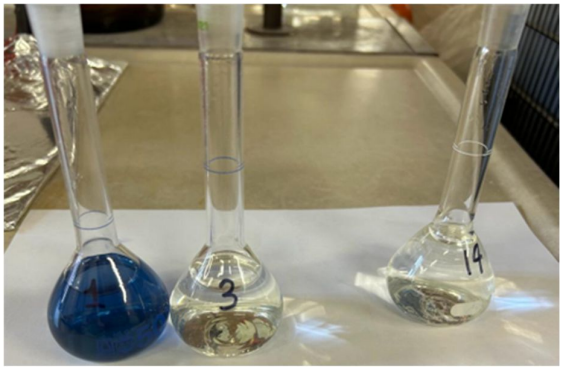

Figure 4.13. Visual assessment of bacterial P-solubilizing ability in presence of rock phosphate (RP) as insoluble inorganic P source. The blue color observed in the flasks is indicative of soluble phosphorus released from RP and corresponds to the chromogenic reaction quantified by UV–visible spectrophotometry. Flask 1: *Pseudomonas putida* RPT12; Flask 3: *Bacillus subtilis* FBS07; Flask 14: uninoculated control.

To investigate whether organic acid production contributed to the solubilization of inorganic phosphate, the pH of the growth medium was measured seven days after inoculation and compared with uninoculated controls containing only phosphorite. In addition, a control medium supplemented with soluble phosphorus in the form of KH_2PO_4 was included, which showed a final pH of approximately 4.

Among the six strains tested, *Pseudomonas putida* RPT12, *Bacillus megaterium* FBM09, and *Bacillus pumilus* FBP01 exhibited the most pronounced reductions in pH, indicating strong acidifying activity likely associated with the production of organic acids. Specifically, *P. putida* RPT12 caused a pH decrease of 3.3 units compared to the control, *B. megaterium* FBM09 decreased the pH by 3.2 units, and *B. pumilus* FBP01 by 2.7 units (Tab. 4.5). These results suggest that these three strains are highly effective in solubilizing insoluble inorganic phosphate under experimental conditions.

In contrast, the remaining three strains showed significantly smaller decreases in pH, with values ranging from approximately 1.2 to 1.5 units. This lower acidification suggests a correspondingly lower capacity for phosphate solubilization, likely reflecting reduced organic acid production. The observed differences in pH reduction among all six strains indicate that the efficiency of phosphate solubilization is closely linked to the quantity and possibly the type of organic acids produced by each bacterium.

Table 4.5. pH values measured in the culture medium after 7 days of incubation of bacterial strains in NBRIP medium containing 1% (w/v) rock phosphate (RP) as the only phosphorus source. Ctrl: uninoculated control; Amy: *Bacillus amyloliquefaciens*; Sub: *B. subtilis* FBS07; Mega: *B. megaterium* FBM09; Pumi: *B. pumilus* FBP01; Po: *Pseudomonas salmasensis* POE54; Pse: *P. putida* RPT12. Different letters indicate values that are significantly different according to one-way ANOVA followed by Bonferroni multiple comparison test ($p < 0.05$).

	Ctrl	Amy	Sub	Mega	Pumi	Po	Pse
NBRIP + RP	**8.0 *a***	**6.8±0.2 *b***	**6.5±0.1 *b***	**4.8±0.2 *d***	**5.3±0.15 *c***	**6.2±0,1 *b***	**4.7±0.1 *d***

4.3. Metabolite profiling of phosphorus-solubilizing bacteria by GC–MS analysis

Among the species used in the present work, four bacterial strains showing the highest phosphorus solubilization activity (*Bacillus megaterium* FBM09*, Bacillus pumilus* FBP01*, Pseudomonas putida* RPT12 and *Pseudomonas salmasensis POE54*), were selected for further analysis. The aim of this experiment was to investigate their metabolic activity under different insoluble phosphorus sources and to characterize the metabolites potentially involved in phosphorus solubilization.

A Principal Component Analysis (PCA) was performed on the metabolites identified via GC-MS across the eight experimental groups. This unsupervised multivariate approach was

employed to simplify the complexity of the metabolomic dataset, allowing for the identification of major patterns, clusters, and outliers. By simplifying the dataset, we aimed to determine the relative influence of two main factors: the innate biological identity of the bacterial strains and the physiological impact of phosphorus (P) supplementation.

PCA revealed distinct clustering patterns based on both strain identity and phosphorus availability (Fig. 4.14). PC1 and PC2 explained 30.9% and 10.1% of the total variance, respectively. PC1 emerged as the primary source of variance, discriminating against the samples mainly by bacterial strain and, to a lesser extent, by the phosphorus source. The metabolic response to phosphorus was most evident in the *B. megaterium* FBM09 (MEGA) strain, where the presence of rock phosphate (MEGA_P) shifted significantly toward the positive axis of PC1, while in presence of tricalcium phosphate samples grouped on the negative side. Similarly, *P. putida* RPT12 (PSE) and *B. pumilus* FBP01 (PUMI) exhibited clear distributional shifts: the *P. putida* RPT12 profile moved from the center-left region to the lower-right quadrant for *P. putida* RPT12 with rock phosphate, whereas the metabolic profile of *B. pumilus* FBP01 grown in presence of rock phosphate moved toward the upper-left quadrant. In contrast, the *P. salmasensis* POE54 (PO) and *P. salmasensis* POE54 with rock phosphate (PO_P) samples showed partial overlaps near the center of the plot, indicating a narrower gap between their metabolic states (Fig. 4.14).

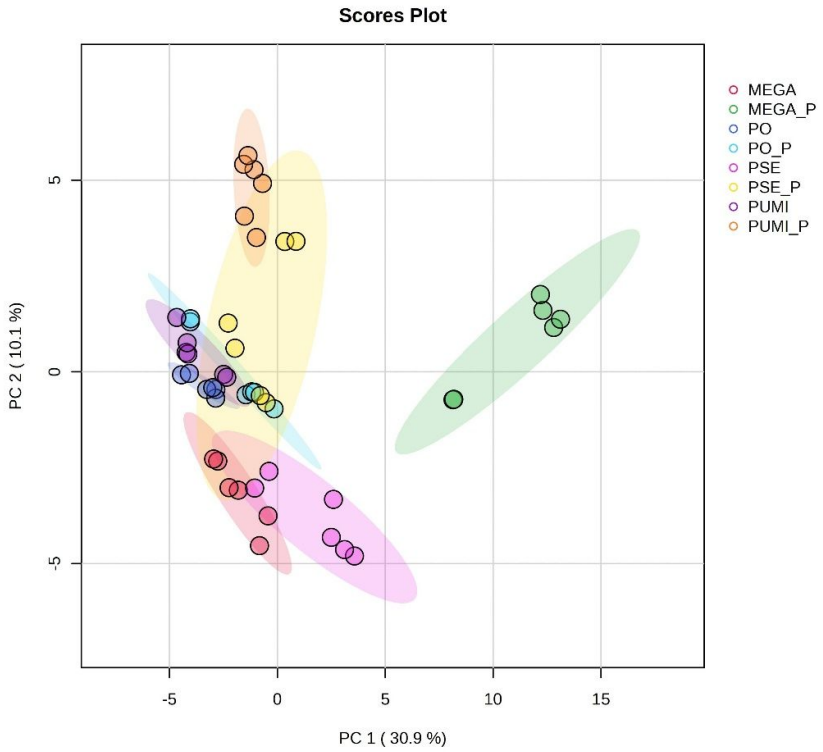

Figure 4.14. Principal Component Analysis (PCA) score plot of GC–MS–identified metabolites produced in liquid culture by *B. megaterium* FBM09, *P. salmasensis* POE54, *P. putida* RPT12, *B. pumilus* FBP01. Bacteria were grown for 7 days in liquid NBRIP containing tricalcium phosphate (MEGA, PO, PSE, PUMI) or rock phosphate as P source (MEGA_P, PO_P, PSE_P, PUMI_P), respectively. Samples cluster according to bacterial strain and phosphorus supplementation (P).

Hierarchical clustering analysis (HCA) combined with heat map visualization was used to compare the relative abundance of GC-MS identified metabolites among bacterial strains grown in presence of different P sources (Fig. 4.15). Results illustrate the similarities and differences in the metabolic profiles across the sample groups, based on the normalized abundance of each identified compound. The heatmap revealed a clear separation of groups; notably, *B. megaterium* FBM09 grown in presence of rock phosphate (MEGA_P) diverged from all other treatments, forming a distinct cluster. This separation is characterized by a high abundance of numerous metabolites (dark red regions) that are present at low levels or entirely absent in the corresponding *B. megaterium* FBM09 control samples (MEGA).

In contrast, the other samples (PO, PO-P, PUMI, PUMI-P, PSE_P) clustered more closely together, indicating a higher degree of similarity in their extracellular metabolite

composition. Distinct strain-specific patterns are also observed: in presence of rock phosphate both *P. putida* RPT12 and *P. salmasensis* POE54 (PSE_P and PO-P, respectively) were primarily defined by lower metabolite abundances (predominantly blue areas), whereas *B. megaterium* FBM09 and *B. pumilus* FBP01 (MEGA_P and PUMI-P, respectively) displayed specific clusters of upregulated molecules.

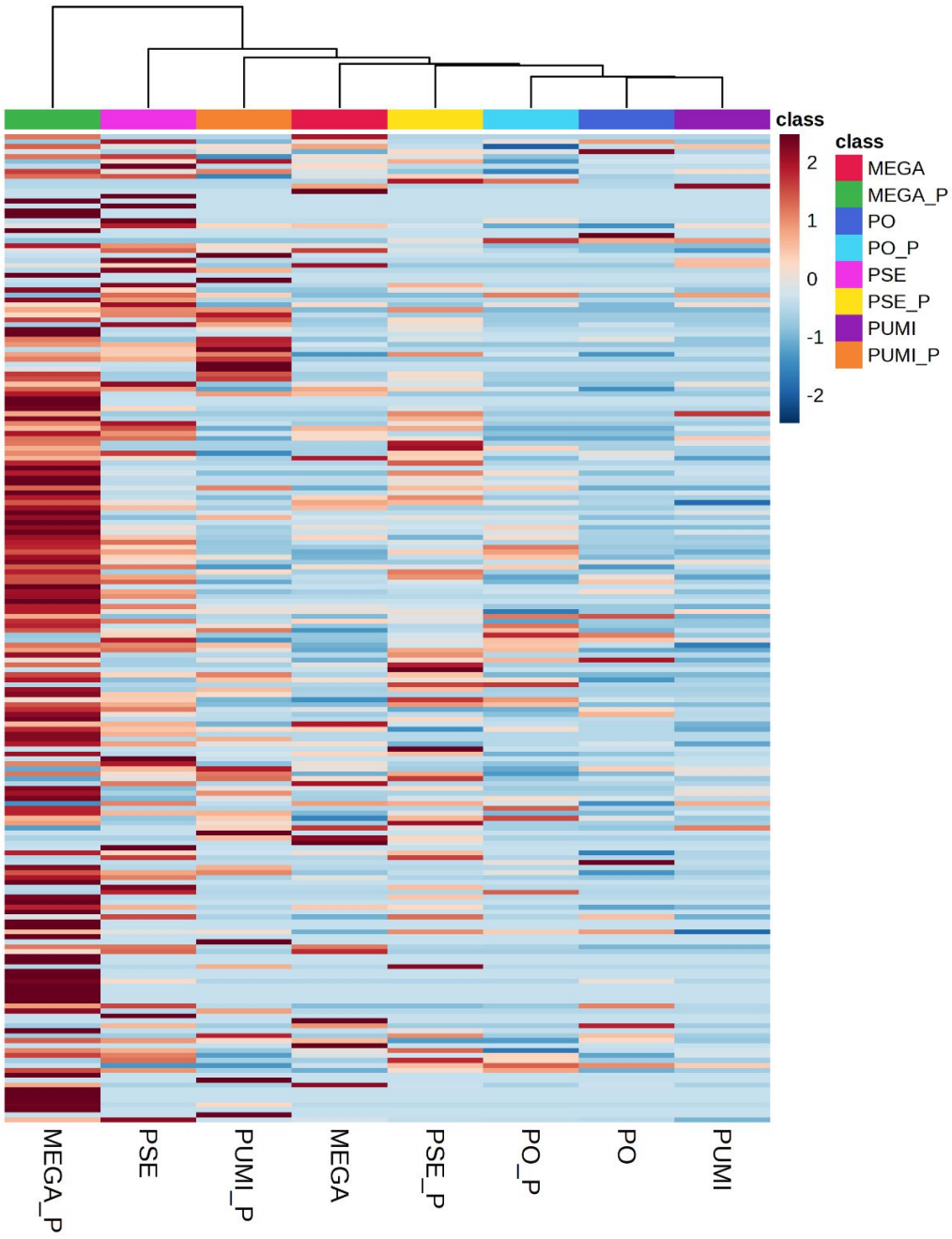

Figure 4.15. Hierarchical clustering heatmap of extracellular metabolic profiles. The heatmap illustrates the differential accumulation of metabolites in culture filtrates of bacteria grown for 7 days in liquid NBRIP containing tricalcium phosphate (MEGA, PO, PSE, PUMI) or rock phosphate as P source (MEGA_P, PO_P, PSE_P, PUMI_P), respectively. Rows represent individual metabolites, while columns represent sample groups. The dendrogram at the top indicates the metabolic similarity between groups based on Euclidean distance. Color intensity reflects the Z-score scaled relative abundance (red: higher abundance; blue: lower abundance).

The GC-MS characterization identified several classes of metabolites, including phenolic derivatives, fatty acids, and nitrogenous compounds (Table 4.6). The quantitative analysis revealed distinct accumulation patterns depending on the strain and phosphorus (P) source.

B. megaterium **FBM09**: in presence of rock phosphate (MEGA_P), a significant upregulation was observed for phenolic compounds (e.g., 4-hydroxybenzoic acid), nitrogenous compounds such as urea, and the diketopiperazine Cyclo(glycylprolyl).

P. putida **RPT12**: In contrast, the presence of rock phosphate instead of tricalcium posphate led to a generalized downregulation of almost all identified metabolites, with a marked decrease in long-chain fatty acids (e.g. palmitic and stearic acids) and the depletion of 4-hydroxybenzaldehyde.

P. salmasensis **POE54*:*** The metabolic profile of PO_P was characterized by the specific upregulation of 3-hydroxybutyric acid, while other markers remained relatively stable compared to the control.

B. pumilus **FBP01**: like *B. megaterium* FBM09, in presence of rock phosphate a significant upregulation was observed for phenolic compounds (e.g., 4-hydroxybenzoic acid), nitrogenous compounds such as urea, and the diketopiperazine Cyclo(glycylprolyl).

Table 4.6. Occurrence and relative regulation of metabolites identified by GC–MS in bacterial cultures grown for 7 days in NBRIP medium containing tricalcium phosphate (MEGA, PO, PSE, PUMI) or rock phosphate (MEGA_P, PO_P, PSE_P, PUMI_P) as phosphorus source.

									Regulation			
Compound	**MEGA**	**MEGA_P**	**PO**	**PO_P**	**PSE**	**PSE_P**	**PUMI**	**PUMI_P**	**MEGA_ vs MEGA**	**PO_P vs PO**	**PSE vs PSE_P**	**PUMI_P vs PUMI**
3-Methylpiperidin-2-one, TMS derivative	A	A	A	A	P	P	A	A	/	/	down	/
4-Hydroxybenzaldehyde, TMS derivative	P	P	A	P	P	P	P	P	up	/	down	down
4-Hydroxybenzoic acid, 2TMS derivative	P	P	A	P	P	P	P	P	up	/	down	up
3-hydroxybutyric acid, 2TMS derivative	P	P	P	P	P	P	A	P	down	up	down	/
Cyclo(glycylprolyl), TMS derivative	P	P	A	A	P	P	A	P	up	/	down	/
Glycerol, 3TMS derivative	P	P	A	P	P	P	P	P	down	/	down	down
Palmitic Acid, TMS derivative	P	P	P	P	P	P	P	P	up	up	down	down
Phenylacetic acid, TMS derivative	P	P	P	P	P	P	P	P	up	down	down	up
Thymine, 2TMS derivative	P	P	P	A	P	P	P	P	down	/	down	up
Stearic acid, TMS derivative	P	P	P	P	P	P	P	P	up	down	down	down
Uracil, 2TMS derivative	A	P	P	P	P	P	P	P	/	down	up	up
Urea, 2TMS derivative	P	P	P	P	P	P	P	P	up	down	up	down
Vanillic Acid, 2TMS derivative	P	P	P	P	P	P	P	P	down	down	down	down

Abbreviations: P: Present; A: Absent; Up/Down: statistical regulation based on Fold Change; (/): calculation not applicable due to metabolite absence in one condition.

4.4 Effects of PSBs on wheat plants (*Triticum aestivum* L.)

Preliminary experiments provide insight into the effects of rock phosphate (RP) concentrations (1–6%) on wheat (*Triticum aestivum* L.) seed germination and early seedling development, evaluated through determination of radicle length and number of germinated seeds in RP-supplemented nutrient agar. Interestingly, the presence of high RP concentrations did not affect seed germination; even when 6% RP was added to the medium, wheat seed germination was not statistically different from the control (Fig. 4.16 A). Lower RP doses did not affect seed germination either.

Radicle elongation was significantly influenced by phosphorite concentration ($p < 0.05$). The presence of 1% phosphorite resulted in a moderate but significant increase in radicle length compared to CTRL (Fig. 4.16 B). However, at higher doses no statistically significant differences were observed.

These results confirm that RP at concentrations ranging from 1-6 % did not alter early-stage development in wheat plants, while at low doses (1% w/v) a growth promotion effect could be expected.

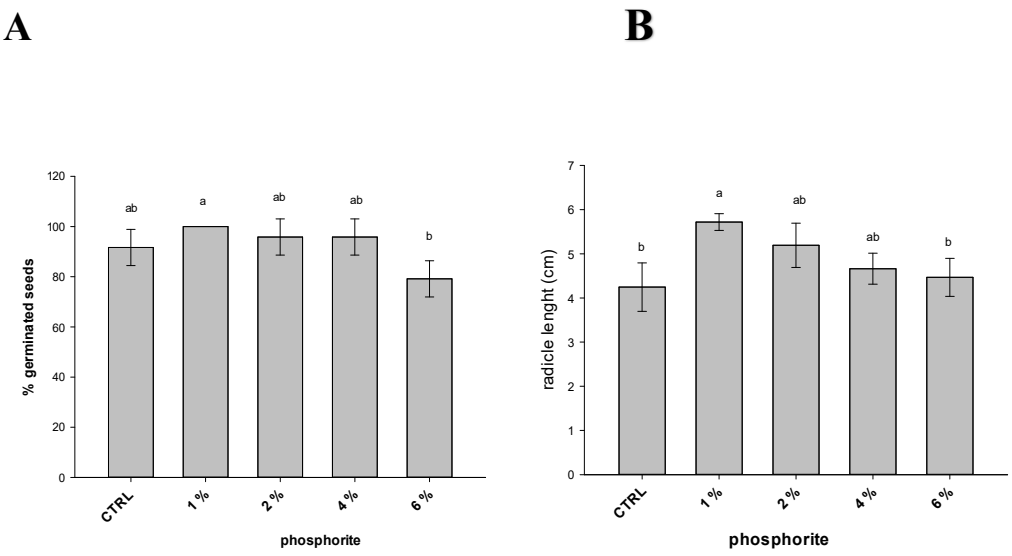

Figure 4.16. Effects of rock phosphate (RP) on wheat (*Triticum aestivum* L.) seed germination (A) and radicle length (B) *in vitro*. Nutrient agar (NA) plates were supplemented with RP at different concentrations (1, 2, 4 or -6 %, w/v). Control samples (CTRL) consisted of NA without RP. Different letters indicate values that are significantly different according to one-way ANOVA followed by Bonferroni multiple comparison test ($p < 0.05$).

Further experiments were carried out to evaluate the effect of selected bacterial strains on wheat (*Triticum aestivum* L.) growth in a controlled growth chamber in presence of rock phosphate (RP) as P source. Plants were grown in vermiculite, here used as an inert growth substrate to minimize background nutrient availability, thus allowing a more accurate assessment of the phosphorus-solubilizing activity of the bacterial strains. Thirty days after sowing, biometric parameters, including culm and root lengths, fresh and dry weights, and chlorophyll content, were measured (Fig. 4.17 – 4.18).

Figure 4.17. Effects of bacterial strain on wheat (*Triticum aestivum* L.) plants grown in a controlled growth chamber for 30 days. Seeds were treated with each bacterial cell suspension (10^7 CFU mL^{-1}) and transferred in pots containing vermiculite. Plants were irrigated every ten days with 20 mL of a modified Hoagland nutrient solution (Hoagland and Arnon, 1950), where RP (1% w/v) was added as P source. 1: uninoculated control; 2: *B. megaterium* FBM09-inoculated plant; 3: *P. putida* RPT12-inoculated plant; 4: *B. pumilus* FBP01-inoculated plant.

Significant differences among treatments were observed among treated plants in terms of culm growth, biomass accumulation, root development, and chlorophyll content compared to controls. However, no differences were observed between uninoculated control that were irrigated either with RP or KH_2PO_4 (Fig. 4.18).

Culm length varied among treatments combining bacterial inoculation with RP. The treatment with *B. megaterium* FBM09 increased culm length by 40% relative to the uninoculated RP-control (Fig. 4.18 A). Similarly, *B. pumilus* FBP01 or *P. putida* RPT12 in presence of RP increased culm length by 32% and 22%, respectively, compared to the RP-control. Overall, no statistical differences were observed among inoculated plants depending by the P source (soluble or insoluble) utilized.

Culm fresh weight was also significantly influenced by the treatments. *P. putida* RPT12 and *B. megaterium* FBM09 increased up to 135% and 112%, respectively, culm fresh weight in presence of RP compared to the uninoculated control (Fig. 4.18 B). *B. pumilus* FBP01 also determined +95% increase in culm fresh weight compared to control. Notably, these effects were not related to the P source supplemented to the plants.

The only treatment statistically affecting root fresh weight compared to control was *B. megaterium* FBM09 (Fig. 4.18 C), where in presence of RP the bacterial inoculation determined a +105% increase of this parameter.

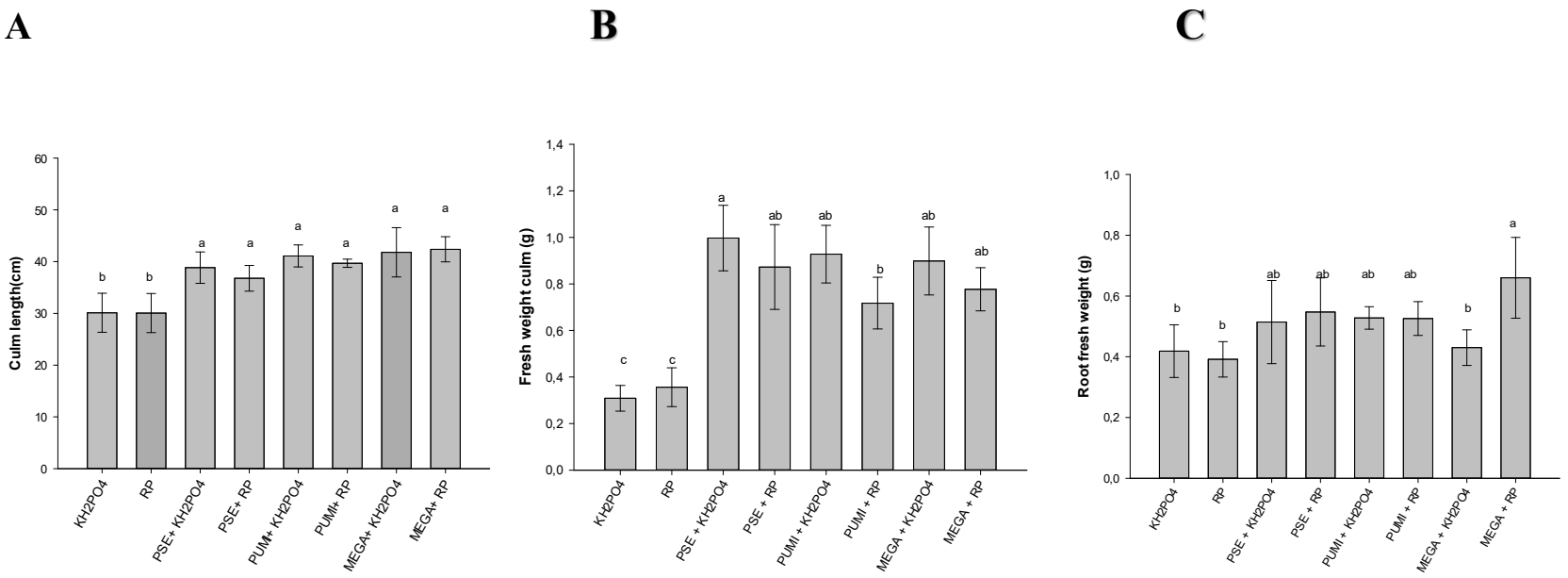

Figure 4.18. Effects of bacterial strain on the growth of wheat (*Triticum aestivum* L.) plants grown in presence of KH_2PO_4 or rock phosphate (RP) as P source. A: Culm length (cm); B: culm fresh weight (g); C. root fresh weight (g). *P. putida* RPT12: PSE. *B. pumilus* FBP01: PUMI. *B. megaterium FBM09*: MEGA. Different letters indicate values that are significantly different according to one-way ANOVA followed by Bonferroni multiple comparison test ($p < 0.05$).

Chlorophyll content was also evaluated and in plants treated with *B. megaterium* FBM09 combined with phosphorite chlorophyll content increased up to 50% compared to the RP-control (data not shown). Root length, as well as culm and root dry weights, were also measured; however, no statistically significant differences were observed among treatments for these parameters.

Overall, the results demonstrate that bacterial inoculation in presence of RP as insoluble P source significantly enhanced plant growth under controlled conditions. The synergistic effect between bacterial strains and insoluble phosphorus suggests improved phosphorus mobilization and availability for the plants.

4.5 Effects of PSMs on tomato plants (*Solanum lycopersicum* L.)

Different experiments were carried out to investigate the efficacy of selected bacteria in promoting growth and productivity, and in enhancing P solubilization and assimilation in tomato plants (*Solanum lycopersicum* L.). Overall, bacterial cell suspensions were inoculated to tomato seeds/plants and rock phosphate (RP) was used as insoluble P source in comparison with KH_2PO_4.

The effects of PSMs were evaluated in terms of plant growth promotion (Experiment #I) or in terms of yield and qualitative parameters of tomato fruits in standard soil condition (Experiment #II) or in P-deficient soil (Experiment III). Overall, no significant differences were observed in Exp. #1 and #2 among the tested conditions with respect to the phosphorus source, including both soluble and insoluble forms applied with each treatment. This result was likely due to the relatively high phosphorus availability in soil (50 ppm), which may have masked any potential effects of the different phosphorus sources on plant response. Therefore, in the presentation of the results in Exp. #1 and #2, only inoculated and control condition were considered. Subsequently, in Exp. #3, plants were grown in P-deficient soil (10 ppm) to better highlight the effects of PSMs inoculations.

4.5.1 Growth promotion activity of PSMs

Tomato plants (*Solanum lycopersicum* L. cv. Tydona) were used to evaluate the plant growth–promoting potential of selected phosphate-solubilizing bacterial strains (*Bacillus megaterium* FBM09, *Bacillus pumilus* FBP01, *Pseudomonas putida* RPT12, and *Pseudomonas salmasensis* POE54*)*. After 60 days significant differences among treated

plants were observed compared to uninoculated controls in terms of stem fresh weight and stem dry weight (Fig. 4.19).

The application of the different PSMs significantly promoted plant growth across all measured parameters compared to the control. Regarding stem biomass, all treatments induced a significant increase in fresh weight compared to uninoculated control (Fig. 4.19 A). Similarly, stem dry weight significantly increased following inoculation with *B. pumilus* FBP01*, B. megaterium* FBM09 and *P. salmasensis* POE54 (Fig. 4.19 B). The most striking differences were observed in root development: *B. megaterium* FBM09 and *P. putida* RPT12 treatments nearly doubled the root dry weight compared to the control, whereas *P. salmasensis* POE54 was the least effective in this regard, showing no statistical difference from the control (Fig. 4.19 C).

Other biometric parameters, including root length, fresh root weight, collar diameter, and number of leaves, showed no statistically significant differences compared to control according to one-way ANOVA ($p < 0.05$; Table 4.7).

Overall, all the selected PSMs showed good growth promotion activity in our experimental conditions.

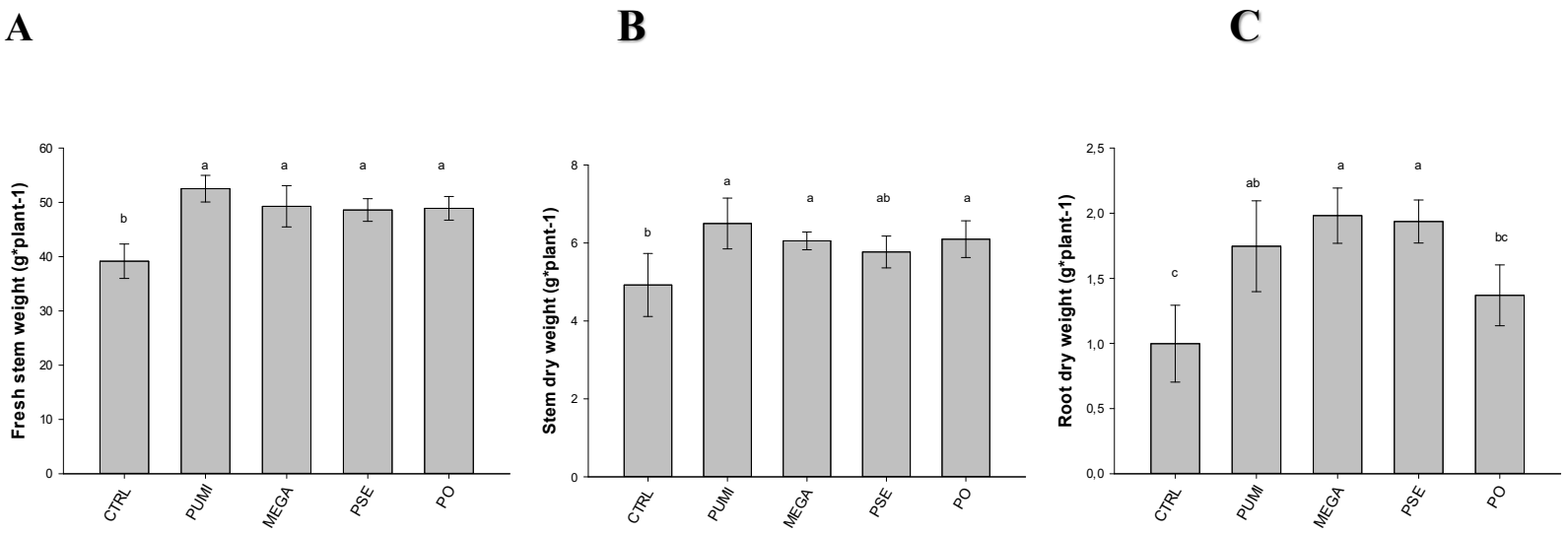

Figure 4.19. Growth promotion activity of *B. pumilus* FBP01 (PUMI), *B. megaterium* FBM09 (MEGA), *P. putida* RPT12 (PSE) and *P. salmasensis* POE54 (PO) on tomato plants (*Solanum lycopersicum* L. cv. Tydona) grown for 60 days in pots under greenhouse conditions (Experiment I). CTRL: uninoculated control. A: Fresh stem weight (g/plant). B: Stem dry weight (g/plant). C: Root dry weight (g/plant). Different letters indicate values that are significantly different according to one-way ANOVA followed by Bonferroni multiple comparison test ($p < 0.05$). Data are the averages of 8 biological replicates.

Table 4.7. Effects of *B. pumilus* FBP01 (PUMI), *B. megaterium* FBM09 (MEGA), *P. putida* RPT12 (PSE) and *P. salmasensis* POE54 (PO) on the growth of tomato plants grown in pots for 60 days under greenhouse conditions (Experiment #I). CTRL: uninoculated control. Different letters indicate values that are significantly different according to one-way ANOVA followed by Bonferroni multiple comparison test ($p < 0.05$). Data are the averages of 8 biological replicates.

Condition	Stem length (cm)	Root length (cm)	Fresh root weight (g)	Collar Ø (cm)	Number of leaves
CTRL	94,2 a	29,5 a	7,3 a	5,3 a	14,2 a
MEGA	99,2 a	33,0 a	8,8 a	5,1 a	15,6 a
PUMI	98,0 a	30,8 a	8,9 a	5,4 a	15,5 a
PSE	94,1 a	31,5 a	9,3 a	5,3 a	15,2 a
PO	98,3 a	32,9 a	8,3 a	5,1 a	15,5 a

Regarding phosphorus accumulation, all treatments significantly enhanced P content in both plant compartments compared to the control, though significant differences were observed (Fig. 4.20). In the shoots (green bars), *B. megaterium* FBM09 and *P. salmasensis* POE54 yielded the highest phosphorus uptake in tomato plants (about 17.4 and 18.7 mg P/plant respectively), significantly outperforming the control.

A similar positive trend was observed in the root system (brownish bars), where *B. megaterium* FBM09 and *P. putida* RPT12 accumulated up to 6.1 and 5.7 mg P/plant, respectively, whereas the roots of uninoculated tomato plants yielded 3.8 mg P/plant. Conversely, *B. pumilus* FBP01 exhibited a more moderate P solubilization effect, and *P. salmasensis* POE54 remaining statistically comparable to the control in the roots, despite the high P accumulation observed in plant shoots (Fig. 4.20). Collectively, these results indicate that while all treatments improve phosphorus solubilization and uptake, *B. megaterium* FBM09 provides the most balanced and effective enhancement of phosphorus nutritional status across the entire plant.

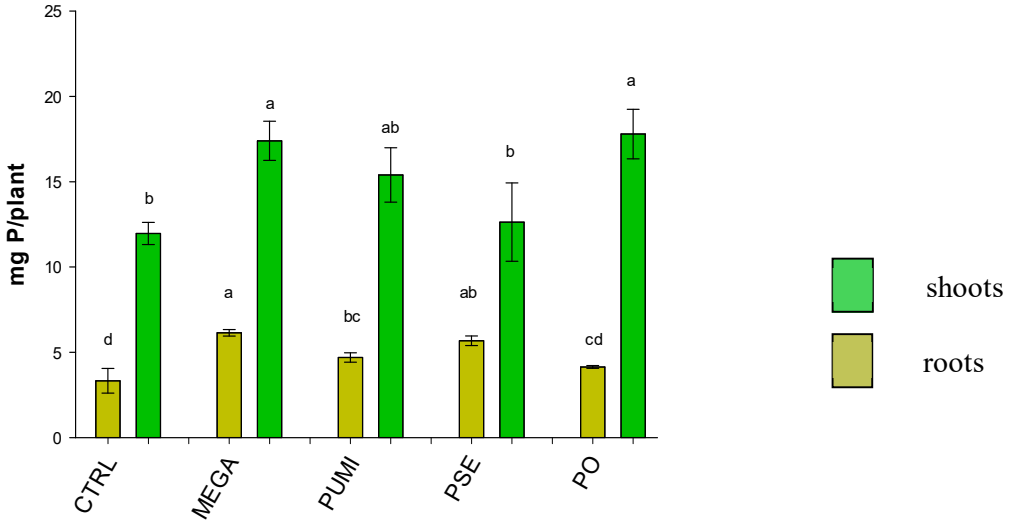

Figure 4.20. Phosphorus (P) content (mg P/plant) accumulated in the shoots (green bars) and in the roots (brownish bars) of tomato plants grown in pots for 60 days in pots under greenhouse conditions and inoculated as reported above (Experiment # I). PUMI: *B. pumilus* FBP01*;* MEGA: *B. megaterium* FBM09*;* PSE: *P. putida* RPT12. PO: *P. salmasensis* POE54. Different letters indicate values that are significantly different according to one-way ANOVA followed by Bonferroni multiple comparison test ($p < 0.05$).

4.5.2 Effects of PSMs on yield and qualitative parameters of tomato fruits

The effects of PSMs on yield and qualitative parameters of tomato fruits are reported in Table 4.8. The application of the different PSMs did not result in significant differences in fruit number and total weight per plant, as all treatments were statistically comparable. However, a moderate increase was observed in the inoculated conditions although it was not significantly different from the control (Table 4.8).

Fruit pH remained relatively stable across treatments, with values ranging between 4.21 and 4.29; however, the *P. salmasensis* POE54 treatment showed a significantly lower pH compared to the other treatments (Table 4.8). Total soluble solids (TSS) varied slightly among treatments, with *B. megaterium* FBM09 showing the highest values, while *B. pumilus* FBP01 exhibited a significantly lower TSS compared to the other treatments. Dry matter content did not show significant differences among treatments, as all values were statistically comparable. However, a slight numerical increase was observed in plants treated with *B. megaterium* FBM09, suggesting a potential, although not statistically supported, improvement in fruit solids accumulation.

Table 4.8. Effects of *B. pumilus* FBP01 (PUMI), *B. megaterium* FBM09 (MEGA), *P. putida* RPT12 (PSE) and *P. salmasensis* POE54 (PO) on the yield and quality of tomato fruits whose plants were grown in a tunnel greenhouse for 90 days (Experiment II). CTRL: uninoculated control. TTS: total soluble solids content (°Brix). Different letters indicate values that are significantly different according to one-way ANOVA followed by Bonferroni multiple comparison test ($p < 0.05$).

Condition	N. fruits/ plant	Fruit total weight /plant	pH	TTS (°Brix)	Dry matter (%)
CTRL	28.3 ± 5.4 a	261.7 ± 57.9 a	4.3 ± 0.02 a	6.9 ± 0.1 ab	11.1 ± 0.3 a
MEGA	32.8 ± 4.2 a	243.5 ± 51.3 a	4.3 ± 0.02 a	7.0 ± 0.1 a	12.5 ± 1.3 a
PUMI	32.4 ± 2.6 a	251.1 ± 39.9 a	4.3 ± 0.05 a	6.5 ± 0.2 b	11.9 ± 0.3 a
PSE	30.8 ± 3.1 a	248.6 ± 54.4 a	4.3 ± 0.03 a	6.6 ± 0.1 ab	11.8 ± 0.4 a
PO	32.4 ± 5.0 a	261.6 ± 42.6 a	4.2 ± 0.05 b	6.7 ± 0.2 ab	11.6 ± 0.2 a

4.5.3 Effects of PSMs on yield and qualitative parameters of tomato fruits in P-deficient soil

The experimental design utilized low-phosphorus soil supplemented with either a highly available soluble source (KH_2PO_4) or an insoluble source (rock phosphate, RP). This setup allows for a direct comparison of how bacterial strains might assist the plant in phosphorus uptake and subsequent fruit development. Details about experimental conditions are reported in Table 3.5.

In terms of effects on fruit yield, the highest total weight values were recorded for the plants inoculated with *B. pumilus* FBP01 or *B. megaterium* FBM09, both supplemented with RP (222.4 g and 212.5 g, respectively; Table 4.9). These results were comparable to the uninoculated control fertilizer supplemented with soluble P form (188.1 g). Conversely, in presence of the insoluble RP, fruit total weight per plant reached 115.1 g (Table 4.9).

The addition of RP to *B. pumilus* FBP01 led to a significant increase in fruit weight, rising from 147.9 g to 222.4 g. A similar positive trend was noted for *P. putida* RPT12 treatment (180.2 g) compared to *P. putida* RPT12 alone (147.7 g).

The qualitative analysis, including pH, soluble solids content (°Brix), and dry matter, revealed statistically significant differences among the experimental conditions (Table 4.9). *P. putida* RPT12, *B. megaterium* FBM09 and *B. pumilus* FBP01 determined a significant increase in fruit pH when RP was supplemented to the soil, compared to the inoculated plants supplemented with KH_2PO_4 or to the uninoculated control supplemented with RP.

Similarly, a significant increase was also observed in total soluble solids (TSS) when bacteria were inoculated in RP supplemented soil (Table 4.9). *B. pumilus* FBP01, *B. megaterium* FBM09 and *P. putida* RPT12 yielded the highest TSS contents (10.9, 10.9 and 10.8 °Brix, respectively), while the RP-control showed 10.1 °Brix. Conversely, applications of bacteria in presence of KH_2PO_4 generally resulted in lower sugar concentrations.

Dry matter also accumulated in higher proportion in fruits from plants inoculated with *B. pumilus* FBP01 or *B. megaterium* FBM09 and supplemented with RP (12.2 % and 12.2 %, respectively), whereas other bacteria or uninoculated control determined lower values (Table 4.9).

Finally, phosphorus accumulation (mg P $plant^{-1}$) significantly increased in *B. megaterium* FBM09 + RP (6.2 mg $plant^{-1}$), followed by *B. pumilus* FBP01 +RP (5.4 mg $plant^{-1}$) and CTRL (5.7 mg $plant^{-1}$). In contrast, the lowest P uptakes were recorded in inoculated plants supplemented with KH_2PO_4 or in uninoculated control supplemented with rock phosphate (RP; Table 4.9).

Overall, the results highlight a consistent trend: the combination of RP with PSMs markedly improved yield, fruit quality, and phosphorus uptake, with *B. pumilus* FBP01 and *B. megaterium* FBM09 being the most effective strains.

Table 4.9. Effects of *B. pumilus* FBP01 (PUMI), *B. megaterium* FBM09 (MEGA), *P. putida* RPT12 (PSE) and *P. salmasensis* POE54 (PO) on the yield and quality of tomato fruits whose plants were grown in pots under greenhouse conditions in P-deficient soil conditions (Experiment III). CTRL: uninoculated control supplemented with KH_2PO_4. RP: uninoculated control supplemented with rock phosphate. TTS: total soluble solids content (°Brix). Different letters indicate values that are significantly different according to one-way ANOVA followed by Bonferroni multiple comparison test ($p < 0.05$).

Condition	Fruit total weight /plant	Ph	TSS (°Brix)	Dry Matter (%)	P content (mg/ plant)
CTRL	188.1 ± 51.5 a	4.32 ± 0.01 a	10.4 ± 0.1 bc	12.1 ± 0.06 a	5.7 ± 0.69 ab
RP	115.1 ± 38.5 c	4.22 ± 0.03 b	10.1 ± 0.1c	10.2 ± 0.4 b	4.5 ± 0.57 bc
PSE	147.7 ± 34.6 c	4.27 ± 0.01 b	10.2 ± 0.1c	9.9 ± 0.68 b	4.9 ± 0 .71 abc
PSE+RP	180.2 ± 51.9 b	4.33 ± 0.02 a	10.8 ± 0.05 a	10.2 ± 0.65 b	4.4 ± 0.3 c
MEGA	182.8 ± 67.4 ab	4.26 ± 0.01 b	10.1 ± 0.1c	9.9 ± 0.2 b	4.4 ± 0.12 bc
MEGA+RP	212.5 ± 36.5 a	4.34 ± 0.02 a	10.9 ± 0.06 a	12.2 ± 0.14 a	6.2 ± 0.37 a
PUMI	147.9 ± 64.2 b	4.25 ± 0.01 b	10.4 ± 0.1 b	9.8 ± 0.18 b	4.2 ± 0.17 bc
PUMI+RP	222.4 ± 18 a	4.33 ± 0.03 a	10.9 ± 0.06 a	12.2 ± 0.48 a	5.4 ± 0.33 ab
PO	140.3 ± 36.8 b	4.21 ± 0.01 b	10.2 ± 0.2 c	9.8 ± 0.1 b	4.5 ± 0.36 bc
PO+RP	148.7 ± 46.9 b	4.27 ± 0.01 b	10.8 ± 0.15 ab	9.9 ± 0.17 b	4.7 ± 0.34 abc

5. DISCUSSION

The solubilization of phosphorus from natural rock phosphate (RP) using phosphate-solubilizing microorganisms (PSMs) as bioinoculants is an important area of research in the agricultural sector. This approach helps reduce the use of chemical phosphate fertilizers, which are often subject to retrogradation, fixation, and immobilization within the soil matrix, which significantly limits their long-term efficiency (Kang et al., 2021). Moreover, the ability of soil microbes to convert insoluble forms of phosphates into plants-accessible forms is an important trait in plant growth-promoting (PGP) bacteria for increasing crop yields, decreasing environmental pollution, and improving the agronomic effectiveness of RP (Maharana e al., 2022).In addition to their ability to solubilize inorganic phosphates, these microorganisms may exhibit a wide range of PGP traits, including phytohormone production, siderophore-mediated iron acquisition, and, in some cases, antagonistic activity against phytopathogens. This functional diversity highlights their potential as multifunctional bio-inoculants for sustainable crop production (Glick, 1995).

The selection of effective microbial candidates for field application requires a comprehensive and multifactorial characterization. The success of a microbial inoculant depends not only on its functional traits, such as nutrient solubilization, but also on its ecological fitness, stress tolerance, and ability to compete within complex and dynamic microbial communities. In this thesis, different isolates of *Bacillus* and *Pseudomonas* species were tested for their PGP traits, biocontrol activity and ability to solubilize inorganic phosphate.

Among the various abiotic stress factors affecting microbial survival in soil, salinity represents a major constraint that can significantly limit microbial persistence and activity in the rhizosphere (Nicotra et al., 2025). In this study, a clear pattern of salt tolerance was observed among the tested isolates, with strains belonging to the *Bacillus* genus exhibiting markedly higher resilience compared to *Pseudomonas* spp., in agreement with previous reports (Ayaz et al., 2022). At 24 h, *B. subtilis* FBS07, *B. pumilus* FBP01, and *B. amyloliquefaciens* FBA21 maintained growth levels comparable to the control even at the highest NaCl concentration tested (1.5 M), indicating a strong intrinsic tolerance to osmotic stress. In contrast, *B. megaterium* FBM09 showed a clear salt-dependent reduction in growth, suggesting a lower capacity to cope with increasing osmotic pressure. Salinity imposes severe physiological constraints on microbial cells, primarily through osmotic imbalance, which can lead to cellular dehydration, plasmolysis, and impairment of enzymatic activity (O'Byrne and Booth, 2002). The ability of several *Bacillus* strains to sustain growth under high salinity conditions may be related to their well-documented

capacity to accumulate compatible solutes and activate osmoadaptive responses (Hoffmann and Bremer, 2017). In addition, the ability of *Bacillus* spp. to form endospores under unfavorable environmental conditions represents a key survival strategy, allowing persistence during stress and rapid recovery when conditions improve.

A markedly different behavior was observed among the species of *Pseudomonas* used in the present study. *P. salmasensis* POE54 emerged as the most sensitive strain, exhibiting a clear and dose-dependent reduction in growth with increasing NaCl concentrations. This suggests a limited capacity to maintain osmotic homeostasis under saline stress. Conversely, *P. putida* RPT12 showed only a slight reduction in growth even at higher salinity levels, indicating a relatively higher tolerance compared to *P. salmasensis* POE54. This behavior may reflect the known metabolic versatility and adaptive capacity of *Pseudomonas* spp. under osmotic stress conditions (Samaddar et al., 2019; Yasmin et al., 2020). Overall, the results highlight a generally higher salinity tolerance among *Bacillus* strains compared to *Pseudomonas*, although species-specific differences were observed within both genera.

The phenotypic profiling obtained through the Biolog GEN III system revealed marked differences in metabolic versatility and stress tolerance among the tested isolates, highlighting distinct ecological strategies between *Bacillus* and *Pseudomonas* genera.

Overall, *Bacillus* strains exhibited a broader metabolic spectrum, particularly toward carbohydrates, including mono-, di-, and polysaccharides. *B. amyloliquefaciens* FBA21 and *B. pumilus* FBP01 showed extensive substrate utilization, such as D-salicin and D-melibiose, reflecting a highly adaptable metabolism capable of efficiently degrading complex carbon sources commonly found in the rhizosphere (Compant et al., 2005; Adesemoye et al., 2009). This metabolic plasticity likely enhances their competitiveness in soil environments, where nutrient availability is heterogeneous and dynamic. Similarly, *B. subtilis FBS07* demonstrated a strong but more selective metabolic profile, combining efficient utilization of specific carbohydrates amino acids (such as L-aspartic acid), and organic acids (such as citric acid) with a degree of substrate specificity. This efficient metabolism of organic acids is particularly relevant for phosphate solubilization and responding to root exudates (Rodríguez and Fraga, 1999; Bais et al., 2006), which may indicate a more specialized ecological niche and a strong potential to establish stable associations with plant roots (Kumar et al., 2018; Ahmad et al., 2022). Furthermore, the high metabolic activity in *B. amyloliquefaciens* FBA21 supports the energy-intensive biosynthesis of antifungal lipopeptides (surfactins, iturins, and fengycins) required for biocontrol activity against pathogens like *Fusarium oxysporum* (Ongena and Jacques, 2008; Chen et al., 2015).

In contrast, *Pseudomonas* isolates displayed a more specialized metabolic strategy, characterized by a limited ability to utilize carbohydrates and a pronounced preference for organic acids (including citric acid, L-lactic acid, and D-glucuronic acid) as well as amino acids. Both *P. putida* RPT12 and *P. salmasensis* POE54 showed strong oxidative activity

toward Krebs cycle intermediates, consistent with the well-known non-fermentative metabolism of the intermediates, consistent with the well-known non-fermentative metabolism of the genus. This metabolic orientation suggests an adaptation to root exudates and supports the establishment of high population densities in the rhizoplane (Compant et al., 2005). While their direct antagonism might be limited, their biocontrol potential relies on indirect mechanisms such as nutrient competition and niche occupation (Raaijmakers et al., 2010).

Siderophore production represents an additional key mechanism contributing to plant growth promotion and microbial competitiveness. In this study, a notable discrepancy was observed between qualitative agar-based assays and quantitative liquid assays, a phenomenon widely reported in the literature. *Bacillus* strains produced relatively small halos on solid media but exhibited high siderophore production in liquid cultures, a difference that can be attributed to the limited diffusion of catecholate-type siderophores, such as bacillibactin, within the agar matrix (Hoffmann and Bremer, 2017; Wilson et al., 2006). High siderophore production was observed in *P. putida* RPT12 (32.7% SU) and *B. subtilis* FBS07 (31.7% SU), highlighting their potential to effectively sequester Fe^{3+} and limit its availability to competing microorganisms, thereby inhibiting the growth of iron-dependent pathogens through nutrient deprivation (Sleator and Hill, 2002). Conversely*, P. salmasensis* POE54 exhibited a large halo but relatively low quantitative siderophore production (11.6%), suggesting the secretion of highly diffusible but less efficient chelators or the activation of surface-specific metabolic pathways (Schwyn and Neilands, 1987).

The differential antagonistic activity observed among the tested bacterial strains highlights the strong strain-dependent nature of biocontrol potential and suggests that distinct mechanisms underlie fungal inhibition. The consistently high efficacy displayed by *B. amyloliquefaciens* FBA21 across all tested pathogens (*Fusarium oxysporum*, *Alternaria alternata*, and *Botrytis cinerea*) strongly supports its role as a highly effective biocontrol agent, likely due to its well-documented capacity to produce a broad spectrum of antifungal secondary metabolites. This evidence indicates that this strain possesses a broad-spectrum antifungal activity, a highly desirable trait for field applications where multiple pathogens often coexist (Kazerooni et al., 2021; Soliman et al., 2023)

B. subtilis FBS07 and *B. pumilus* FBP01 showed a more moderate but still relevant antagonistic potential, which may reflect differences in the quantity or composition of the antimicrobial compounds produced. In these cases, fungal inhibition is likely the result of a combination of mechanisms, including antibiosis, competition for nutrients, and possibly the production of volatile organic compounds, rather than the dominance of a single highly potent pathway. This variability among *Bacillus* species further emphasizes that even closely related taxa can exhibit markedly different functional traits, reinforcing the importance of strain-level selection in the development of microbial inoculants.

The limited antagonistic activity observed for *B. megaterium* FBM09 is consistent with previous reports indicating that this species generally exhibits weak or inconsistent

antifungal activity *in vitro*, particularly when compared to more specialized biocontrol agents such as *B. amyloliquefaciens* (Chen et al., 2006). Rather than relying on direct antibiosis, *B. megaterium* FBM09 is primarily recognized for its role in nutrient mobilization and plant growth promotion, and its contribution to pathogen suppression may occur predominantly through indirect mechanisms, such as improved plant nutritional status or modulation of plant defense responses (Raaijmakers et al., 2010).

Similarly, *Pseudomonas* strains showed limited inhibition of pathogen growth, thus suggesting that these microorganisms may rely on alternative strategies that are not effectively observed *in vitro*. Under *in vivo* conditions, these strains may exert significant effects through indirect mechanisms, including rhizosphere colonization, nutrient competition mediated by siderophore production, and the induction of plant systemic resistance (Hofte et al., 2007). Indeed, it is well established that many *Pseudomonas* spp. exert their biocontrol activity primarily through indirect mechanisms, such as competition for iron mediated by siderophore production, niche colonization, and the induction of systemic resistance in plants, rather than through the secretion of diffusible antifungal compounds (Raaijmakers et al., 2010). This interpretation is particularly relevant considering the strong siderophore production previously observed in *P. putida* RPT12, which may contribute to pathogen suppression *in vivo* by limiting iron availability rather than directly inhibiting mycelial growth.

These findings highlight an important limitation of *in vitro* dual culture assays, which, although useful for preliminary screening, mainly detect direct antagonistic interactions and may therefore underestimate the contribution of indirect or plant-mediated mechanisms that are highly relevant under natural conditions (Compant et al., 2005). Consequently, strains showing limited inhibition *in vitro* should not be excluded a priori from further evaluation, as their effectiveness may become more evident in more complex systems involving plant hosts.

The literature reports that the efficiency of phosphorite solubilization by phosphate-solubilizing bacteria is strongly influenced by the production and concentration of organic acids, which play a major role in mobilizing insoluble phosphate into solution. The solubilization of insoluble phosphate mainly results from the production of low-molecular-weight organic acids and protons during carbon source metabolism, which acidify the surrounding medium and promote phosphate mobilization (Sharma et al., 2013; Wei et al., 2018). In this context, organic acid composition, pH dynamics, and bacterial community structure play a crucial role in determining both phosphate solubilization efficiency and phosphorus availability (Saeid et al., 2018). Accordingly, the variability observed in P concentrations among treatments can be attributed to strain-specific differences in both the type and quantity of organic acids produced, as well as in the efficiency of their secretion systems.

Consistent with this framework, plate assays provided initial evidence of phosphate solubilization capacity, as *P. salmasensis* POE54, *B. pumilus* FBP01, and *P. putida* RPT12

produced clear halos on both PVK and NBRIP media. The higher sensitivity of NBRIP, attributed to its lower buffering capacity, likely enhanced the visual expression of solubilization activity, resulting in more pronounced halo formation compared to PVK (Nautiyal, 1998). By measuring the ratio of the halo diameter to the colony diameter, a solubilization index (SI) was determined, which aligns with similar results reported in literature for numerous bacterial strains, including *Pseudomonas* and *Bacillus* species (Ahmad et al., 2022; Bouizgarne et al., 2023; Bakki et al., 2024). Among the tested strains, *P. salmasensis* POE54 exhibited the highest index (SI = 1.95), followed by *B. pumilus* FBP01 (SI=1.9) and *P. putida* RPT12 (SI= 1.4), supporting the well-documented ability of *Pseudomonas* species to acidify their microenvironment through the production of gluconic acid and related metabolites (Panchal et al., 2021). Furthermore, these results obtained on solid media were corroborated by findings in liquid media, where a significant decrease in the pH of the culture medium was observed when the bacterial strains were grown in the presence of rock phosphate.

In contrast, *B. megaterium* FBM09, *B. subtilis* FBS07, and *B. amyloliquefaciens* FBA21did not produce detectable halos on solid media despite their ability to grow in liquid PVK supplemented with phosphorite. This discrepancy suggests that these strains may rely on solubilization mechanisms that are not associated with strong localized acidification or that do not generate visible clearing zones under solid-state conditions, as previously reported. This observation further emphasizes that plate-based assays alone are not sufficient to fully assess phosphate-solubilizing capacity and should always be complemented by quantitative analyses in liquid systems. The ability of some strains to efficiently solubilize phosphate without producing visible halos highlights the diversity of underlying biochemical mechanisms.

This interpretation is supported by results obtained in liquid culture, where a clear acidification of the medium was observed together with increased soluble phosphorus concentrations, confirming the central role of organic acid production in phosphate mobilization (Nautiyal et al., 2000). The differences in both pH reduction and P release among strains indicate that solubilization efficiency is strongly dependent on metabolic strategy and regulation of organic acid biosynthesis pathways. In particular, the pronounced acidification observed in *P. putida* RPT12, *B. megaterium* FBM09, and *B. pumilus* FBP01 suggests the activation of efficient biochemical routes involved in the secretion of low-molecular-weight organic acids.

The strong performance of *P. putida* RPT12 is consistent with its well-established ability to oxidize glucose into gluconic acid via membrane-bound dehydrogenases, a mechanism considered one of the most effective pathways for phosphate mobilization in Gram-negative bacteria (Walpola and Yoon, 2013). Similarly, the high solubilization capacity observed in *B. megaterium* FBM09 and *B. pumilus* FBP01 indicates that, despite phylogenetic differences, these strains converge toward functionally efficient strategies for mineral phosphate mobilization, likely involving distinct but equally effective organic acid profiles.

Quantitative analysis of soluble phosphorus further confirmed these trends, revealing clear strain-dependent differences. Among the phosphorite-supplemented treatments, *P. putida* RPT12 showed the highest solubilization capacity (11.56 mg L^{-1}), followed by *B. pumilus* FBP01 (10.02 mg L^{-1}) and *B. megaterium* FBM09 (8.12 mg L^{-1}). In contrast, *B. subtilis* FBS07 and *B. amyloliquefaciens* FBA21 exhibited reduced solubilization (0.39 mg L^{-1}), despite their ability to persist in phosphorite-containing media (Wyciszkiewics et al., 2015). These findings indicate that tolerance to insoluble phosphorus sources is not necessarily linked to active phosphate mobilization but rather reflects distinct metabolic capabilities and regulatory responses to phosphorus limitation.

The extremely low phosphorus concentration measured in the abiotic control (0.029 mg L^{-1}) confirms that phosphorite dissolution under the tested conditions is negligible in the absence of microbial activity, thereby emphasizing the central role of bacterial metabolism in regulating phosphorus availability. The several-fold increase observed in the most efficient strains further highlights their strong potential to mobilize otherwise inaccessible phosphorus pools, although this mobilization remains substantially lower than that achieved with fully soluble fertilizers (Rodríguez and Fraga, 1999).

Importantly, the consistent association between pH reduction and soluble phosphorus concentration suggests a direct functional link between acidification and phosphate mobilization. This relationship reinforces the role of organic acid-mediated processes as the dominant mechanism under experimental conditions. While this negative correlation between pH and phosphorus availability has been widely reported (Halder et al., 1990; Goldstein, 1995; Illmer and Schinner, 1995; Kim et al., 1998; Hwangbo et al., 2003; Rashid et al., 2004), the present results further indicate that not all strains capable of growing under phosphorus-limited conditions contribute equally to solubilization, suggesting that only some released the organic acids responsible for the lowering of the pH into the liquid medium (Hwangbo et al., 2003). Literature reports that PSB-mediated rock phosphate solubilization is influenced by the higher concentrations of organic acids required to mobilize large quantities of insoluble phosphate into the solution via direct phosphate oxidation, which occurs on the outer surface of the cytoplasmic membrane (Pande et al., 2017). These microbial metabolites convert phosphate into soluble forms by chelating the cations bound to the phosphate through their hydroxyl and carboxyl groups (Mardad et al., 2013).

In this regard, *B. subtilis* FBS07 and *B. amyloliquefaciens* FBA21 represent a clear example of strains that, despite successful growth in phosphorite-containing media, exhibit limited phosphate-solubilizing activity. This suggests that survival under nutrient-limited conditions does not necessarily imply active nutrient mobilization but may instead involve alternative metabolic adaptations that do not rely on significant organic acid secretion, or that produce acids at levels insufficient to affect bulk solution chemistry. Similar patterns have been reported in other studies, where qualitative growth responses do not always correlate with quantitative solubilization performance in liquid assays (Fankem et al., 2014).

Finally, the comparison with the soluble phosphate control (KH_2PO_4) highlights the substantial difference between biologically mobilized phosphorus and readily available inorganic phosphate. Although microbial solubilization does not reach the efficiency of synthetic fertilizers, the observed increases in soluble phosphorus demonstrate a meaningful contribution to nutrient availability. From an applied perspective, even partial mobilization of native or mineral-bound phosphorus can improve soil fertility and nutrient use efficiency while reducing dependence on chemical inputs. Moreover, under natural soil conditions, long-term microbial activity combined with plant–microbe interactions may amplify these effects, producing cumulative benefits that are not fully captured in short-term *in vitro* experiments.

To gain deeper insight into the metabolic basis underlying these functional differences, a GC–MS metabolomic analysis was performed. Multivariate statistical approaches, including PCA and HCA, revealed that bacterial strain identity is the primary determinant of metabolic variation, while P availability acts as a key regulatory factor shaping extracellular profiles (Fig. 4.14, 4.15). This metabolomic reprogramming provides a functional link to the observed differences in phosphate solubilization efficiency among the tested strains.

The production and modulation of low-molecular-weight organic acids are widely recognized as the primary drivers of mineral phosphate mobilization through medium acidification and chelation (Sharma et al., 2013; Wei et al., 2018). Our findings confirm that strains exhibiting the most pronounced metabolic adjustments under phosphorus-limited conditions (rock phosphate) are also the most effective solubilizers. For instance, *B. megaterium* FBM09 and *B. pumilus* FBP01 showed a significant upregulation of phenolic compounds, such as 4-hydroxybenzoic acid, and nitrogenous metabolites, including urea and the diketopiperazine Cyclo(glycylprolyl). The enrichment of these compounds likely reflects a sophisticated modulation of secondary metabolic pathways and microbial signaling in response to P-availability (Holden et al., 1999; Pech et al., 2022).

In contrast, *P. putida* RPT12 and *P. salmasensis* POE54 exhibited distinct adaptive strategies. In *P. salmasensis* POE54, the specific accumulation of 3-hydroxybutyric acid under rock phosphate conditions suggests a shift toward carbon storage mechanisms, such as polyhydroxyalkanoate (PHA) biosynthesis, likely as a response to nutrient stress (Sudesh et al., 2000). Conversely, *P. putida* RPT12 showed a generalized downregulation of most extracellular metabolites (e.g., palmitic and stearic acids) when grown with rock phosphate, suggesting a metabolic strategy oriented toward resource conservation and intracellular reallocation. Despite this reduction, the persistent presence of urea in *Pseudomonas* strains points toward a maintained nitrogen homeostasis under fluctuating nutrient conditions (Sharon et al., 2016). Interestingly, the widespread depletion of vanillic acid across all multiple strains suggests a common metabolic rerouting, where intermediate phenolic compounds are potentially redirected toward the biosynthesis of functionally relevant metabolites, such as catecholate-type siderophores (e.g., bacillibactin) involved in iron acquisition (Miethke et al., 2006). Collectively, these results demonstrate that phosphorus

availability acts as a central regulatory signal that reshapes bacterial metabolic networks in a strain-dependent manner.

The pot experiment conducted on wheat (*Triticum aestivum*) provided strong biological validation of the phosphate-solubilizing potential previously identified under *in vitro* conditions, confirming that these microbial traits can effectively translate into plant growth promotion. Many commercially available biofertilizers are primarily based on plant growth-promoting rhizobacteria (PGPR), which exert beneficial effects on plant development largely through improved nutrient availability to the host plant.

The effect observed in the condition when bacteria were inoculated in presence of RP supports the hypothesis that microbial activity represents a key factor in the mobilization of nutrients from insoluble mineral sources. This observation is consistent with previous studies demonstrating that the combined application of phosphate-solubilizing bacteria and insoluble phosphate sources significantly enhances phosphorus availability and plant performance compared to single treatments (Afzal and Bano, 2008; Zabihi et al., 2010; Rezakhani et al., 2019; Wang et al., 2022).

The quantitative results revealed strain-specific efficiencies in enhancing plant parameters. *B. megaterium* FBM09 was the most effective treatment when inoculated in presence of RP, increasing culm length by 40% relative to the uninoculated control, followed by *B. pumilus* FBP01 (+32%) and *P. putida* RPT12 (+22%). However, the most interesting results were observed in biomass accumulation. *P. putida* RPT12 led to a 135% increase in fresh culm weight, highlighting its superior effectiveness in enhancing fresh biomass. Similarly, *B. megaterium* FBM09 and *B. pumilus* FBP01 showed marked positive effects, increasing fresh culm weight by 112% and 95%, respectively, compared to control. These substantial increases highlight the high efficiency of these strains in converting phosphorite into plant-available forms, effectively acting as mediators between the mineral substrate and the plant (Adesemoye et al., 2008; Mpanga et al., 2019; Wang et al., 2022).

The observed growth enhancement likely reflects a multifactorial mechanism involving both nutrient solubilization and the production of bioactive compounds. For instance, *B. megaterium* FBM09 not only enhanced the epigeal part but also doubled the root fresh weight (+105%). Metabolomic data obtained through GC–MS analysis suggest that the secretion of compounds such as phenylacetic acid (PAA) by *B. megaterium* FBM09 may trigger hormone-mediated signaling pathways that improve root architecture and nutrient acquisition (Elhaissoufi et al., 2020). Furthermore, the 50% increase in chlorophyll content observed in the *B. megaterium* FBM09 treatment supports an improved physiological status. Since phosphorus is central to energy metabolism, its increased availability is directly associated with enhanced chloroplast development and photosynthetic efficiency.

The contribution of *B. pumilus* FBP01 can be further interpreted through the metabolic shifts identified via GC–MS, particularly the increased abundance of saturated fatty acids like stearic and palmitic acids. These compounds are involved in membrane remodeling, which

may optimize rhizosphere interactions and nutrient exchange efficiency (Compant et al., 2005; Kumar et al., 2018; Ahmad et al., 2022). While some parameters, such as root length and dry weights, did not show statistically significant differences, the overall results provide compelling evidence that *P. putida* RPT12, *B. megaterium* FBM09, and *B. pumilus* FBP01 are promising candidates for biofertilizers. These findings are consistent with the literature (Mahmud et al., 2021; Batool et al., 2019; Kang et al., 2021) and demonstrate benefits across multiple crops including wheat (Benbrik et al., 2021), maize, faba bean (Borgi et al., 2020), and tomato (El Maaloum et al., 2020), ultimately aiming at improving phosphorus use efficiency in sustainable agriculture (Bargaz et al., 2021).

The tomato pot experiment confirmed the ability of PSMs to promote plant growth even under conditions where P availability is not limited. The absence of significant differences between soluble and insoluble P treatments indicates that the baseline soil P content was sufficient to sustain plant growth, thereby reducing plant dependence on microbial-mediated P mobilization. Similar observations have been reported in systems where high nutrient availability masks the functional contribution of PGPR (Rodríguez and Fraga, 1999; Richardson and Simpson, 2011). Despite these conditions, bacterial inoculation significantly enhanced plant biomass, highlighting the multifunctional nature of the selected strains. *B. pumilus* FBP01 showed the strongest effect on above-ground biomass, while *B. megaterium* FBM09 and *P. salmasensis* POE54 also significantly improved stem dry weight. These effects are likely not solely attributable to P solubilization, but rather to a combination of mechanisms including phytohormone production, improved nutrient uptake, and modulation of plant metabolism (Vessey, 2003; Adesemoye et al., 2009).

B. megaterium FBM09 and *P. putida* RPT12 nearly doubled root dry weight, suggesting a strong influence on root system architecture. The lack of significant differences in root length and other morphological parameters indicates that these bacteria may enhance root density and lateral branching rather than elongation, a response commonly associated with PGPR-mediated hormonal regulation (Tahir et al., 2017). Phosphorus accumulation data further support these findings. All treatments increased P content in both shoots and roots, although with distinct patterns. *B. megaterium* FBM09 showed the most balanced effect across plant compartments, while *P. salmasensis* POE54 and *P. putida* RPT12 displayed preferential accumulation in shoots and roots, respectively. These differences likely reflect strain-specific strategies related to rhizosphere colonization, organic acid production, and nutrient exchange dynamics (Richardson et al., 2009). Overall, these results demonstrate that PSB can enhance plant growth under non-limiting P conditions through mechanisms that extend beyond phosphate solubilization, reinforcing their role as multifunctional bioinoculants.

Under standard soil conditions, bacterial inoculation had a limited effect on tomato yield, with no statistically significant differences observed in fruit number or total fruit weight among treatments. This result is consistent with the high baseline fertility of the system, which likely reduced the relative contribution of microbial activity to plant productivity.

Under nutrient-rich conditions, plants can directly access available nutrients, thereby limiting the expression of microbial traits associated with nutrient mobilization (Richardson and Simpson, 2011). However, moderate effects were observed on fruit quality parameters. Total soluble solids (TSS), a key indicator of fruit quality, were slightly enhanced in plants treated with *B. megaterium* FBM09, suggesting a potential role of this strain in improving carbon allocation and sugar accumulation. Conversely, *B. pumilus* FBP01 showed lower TSS values, indicating variability in strain-specific metabolic effects on fruit composition. Fruit pH remained relatively stable across treatments, with only minor variations, while dry matter content showed no significant differences, although a slight increasing trend was observed in *B. megaterium* FBM09-treated plants. Overall, the results highlight that under optimal growing conditions, the benefits of microbial inoculation are less pronounced, particularly in terms of yield, and are mainly restricted to minor improvements in fruit quality attributes.

Conversely, phosphorus-deficient conditions clearly highlighted the functional role of PSB in improving plant performance. Phosphorus is an essential macronutrient for tomato cultivation, playing a central role in plant growth and development. Tomato crops typically require approximately 50 kg/ha of phosphorus during the growing season. This nutrient is particularly important during early developmental stages following transplanting, where it promotes root establishment, and later during flowering and fruit set, where it supports reproductive development. The significant reduction in yield observed in the RP control confirmed that P availability was a limiting factor. However, the inoculation with PSB effectively mitigated this limitation, demonstrating their capacity to mobilize insoluble phosphorus and enhance its bioavailability to plants. This function, where bacteria facilitate the transfer of nutrients from mineral sources to the plant in P-poor environments, is well-documented in literature (Kim et al., 1998; Galavi et al., 2011). The combination of PSB with RP resulted in a substantial increase in fruit yield, with *Bacillus pumilus* FBP01 and *Bacillus megaterium* FBM09 showing the highest performance. These treatments not only restored productivity levels comparable to the soluble P control (KH_2PO_4), but in some cases exceeded them, indicating a highly efficient microbial-mediated mobilization of phosphorus. Similar effects between PSB and insoluble P sources have been widely reported (Khan et al., 2009; Sharma et al., 2013). Fruit quality parameters were also significantly improved under P-limiting conditions. Inoculated plants grown with RP showed higher TSS and increased dry matter content, particularly with *B. pumilus* FBP01 and *B. megaterium* FBM09. This enhancement in fruit quality is directly linked to improved phosphorus nutrition, which is essential for energy metabolism and carbon partitioning (Raghothama, 1999; Copetta et al.,2011). Our findings align with studies by Al-Erwy et al. (2016) and Bona et al. (2017), which demonstrated that PSB inoculation under low-nutrient inputs triggers metabolic shifts in tomato fruits, leading to higher sugar accumulation and improved nutritional value.

Phosphorus uptake data further confirmed the effectiveness of microbial inoculations. The highest P-accumulation was observed when *B. megaterium* FBM09 or *B. pumilus* FBP01 were inoculated in soil supplemented with RP. The ability of these strains to transfer phosphorus to the plant suggests high rhizosphere competence and efficient nutrient exchange dynamics (Richardson et al., 2009). Furthermore, the observed changes in root architecture, characterized by increased density rather than simple elongation, support the hypothesis that PSBs maximize the soil exploration area in response to P-stress (Vacheron et al., 2013). While the impact of PSB is masked in nutrient-rich systems, their role becomes crucial under phosphorus limitation, where they act as key drivers of nutrient mobilization, plant productivity, and fruit quality. Among the tested strains, *B. megaterium* FBM09 and B. *pumilus* FBP01 emerged as the most promising candidates for sustainable biofertilizer applications in P-deficient agricultural soils.

Overall, this study demonstrates that the effectiveness of phosphate-solubilizing bacteria is strongly context-dependent, but under phosphorus-limited conditions they emerge as key drivers of nutrient mobilization and plant performance, supporting their promising application as sustainable bioinoculants for improving phosphorus use efficiency in agricultural systems. Compared to conventional chemical methods, this biological strategy, using *Bacillus megaterium* FBM09 and *B. pumilus* FBP01 to release phosphate from RP, is considered a more cost-effective and energy-efficient alternative. However, to better understand the phytoavailability of phosphorus in soils treated with rock phosphate and *Bacillus* spp., further in-depth studies are required. In addition, the compatibility among strains exhibiting plant growth–promoting and/or phosphate-solubilizing activities should be more thoroughly investigated to maximize their stimulatory effects, as their application represents an ecologically and economically sustainable approach.

6. CONCLUSIONS

This work investigated the role of plant growth-promoting microorganisms, with particular emphasis on phosphate-solubilizing microorganisms (PSMs), highlighting their potential in enhancing nutrient availability and improving crop performance.

The integrated phenotypic and physiological characterization and the quantitative assays confirmed the superior ability of strains such as *Pseudomonas putida* RPT12*, Bacillus pumilus* FBP01, and *Bacillus megaterium* FBM09 to mobilize phosphorus from insoluble sources like rock phosphate. The metabolic profiling via GC-MS revealed that these effects are linked to complex metabolic reprogramming, involving not only acidification but also the production of secondary metabolites, including phenolic acids and nitrogenous compounds, that vary significantly depending on the phosphorus source and the microbial species.

In vivo experiments on wheat and tomato plants confirmed these findings, demonstrating that microbial inoculation can significantly increase plant biomass and phosphorus accumulation, even under limiting nutrient conditions. A particularly relevant aspect emerged from the preliminary compatibility assays, which identified non-antagonistic combinations of best-performing strains, representing a fundamental step toward the development of tailor-made functional microbial consortia.

While the effectiveness of these bioinoculants is clear under controlled conditions, the complexity of plant–soil–microbiome interactions in the field remains a challenge. However, this work provides a robust framework for the selection of multifunctional strains and lays the groundwork for innovative, sustainable fertilization strategies. The integration of microbiological, metabolomic, and physiological approaches proves to be a key path toward reducing chemical inputs and enhancing the resilience of modern agricultural systems.

7. REFERENCES

Ab Rahman, S. F. S., Singh, E., Pieterse, C. M., Schenk, P. M. (2018). Emerging microbial biocontrol strategies for plant pathogens. *Plant Science*, 267, 102-111.

Adedayo, A. A., & Babalola, O. O. (2023). Fungi that promote plant growth in the rhizosphere boost crop growth. *Journal of Fungi*, 9(2), 239.

Adesemoye, A. O., Torbert, H. A., & Kloepper, J. W. (2008). Enhanced plant nutrient use efficiency with PGPR and AMF in an integrated nutrient management system. *Canadian journal of microbiology*, 54(10), 876-886.

Afzal, A. A., & Asghari Bano, A. B. (2008). Rhizobium and phosphate solubilizing bacteria improve the yield and phosphorus uptake in wheat (*Triticum aestivum*). *International Journal of Agriculture and Biology*, 2008, Volume 10 (1), 85-88.

Ahemad, M., & Kibret, M. (2014). Mechanisms and applications of plant growth promoting rhizobacteria: current perspective. *Journal of King saud University-science*, 26(1), 1-20.

Ahmad, A., Moin, S. F., Liaqat, I., Saleem, S., Muhammad, F., Mujahid, T., & Zafar, U. (2023). Isolation, solubilization of inorganic phosphate, and production of organic acids by individual and co-inoculated microorganisms. *Geomicrobiology Journal*, 40(1), 111-121.

Alam, S., Khalil, S., Ayub, N., & Rashid, M. (2002). In vitro solubilization of inorganic phosphate by phosphate solubilizing microorganisms (PSM) from maize rhizosphere. *Int J Agric Biol*, 4(4), 454-458.

Al-Erwy, A. S., Bafeel, S. O., & Al-Toukhy, A. (2016). Effect of chemical, organic and bio fertilizers on germination, growth and yield of wheat (*Triticum aestivum* L.) plants irrigated with sea water. seeds, 10(100.1).

Alfa, M. I., Adie, D. B., Igboro, S. B., Oranusi, U. S., Dahunsi, S. O., & Akali, D. M. (2014). Assessment of biofertilizer quality and health implications of anaerobic digestion effluent of cow dung and chicken droppings. *Renewable energy*, 63, 681-686.

Argentel-Martínez, L., Peñuelas-Rubio, O., Herrera-Sepúlveda, A., González-Aguilera, J., Sudheer, S., Salim, L. M., ... & Azizoglu, U. (2025). Biotechnological advances in plant growth-promoting rhizobacteria for sustainable agriculture. *World Journal of Microbiology and Biotechnology*, 41(1), 21.

Aseri, G. K., Jain, N., & Tarafdar, J. C. (2009). Hydrolysis of organic phosphate forms by phosphatases and phytase producing fungi of arid and semi-arid soils of India. *Am Eurasian J Agric Environ Sci*, *5*(4), 564-570.

Asghar, W., Craven, K. D., Kataoka, R., Mahmood, A., Asghar, N., Raza, T., & Iftikhar, F. (2024). The application of *Trichoderma* spp., an old but new useful fungus, in sustainable soil health intensification: A comprehensive strategy for addressing challenges. *Plant Stress*, 100455.

Ayaz, M., Ali, Q., Jiang, Q., Wang, R., Wang, Z., Mu, G., ... & Gu, Q. (2022). Salt tolerant *Bacillus* strains improve plant growth traits and regulation of phytohormones in wheat under salinity stress. *Plants, 11* (20), 2769.

Backer, R., Rokem, J. S., Ilangumaran, G., Lamont, J., Praslickova, D., Ricci, E., ... & Smith, D. L. (2018). Plant growth-promoting rhizobacteria: context, mechanisms of action, and roadmap to commercialization of biostimulants for sustainable agriculture. *Frontiers in plant science*, 9, 1473.

Bais, H. P., Weir, T. L., Perry, L. G., Gilroy, S., & Vivanco, J. M. (2006). The role of root exudates in rhizosphere interactions with plants and other organisms. *Annu. Rev. Plant Biol.*, 57(1), 233-266.

Bakki, M., Banane, B., Marhane, O., Esmaeel, Q., Hatimi, A., Barka, E. A., ... & Bouizgarne, B. (2024). Phosphate solubilizing Pseudomonas and Bacillus combined with rock phosphates promoting tomato growth and reducing bacterial canker disease. *Frontiers in Microbiology*, 15, 1289466.

Baldotto, M. A., & Baldotto, L. E. B. (2013). Gladiolus development in response to bulb treatment with different concentrations of humic acids. *Revista ceres*, 60(1), 138-142.

Bardin, M., & Pugliese, M. (2020). Biocontrol agents against diseases. Integrated pest and disease management in greenhouse crops, 385-407. Cham: Springer International Publishing.

Bargaz, A. (2020) Phosphate Solubilizing Rhizobacteria Could Have a Stronger Influence on Wheat Root Traits and Aboveground Physiology Than Rhizosphere P Solubilization. *Front. Plant Sci.* 11:979.

Batista, B. D., & Singh, B. K. (2021). Realities and hopes in the application of microbial tools in agriculture. *Microbial Biotechnology*, 14(4), 1258-1268.

Batool, S., Iqbal, A. (2019) Phosphate solubilizing rhizobacteria as alternative of chemical fertilizer for growth and yield of *Triticum aestivum* (Var. Galaxy 2013). *Saudi J. Biol. Sci.* 26, 1400–1410.

Benbrik, B., Elabed, A., Iraqui, M., Ghachtouli, N.E., Douira, A., Amir, S., Filali-Maltouf, A., El Abed, S., El Modafar, C., Ibnsouda-Koraichi, S. (2021) A phosphocompost amendment enriched with PGPR consortium enhancing plants growth in deficient soil. *Commun. Soil Sci. Plant. Anal*. 52, 1236–1247.

Berlyn, G. P., & Russo, R. O. (1990). The use of organic biostimulants in nitrogen fixing trees. CABI digital library, 78-80.

Bona, E., Cantamessa, S., Massa, N., Manassero, P., Marsano, F., Copetta, A., ... & Berta, G. (2017). Arbuscular mycorrhizal fungi and plant growth-promoting pseudomonads improve yield, quality and nutritional value of tomato: a field study. *Mycorrhiza*, 27(1), 1-11.

Borgi, M.A., Saidi, I., Moula, A., Rhimi, S., Rhimi, M. (2020) The attractive *Serratia plymuthica* BMA1 strain with high rock phosphate-solubilizing activity and its effect on the growth and phosphorus uptake by vicia faba L. plants. *Geomicrobiol. J.* 37, 437–445.

Bouizgarne, B., Bakki, M., Boutasknit, A., Banane, B., El Ouarrat, H., Ait El Maalem, S., ... & Meddich, A. (2023). Phosphate and potash solubilizing bacteria from Moroccan phosphate mine showing antagonism to bacterial canker agent and inducing effective tomato growth promotion. *Frontiers in Plant Science*, 14, 970382.

Brown, P., & Saa, S. (2015). Biostimulants in agriculture. *Frontiers in plant science*, 6, 671.

Carvalho, A. F. A., de Oliva Neto, P., Da Silva, D. F., & Pastore, G. M. (2013). Xylo-oligosaccharides from lignocellulosic materials: chemical structure, health benefits and production by chemical and enzymatic hydrolysis. *Food Research International*, 51(1), 75-85.

Chen, Y. L., Lee, C. C., Lin, Y. L., Yin, K. M., Ho, C. L., & Liu, T. (2015). Obtaining long 16S rDNA sequences using multiple primers and its application on dioxin-containing samples. *BMC bioinformatics*, 16(Suppl 18), S13.

Chen, Y.P. P.D. Rekha, P.D., A.B. Arun, A.B., F.T. Shen, F.T., Lai, W.A., Young, C.C. (2006) Phosphate solubilizing bacteria from subtropical soil and their tricalcium phosphate solubilizing abilities. *Applied Soil Ecology*, Volume 34 (1), 33-41.

Choi, J., Choi, D., Lee, S., Ryu, C. M., & Hwang, I. (2011). Cytokinins and plant immunity: old foes or new friends? *Trends in plant science*, 16(7), 388-394.

Choudhary, D. K., Prakash, A., & Johri, B. N. (2007). Induced systemic resistance (ISR) in plants: mechanism of action. *Indian journal of microbiology*, 47, 289-297.

Cohen, A. C., Bottini, R., & Piccoli, P. (2015). Role of abscisic acid producing PGPR in sustainable agriculture. *Bacterial metabolites in sustainable agroecosystem*, 259-282.

Colla, G., Hoagland, L., Ruzzi, M., Cardarelli, M., Bonini, P., Canaguier, R., & Rouphael, Y. (2017). Biostimulant action of protein hydrolysates: Unraveling their effects on plant physiology and microbiome. *Frontiers in plant science*, *8*, 327435.

Comerford NB (1998) Soil phosphorus bioavailability. In: Lynch JP, Deikman J (eds) Phosphorus in plant biology: regulatory roles in molecular, cellular, organismic, and ecosystem processes. American Society of Plant Physiologists, *Rockville*, pp 136–147

Compant S, Duffy B, Nowak J, Clément C, Barka EA (2005). Use of Plant Growth-Promoting Bacteria for Biocontrol of Plant Diseases: Principles, Mechanisms of Action, and Future Prospects. *Applied Environ*mental *Microbiology* 71 (9)

Compant, S., Cassan, F., Kostić, T., Johnson, L., Brader, G., Trognitz, F., & Sessitsch, A. (2024). Harnessing the plant microbiome for sustainable crop production. *Nature Reviews Microbiology*, 1-15.

Compant, S., Duffy, B., Nowak, J., Clément, C., & Barka, E. A. (2005). Use of plant growth-promoting bacteria for biocontrol of plant diseases: principles, mechanisms of action, and future prospects. *Applied and environmental microbiology*, 71(9), 4951-4959.

Conrath, U. (2006). Systemic acquired resistance. *Plant signaling & behavior*, 1(4), 179-184.

Correaa, O. S., Montecchiaa, M. S., Bertia, M.F., Ferraria, M.F., Pucheub, N.L., Kerberb, N.L., Garcı´a, A.F. (2009) *Bacillus amyloliquefaciens* BNM122, a potential microbial biocontrol agent applied on soybean seeds, causes a minor impact on rhizosphere and soil microbial communities *Applied soil ecology* 41, 185–194.

Das, P. P., Singh, K. R., Nagpure, G., Mansoori, A., Singh, R. P., Ghazi, I. A., ... & Singh, J. (2022). Plant-soil-microbes: A tripartite interaction for nutrient acquisition and better plant growth for sustainable agricultural practices. *Environmental Research*, 214, 113821.

de Groot, C. C., Marcelis, L. F., van den Boogaard, R., Kaiser, W. M., & Lambers, H. (2003). Interaction of nitrogen and phosphorus nutrition in determining growth. *Plant and Soil*, 248(1), 257-268.

De Pascale, S., Rouphael, Y., & Colla, G. (2017). Plant biostimulants: Innovative tool for enhancing plant nutrition in organic farming. *Eur. J. Hortic. Sci*, 82(6), 277-285.

De Ridder, M., De Jong, S., Polchar, J., & Lingemann, S. (2012, December). Risks and opportunities in the global phosphate rock market: robust strategies in times of uncertainty.

Ding, Y., Yi, Z., Fang, Y., He, S., Li, Y., He, K., Zhao, H., Jin, Y. (2021). Multi-omics reveal the efficient phosphate-solubilizing mechanism of bacteria on rocky soil. *Frontiers in Microbiology*, 12, 761972.

Dodor, D. E., & Tabatabai, M. A. (2003). Effect of cropping systems on phosphatases in soils. *Journal of Plant Nutrition and Soil Science*, 166(1), 7-13.

Duponnois, R., Kisa, M., & Plenchette, C. (2006). Phosphate-solubilizing potential of the nematophagous fungus *Arthrobotrys oligospora*. *Journal of Plant Nutrition and Soil Science*, 169(2), 280-282.

Edi Premono, M., Moawad, A. M., & Vlek, P. L. G. (1996). Effect of phosphate-solublizing Pseudomonas putida on the growth of maize and its survival in the rhizosphere. CABI digital library, 13-23.

Egamberdieva, D., Wirth, S. J., Alqarawi, A. A., Abd_Allah, E. F., & Hashem, A. (2017). Phytohormones and beneficial microbes: essential components for plants to balance stress and fitness. *Frontiers microbiology*, in 8, 2104.

El Maaloum, S., Elabed, A., Alaoui-Talibi, Z.E., Meddich, A., Filali-Maltouf, A., Douira, A., Ibnsouda-Koraichi, S., Amir, S., El Modafar, C. (2020). Effect of arbuscular mycorrhizal fungi and phosphate-solubilizing bacteria consortia associated with phospho-compost on phosphorus solubilization and growth of tomato seedlings (*Solanum lycopersicum* L.). *Commun. Soil Sci. Plant. Anal*. 51, 622–634.

Elhaissoufi, W., Khourchi, S., Ibnyasser, A., Ghoulam, C., Rchiad, Z., Zeroual, Y., ... & Bargaz, A. (2020). Phosphate solubilizing rhizobacteria could have a stronger influence on wheat root traits and aboveground physiology than rhizosphere P solubilization. *Frontiers in plant science*, 11, 979.

El-Hasan, A., Walker, F., Schöne, J., & Buchenauer, H. (2007). Antagonistische Wirkung von 6-Pentyl-alpha-pyron aus Trichoderma harzianum gegen Fusarium moniliforme. *Journal of Plant Diseases and Protection*, 114, 62-68.

El-Saadony, M. T., Saad, A. M., Soliman, S. M., Salem, H. M., Ahmed, A. I., Mahmood, M., ... & AbuQamar, S. F. (2022). Plant growth-promoting microorganisms as biocontrol agents of plant diseases: Mechanisms, challenges and future perspectives. *Frontiers in plant science*, 13, 923880.

Elser, J. J., Bracken, M. E., Cleland, E. E., Gruner, D. S., Harpole, W. S., Hillebrand, H., ... & Smith, J. E. (2007). Global analysis of nitrogen and phosphorus limitation of primary producers in freshwater, marine and terrestrial ecosystems. *Ecology letters*, 10(12), 1135-1142.

Ertani, A., Francioso, O., Tugnoli, V., Righi, V., & Nardi, S. (2011). Effect of commercial lignosulfonate-humate on *Zea mays* L. metabolism. *Journal of agricultural and food chemistry,* 59(22), 11940-11948.

Fahad, S., Hussain, S., Matloob, A., Khan, F. A., Khaliq, A., Saud, S., ... & Huang, J. (2015). Phytohormones and plant responses to salinity stress: a review. *Plant growth regulation,* 75, 391-404.

Fankem, H., Tchakounte, G. T., Nkot, L. N., Mafokoua, H. L., Dondjou, D. T., Simo, C., ... & Etoa, F. X. (2015). Common bean (*Phaseolus vulgaris* L.) and soya bean (Glycine max) growth and nodulation as influenced by rock phosphate solubilising bacteria under pot grown conditions. *International Journal of Agricultural Policy and Research*, 3(5), 242–250.

Fasim, F., Ahmed, N., Parsons, R., & Gadd, G. M. (2002). Solubilization of zinc salts by a bacterium isolated from the air environment of a tannery. *FEMS microbiology letters*, 213(1), 1-6.

Furihata, T., Suzuki, M., Sakurai, H. (1992) Kinetic characterization of two phosphate uptake systems with different affinities in suspension-cultured Catharanthus roseus protoplasts. *Plant Cell Physiology* 33, 1151–1157

Galavi, M., Yosefi, K., Ramrodi, M., & Mousavi, S. R. (2011). Effect of bio-phosphate and chemical phosphorus fertilizer accompanied with foliar application of micronutrients on yield, quality and phosphorus and zinc concentration of maize. *Journal of Agricultural Science*, *3*(4), 22.

Gao, Q. M., Zhu, S., Kachroo, P., & Kachroo, A. (2015). Signal regulators of systemic acquired resistance. *Frontiers in plant science*, 6, 228.

Ghorbanpour, M., Omidvari, M., Abbaszadeh-Dahaji, P., Omidvar, R., & Kariman, K. (2018). Mechanisms underlying the protective effects of beneficial fungi against plant diseases. *Biological Control*, 117, 147-157.

Glick, B. R. (2012). Plant growth-promoting bacteria: mechanisms and applications. Scientifica, 2012(1), 963401.

Goldstein, A. H. (1995). Recent Progress in Understanding the Molecular Genetics and Biochemistry of Calcium Phosphate Solubilization by Gram Negative Bacteria. *Biological Agriculture & Horticulture*, 12(2), 185–193.

Goldstein, A. H., Braverman, K., & Osorio, N. (1999). Evidence for mutualism between a plant growing in a phosphate-limited desert environment and a mineral phosphate solubilizing (MPS) rhizobacterium. *FEMS microbiology ecology*, 30(4), 295-300.

Goswami, M., & Suresh, D. E. K. A. (2020). Plant growth-promoting rhizobacteria—alleviators of abiotic stresses in soil: a review. *Pedosphere*, 30(1), 40-61.

Gozzo, F. (2003). Systemic acquired resistance in crop protection: from nature to a chemical approach. *Journal of Agricultural and Food Chemistry*, 51(16), 4487-4503.

Grant, C. A., Flaten, D. N., Tomasiewicz, D. J., & Sheppard, S. C. (2001). The importance of early season phosphorus nutrition. *Canadian journal of plant science*, 81(2), 211-224.

Halbleib, C. M., & Ludden, P. W. (2000). Regulation of biological nitrogen fixation. *The Journal of nutrition*, 130(5), 1081-1084.

Halder, AK., Mishra, AK., Bhattacharya, P., Chakrabarthy, PK. (1990) Solubilization of rock phosphate by Rhizobium and Bradyrhizobium. *Journal of general Applied Microbiology*, 36, 81–92.

Hamdali, H., Moursalou, K., Tchangbedji, G., Ouhdouch, Y., & Hafidi, M. (2012). Isolation and characterization of rock phosphate solubilizing actinobacteria from a Togolese phosphate mine. African Journal of Biotechnology, 11(2), 312.

Hamza, B., & Suggars, A. (2001). Biostimulants: myths and realities. *TurfGrass Trends*, 8, 6-10.

Harman, G. E., Howell, C. R., Viterbo, A., Chet, I., & Lorito, M. (2004). *Trichoderma* species—opportunistic, avirulent plant symbionts. *Nature reviews microbiology*, 2(1), 43-56.

Harman, G., Khadka, R., Doni, F., & Uphoff, N. (2021). Benefits to plant health and productivity from enhancing plant microbial symbionts. *Frontiers in plant science*, 11, 610065.

Herlemann, D.P.R., Labrenz, M., Jürgens, K., Bertilsson, S., Waniek, J.J., Andersson, A.F. (2011). Transitions in bacterial communities along the 2000 km salinity gradient of the Baltic Sea Autori , *The ISME Journal (International Society for Microbial Ecology)*, 5(10), 1571-1579.

Hidangmayum, A., & Sharma, R. (2017). Effect of different concentrations of commercial seaweed liquid extract of *Ascophyllum nodosum* as a plant bio stimulant on growth, yield and biochemical constituents of onion (*Allium cepa* L.). *J. Pharmacogn. Phytochem*, *6*(4), 658-663.

Hinsinger, P. (2001). Bioavailability of soil inorganic P in the rhizosphere as affected by root-induced chemical changes. *Plant and Soil*, 237, 173–195.

Hoagland, D. R., & Arnon, D. I. (1938). The water-culture method for growing plants without soil. *Circular. California Agricultural Experiment Station*, Vol. 347, 39.

Hoffmann, T., Bremer, E. (2017) Guardians in a stressful world: the Opu family of compatible solute transporters from *Bacillus subtilis*. *Biological Chemistry*, volume 398 (2), 193-214.

Höfte, M., & Bakker, P. A. (2007). Competition for iron and induced systemic resistance by siderophores of plant growth promoting rhizobacteria. *In Microbial siderophores* (pp. 121-133). Berlin, Heidelberg: Springer Berlin Heidelberg.

Holden, M.T.G., Ram Chhabra, S., De Nys, R., Stead, P., Bainton, N.J., Hill, P.J., Manefield, M., Kumar, N., Labatte, M., England, D., Rice, S., Givskov, M., Salmond, G.P.C., Stewart, G.S.A.B., Bycroft, B.W., Kjelleberg, S., Williams, P. (1999), Quorum-sensing cross talk: isolation and chemical characterization of cyclic dipeptides from *Pseudomonas aeruginosa* and other Gram-negative bacteria. *Molecular Microbiology*, 33: 1254-1266.

Holford, I. C. R. (1997). Soil phosphorus: its measurement, and its uptake by plants. *Australian Journal of Soil Research*, 35 (2), 227–239.

Hossain, M. M., & Sultana, F. (2020). Application and mechanisms of plant growth promoting fungi (PGPF) for phytostimulation. *Organic agriculture*, 1, 31.

Hossain, M.M., Sultana, F., Islam, S. (2017). Plant Growth-Promoting Fungi (PGPF): Phytostimulation and Induced Systemic Resistance. In: Singh, D., Singh, H., Prabha, R. (eds) Plant-Microbe Interactions in Agro-Ecological Perspectives. Springer, Singapore.

Huang, C. Y., Shirley, N., Genc, Y., Shi, B., & Langridge, P. (2011). Phosphate utilization efficiency correlates with expression of low-affinity phosphate transporters and noncoding RNA, IPS1, in barley. Plant Physiology, 156(3), 1217-1229.

Hurtado, MD, Carmona, S., & Delgado, A. (2008). Automated modification of the molybdenum blue colorimetric method for phosphorus determination in soil extracts. *Communications in soil science and plant analysis*, 39 (15-16), 2250-2257.

Hwangbo, H., Park, R. D., Kim, Y. W., Rim, Y. S., Park, K. H., Kim, T. H., ... & Kim, K. Y. (2003). 2-Ketogluconic acid production and phosphate solubilization by Enterobacter intermedium. *Current microbiology*, *47*(2), 0087-0092.

Illmer, P., & Schinner, F. (1995). Solubilization of inorganic calcium phosphates—solubilization mechanisms. *Soil Biology and Biochemistry*, *27*(3), 257-263.

Islam, M. T., & Hossain, M. M. (2012). Plant Probiotics in Phosphorus Nutrition in Crops, with Special Reference to Rice. In: D. K. Maheshwari (Ed.), Bacteria in Agrobiology: Plant Probiotics (pp. 325-363), Springer, Berlin Heidelberg.

Islam, M. T., Deora, A., Hashidoko, Y., Rahman, A., Ito, T., & Tahara S. (2007). Isolation and Identification of Potential Phosphate Solubilizing Bacteria from the Rhizoplane of Oryza sativa L. cv. *BR29 of Bangladesh. Zeitschrift für Naturforschung* C, 62, 103-110.

Jain, R., Saxena, J., & Sharma, V. (2010). The evaluation of free and encapsulated Aspergillus awamori for phosphate solubilization in fermentation and soil–plant system. *Applied Soil Ecology*, 46(1), 90-94.

Jeschke, W. D., Kirkby, E. A., Peuke, A. D., Pate, J. S., & Hartung, W. (1997). Effects of P deficiency on assimilation and transport of nitrate and phosphate in intact plants of castor bean (*Ricinus communis* L.). *Journal of Experimental Botany*, 48(1), 75-91.

Kalayu, G. (2019). Phosphate solubilizing microorganisms: promising approach as biofertilizers. International Journal of Agronomy, 2019(1), 4917256.

Kamilova, F., Validov, S., Azarova, T., Mulders, I., & Lugtenberg, B. (2005). Enrichment for enhanced competitive plant root tip colonizers selects for a new class of biocontrol bacteria. *Environmental microbiology*, 7(11), 1809-1817.

Kang, S.M., Khan, M.A., Hamayun, M., Kim, L.R., Kwon, E.H., Kang, Y.S., Kim, K.Y., Park, J.J., Lee, I.J. (2021). Phosphate-solubilizing *Enterobacter ludwigii* AFFR02 and *Bacillus megaterium* Mj1212 rescues alfalfa's growth under post-drought stress. *Agriculture* 11, 485.

Kauffman, G. L., Kneivel, D. P., & Watschke, T. L. (2007). Effects of a biostimulant on the heat tolerance associated with photosynthetic capacity, membrane thermostability, and polyphenol production of perennial ryegrass. *Crop science*, 47(1), 261-267.

Kazerooni, E. A., Maharachchikumbura, S. S., Al-Sadi, A. M., Kang, S. M., Yun, B. W., & Lee, I. J. (2021). Biocontrol potential of *Bacillus amyloliquefaciens* against *Botrytis pelargonii* and *Alternaria alternata* on *Capsicum annuum. Journal of fungi*, 7(6), 472.

Khamsuk, K., Dell, B., Pathom-Aree, W., Pathaichindachote, W., Suphrom, N., Nakaew, N., & Jumpathong, J. (2024). Screening plant growth-promoting bacteria with antimicrobial properties for upland rice. *Journal of microbiology and biotechnology*, 34(5), 1029.

Khan, A. A., Jilani, G., Akhtar, M. S., Naqvi, S. M. S., & Rasheed, M. (2009). Phosphorus solubilizing bacteria: occurrence, mechanisms and their role in crop production. *J. agric. biol. sci*, 1(1), 48-58.

Khan, A. R., Mustafa, A., Hyder, S., Valipour, M., Rizvi, Z. F., Gondal, A. S., ... & Daraz, U. (2022). *Bacillus* spp. as bioagents: uses and application for sustainable agriculture. *Biology*, 11(12), 1763.

Kim, KY., Jordan, D., Mcdonald, G.A. (1998). *Enterobacter agglomerans*, phosphate solubilizing bacteria, and microbial activity in soil: effect of carbon source. *Soil Biology Biochemistry* 30, 995–1003.

Klindworth, A., Pruesse, E., Schweer, T., Peplies, J., Quast, C., Horn, M., & Glöckner, F. O. (2013). Evaluation of general 16S ribosomal RNA gene PCR primers for classical and next-generation sequencing-based diversity studies. Nucleic acids research, 41(1), e1-e1.

Kolomazník, K., Pecha, J., Friebrová, V., Janáčová, D., & Vašek, V. (2012). Diffusion of biostimulators into plant tissues. Heat and mass transfer, 48(9), 1505-1512.

Kpomblekou-a, K., & Tabatabai, M. A. (1994). Effect of organic acids on release of phosphorus from phosphate rocks1. Soil Science, 158(6), 442-453.

Kumar, A., Kumar, A., & Patel, H. (2018). Role of microbes in phosphorus availability and acquisition by plants. International journal of current microbiology and applied Sciences, 7(5), 1344-1347.

Kumar, N., Srivastava, P., Vishwakarma, K., Kumar, R., Kuppala, H., Maheshwari, S. K., & Vats, S. (2020). The rhizobium–plant symbiosis: state of the art. *Plant microbe symbiosis*, 1-20.

Kunicki, E., Grabowska, A., Sękara, A., & Wojciechowska, R. (2010). The effect of cultivar type, time of cultivation, and biostimulant treatment on the yield of spinach (*Spinacia oleracea* L.). *Folia Horticulturae*, 22(2), 9-13.

Lahlali, R., Ezrari, S., Radouane, N., Kenfaoui, J., Esmaeel, Q., El Hamss, H., ... & Barka, E. A. (2022). Biological control of plant pathogens: A global perspective. *Microorganisms,* 10(3), 596.

Lin DaoHui, L. D., & Xing, B. S. (2007). Phytotoxicity of nanoparticles: inhibition of seed germination and root growth.

Liu, F., Xing, S., Ma, H., Du, Z., & Ma, B. (2013). Cytokinin-producing, plant growth-promoting rhizobacteria that confer resistance to drought stress in *Platycladus orientalis* container seedlings. *Applied microbiology and biotechnology*, 97, 9155-9164.

Lopes, M. J., Filho, M. B. D., Reis Castro, T. H., Filippi, M. C. C., and Silva, G. B. (2018a). Effect of *Pseudomonas fluorescens* and *Burkholderia pyrrocinia* on the growth improvement and physiological responses in *Brachiaria brizantha*. *Am. J. Plant Sci.* 9, 250–265. doi: 10.4236/ajps.2018.92021

López-Bucio, J., Pelagio-Flores, R., & Herrera-Estrella, A. (2015). Trichoderma as biostimulant: exploiting the multilevel properties of a plant beneficial fungus. *Scientia horticulturae*, 196, 109-123.

Louden, B. C., Haarmann, D., & Lynne, A. M. (2011). Use of blue agar CAS assay for siderophore detection. Journal of microbiology & biology education, 12(1), 51-53.

Lugtenberg, B. J., Chin-A-Woeng, T. F., & Bloemberg, G. V. (2002). Microbe–plant interactions: principles and mechanisms. *Antonie Van Leeuwenhoek*, 81, 373-383.

Ma, Y., Li, Y., Yang, S., Li, Y., & Zhu, Z. (2023). Biocontrol potential of *Trichoderma asperellum* strain 576 against *Exserohilum turcicum* in *Zea mays*. *Journal of Fungi*, 9(9), 936.

Magaya, S., Magid, J., Hermann, L., & Schulp, C. J. E. (2024). Phosphorus removal and use in organic crop farming in the EU. Nutrient Cycling in Agroecosystems, 1-20.

Mahmud, A.A., Upadhyay, S.K., Srivastava, A.K., Bhojiya, A.A. (2021). Biofertilizers: a nexus between soil fertility and crop productivity under abiotic stress. *Curr. Opin. Environ. Sustain.* 3, 100063.

Malhotra, A., & Habibovic, P. (2016). Calcium phosphates and angiogenesis: implications and advances for bone regeneration. Trends in biotechnology, 34(12), 983-992.

Mardad, I., Serrano, A., & Soukri, A. (2013). Solubilization of inorganic phosphate and production of organic acids by bacteria isolated from a Moroccan mineral phosphate deposit.

Marschner, P. (2012). Marschner's Mineral Nutrition of Higher Plants (3rd ed.). *Academic Press.*

Mendoza-Arroyo, G. E., Chan-Bacab, M. J., Aguila-Ramírez, R. N., Ortega-Morales, B. O., Canché Solís, R. E., Chab-Ruiz, A. O., ... & Camacho-Chab, J. C. (2020). Inorganic phosphate solubilization by a novel isolated bacterial strain Enterobacter sp. ITCB-09 and its application potential as biofertilizer. *Agriculture*, 10(9), 383.

Miethke, M., Klotz, O., Linne, U., May, J. J., Beckering, C. L., & Marahiel, M. A. (2006). Ferri-bacillibactin uptake and hydrolysis in *Bacillus subtilis*. *Molecular microbiology*, *61*(6), 1413-1427.

Mittal, V., Singh, O., Nayyar, H., Kaur, J., & Tewari, R. (2008). Stimulatory effect of phosphate-solubilizing fungal strains (*Aspergillus awamori* and *Penicillium citrinum*) on the yield of chickpea (*Cicer arietinum* L. cv. GPF2). *Soil Biology and Biochemistry*, 40(3), 718-727.

Montanarella, L., & Panagos, P. (2021). The relevance of sustainable soil management within the European Green Deal. Land use policy, 100, 104950.

Mpanga, I. K., Nkebiwe, P. M., Kuhlmann, M., Cozzolino, V., Piccolo, A., Geistlinger, J., ... & Neumann, G. (2019). The form of N supply determines plant growth promotion by P-solubilizing microorganisms in maize. *Microorganisms*, *7*(2), 38.

Murphy, J. A. M. E. S., & Riley, J. P. (1962). A modified single solution method for the determination of phosphate in natural waters. *Analytica chimica acta*, 27, 31-36.

Nardi, S., Pizzeghello, D., Schiavon, M., & Ertani, A. (2016). Plant biostimulants: physiological responses induced by protein hydrolyzed-based products and humic substances in plant metabolism. *Scientia Agricola*, *73*, 18-23.

Nautiyal, C. S. (1999). An efficient microbiological growth medium for screening phosphate solubilizing microorganisms. *FEMS microbiology Letters*, 170(1), 265-270.

Nesme, T., & Withers, P. J. (2016). Sustainable strategies towards a phosphorus circular economy. Nutrient Cycling in Agroecosystems, 104, 259-264.

Nicotra, D., Mosca, A., Dimaria, G., Massimino, M. E., Di Stabile, M., La Bella, E., ... & Catara, V. (2025). Mitigating Water Stress in Plants with Beneficial Bacteria: Effects on Growth and Rhizosphere Bacterial Communities. *International Journal of Molecular Sciences*, 26(4), 1467.

Nicotra, D., Mosca, A., Dimaria, G., Tessitori, M., Vetukuri, R. R., & Catara, V. (2024). Temporal Dynamics of the Tomato Rhizosphere Microbiome in Response to Synthetic Communities of Plant Growth-Promoting Rhizobacteria. *bioRxiv*, 2024-12.

Nicotra, D., Ghadamgahi, F., Ghosh, S., Anzalone, A., Dimaria, G., Mosca, A., Massimino, M.E., Vetukuri, R.R. and Catara, V. (2024). Genomic insights and biocontrol potential of ten bacterial strains from the tomato core microbiome. *Frontiers in Plant Science*, 15, 1437947.

Nobahar, A., Sarikhani, M. R., & Chalabianlou, N. (2017). Buffering capacity affects phosphorous solubilization assays in rhizobacteria. *Rhizosphere,* 4, 119-125.

Norrie, J., & Keathley, J. P. (2005, June). Benefits of *Ascophyllum nodosum* marine-plant extract applications to "Thompson Seedless" grape production. *In X International Symposium on Plant Bioregulators in Fruit Production* 727 (pp. 243-248).

O'Brien, P. A. (2017). Biological control of plant diseases. *Australasian Plant Pathology*, 46, 293-304.

O'Byrne, C. P., & Booth, I. R. (2002). Osmoregulation and its importance to food safety. *International Journal of Food Microbiology*, 74(3), 203-216

Olanrewaju, O. S., Glick, B. R., & Babalola, O. O. (2017). Mechanisms of action of plant growth promoting bacteria. *World Journal of Microbiology and Biotechnology*, 33, 1-16.

Olsen, S. R. (1954). Estimation of available phosphorus in soils by extraction with sodium bicarbonate (No. 939). *US Department of Agriculture*.

Ongena, M., & Jacques, P. (2008). Bacillus lipopeptides: versatile weapons for plant disease biocontrol. Trends in microbiology, 16(3), 115-125.

Panchal, P., Miller, A. J., & Giri, J. (2021). Organic acids: versatile stress-response roles in plants. *Journal of Experimental Botany*, 72(11), 4038-4052.

Pande, A., Pandey, P., Mehra, S., Singh, M., & Kaushik, S. (2017). Phenotypic and genotypic characterization of phosphate solubilizing bacteria and their efficiency on the growth of maize. *Journal of Genetic Engineering and Biotechnology*, *15*(2), 379-391.

Pikovskaya, R. I. (1948). Mobilization of phosphorus in soil connection with the vital activity of some microbial species. *Microbiologiya* 17 : 362–370

Poirier, Y., & Bucher, M. (2002). Phosphate transport and homeostasis in Arabidopsis. The Arabidopsis book/*American Society of Plant Biologists*, 1, e0024.

Povero, G., Mejia, J. F., Di Tommaso, D., Piaggesi, A., & Warrior, P. (2016). A systematic approach to discover and characterize natural plant biostimulants. *Frontiers in plant science*, 7, 435.

Qiao, J. Q., Wu, H. J., Huo, R., Gao, X. W., & Borriss, R. (2014). Stimulation of plant growth and biocontrol by Bacillus amyloliquefaciens FBA21subsp. plantarum FZB42 engineered for improved action. *Chemical and Biological Technologies in Agriculture*, 1(1), 12.

Raaijmakers, J. M., De Bruijn, I., Nybroe, O., & Ongena, M. (2010). Natural functions of lipopeptides from Bacillus and Pseudomonas: more than surfactants and antibiotics. *FEMS microbiology reviews*, 34(6), 1037-1062.

Raghothama, K.G. (1999) Phosphorus metabolism. *Annual Review of Plant Biology*, Volume 50, 665-693.

Rashid, M., Khalil, S., Ayub, N., Alam, S., Latif, F. (2004) Organic acids production and phosphate solubilization by phosphate solubilizing microorganisms (PSM) under *vitro* conditions. *Pak J Biol Sci*, 7, 187–196

Rawat, P., Das, S., Shankhdhar, D., & Shankhdhar, S. C. (2021). Phosphate-solubilizing microorganisms: mechanism and their role in phosphate solubilization and uptake. Journal of Soil *Science and Plant Nutrition*, 21(1), 49-68.

Re, R., Pellegrini, N., Proteggente, A., Pannala, A., Yang, M., & Rice-Evans, C. (1999). Antioxidant activity applying an improved ABTS radical cation decolorization assay. *Free radical biology and medicine*, 26(9-10), 1231-1237.

Reyes, I., Bernier, L., Simard, R. R., & Antoun, H. (1999). Effect of nitrogen source on the solubilization of different inorganic phosphates by an isolate of *Penicillium rugulosum* and two UV-induced mutants. *FEMS Microbiology Ecology*, 28(3), 281-290.

Rezakhani, L., Motesharezadeh, B., Tehrani, M. M., Etesami, H., & Hosseini, H. M. (2019). Phosphate–solubilizing bacteria and silicon synergistically augment phosphorus (P) uptake by wheat (*Triticum aestivum* L.) plant fertilized with soluble or insoluble P source. *Ecotoxicology and Environmental Safety*, 173, 504-513.

Richardson, A. E., & Simpson, R. J. (2011). Soil microorganisms mediating phosphorus availability. Volume 156 (3), 989–996.

Rodríguez, H., & Fraga, R. (1999). Phosphate solubilizing bacteria and their role in plant growth promotion. *Biotechnology advances*, 17(4-5), 319-339.

Romeiro, R. S. (2007). Controle biológico de doenças de plantas: procedimentos. Viçosa, MG: Universidade Federal de Viçosa. 172p.

Romera, F. J., García, M. J., Lucena, C., Martínez-Medina, A., Aparicio, M. A., Ramos, J., ... & Pérez-Vicente, R. (2019). Induced systemic resistance (ISR) and Fe deficiency responses in dicot plants. *Frontiers in Plant Science,* 10, 287.

Rouphael, Y., & Colla, G. (2020). Biostimulants in agriculture. *Frontiers in plant science*, *11*, 40.

Rutherford, P. M., Dudas, M. J., & Arocena, J. M. (1995). Trace elements and fluoride in phosphogypsum leachates. *Environmental technology*, 16(4), 343-354.

Sabaratnam, S., & Traquair, J. A. (2015). Mechanism of antagonism by *Streptomyces griseocarneus* (strain Di944) against fungal pathogens of greenhouse-grown tomato transplants. *Canadian Journal of Plant Pathology*, 37(2), 197-211.

Saeed, Q.; Xiukang, W.; Haider, F.U.; Kučerik, J.; Mumtaz, M.Z.; Holatko, J.; Naseem, M.; Kintl, A.; Ejaz, M.; Naveed, M.; et al. Rhizosphere Bacteria in Plant Growth Promotion, Biocontrol, and Bioremediation of Contaminated Sites: A Comprehensive Review of Effects and Mechanisms. Int. J. Mol. Sci. 2021, 22, 10529.

Saeid, A., Prochownik, E., & Dobrowolska-Iwanek, J. (2018). Phosphorus solubilization by Bacillus species. *Molecules*, 23(11), 2897.

Sakano, K. (1990). Proton/phosphate stoichiometry in uptake of inorganic phosphate by cultured cells of *Catharanthus roseus* (L.) *G. Don. Plant Physiology*, 93(2), 479-483.

Saleem, M., Arshad, M., Hussain, S., & Bhatti, A. S. (2007). Perspective of plant growth promoting rhizobacteria (PGPR) containing ACC deaminase in stress agriculture. *Journal of industrial Microbiology and Biotechnology*, 34(10), 635-648.

Samaddar, S., Chatterjee, P., Choudhury, A.R., Ahmed, S., Sa, T. (2019) Interactions between *Pseudomonas* spp. and their role in improving the red pepper plant growth under salinity stress. *Microbiological Research* Volume 219, 66-73

Sánchez-Calderón, L., Chacon-López, A., Pérez-Torres, C. A., & Herrera-Estrella, L. (2010). Phosphorus: plant strategies to cope with its scarcity. *Cell biology of metals and nutrients*, 173-198.

Sani, M. N. H., Islam, M. N., Uddain, J., Chowdhury, M. S. N., & Subramaniam, S. (2020). Synergistic effect of microbial and nonmicrobial biostimulants on growth, yield, and nutritional quality of organic tomato. *Crop Science*, 60(4), 2102-2114.

Santana, E. B., Marques, E. L. S., & Dias, J. C. T. (2016). Effects of phosphate-solubilizing bacteria, native microorganisms, and rock dust on *Jatropha curcas* L. growth. Genetics and Molecular Research, 15(4), 15048729.

Sanyal, SK., De Datta, SK. (1991). Chemistry of phosphorus transformations in soil. *Advances in Soil Science* (Volume 16) 1–120.

Sarker, A., Islam, M. T., Biswas, G. C., Alam, M. S., & Talukder, N. M. (2012). Screening for phosphate solubilizing bacteria inhibiting the rhizoplane of rice grown in acidic soil of Bangladesh. *Acta Microbiologica et Immunologica Hungarica*, 59(2), 199-203.

Satyaprakash, M., Nikitha, T., Reddi, E. U. B., Sadhana, B., & Vani, S. S. (2017). Phosphorous and phosphate solubilising bacteria and their role in plant nutrition. *International Journal of Current Microbiology and Applied Sciences*, 6(4), 2133-2144.

Satyendra Singh, S., Balodi, R., Meena, P.N., Singhal, S. (2021) Biocontrol activity of *Trichoderma harzianum, Bacillus subtilis* FBS07 and *Pseudomonas fluorescens* against *Meloidogyne incognita, Fusariumoxysporum* and *Rhizoctonia solani. Indian Phytopathology* 74, 703–714

Schachtman, D. P., Reid, R. J., & Ayling, S. M. (1998). Phosphorus uptake by plants: from soil to cell. *Plant Physiology*, 116, 447–453.

Schwyn, B., & Neilands, J. B. (1987). Universal chemical assay for the detection and determination of siderophores. *Analytical Biochemistry*, 160(1), 47-56.

Sellitto, V. M. (2020). I microrganismi utili in agricoltura. *Edagricole*, Bologna.

Selvi, K. B., Paul, J. J. A., Vijaya, V., & Saraswathi, K. (2017). Analyzing the efficacy of phosphate solubilizing microorganisms by enrichment culture techniques. *Biochemistry and Molecular Biology Journal*, 3(1), 1-7.

Shaharoona, B., Arshad, M., Waqas, R., & Khalid, A. (2011). Role of ethylene and plant growth-promoting rhizobacteria in stressed crop plants. *In Crop stress and its management: perspectives and strategies* (pp. 429-446).

Sharif, M., Khattak, R. A., & Sarir, M. S. (2002). Effect of different levels of lignitic coal derived humic acid on growth of maize plants. *Communications in soil science and plant analysis*, 33(19-20), 3567-3580.

Sharma, S. B., Sayyed, R. Z., Trivedi, M. H., & Gobi, T. A. (2013). Phosphate solubilizing microbes: sustainable approach for managing phosphorus deficiency in agricultural soils. *SpringerPlus*, *2*(1), 587.

Sharma BK, Yadav SK, Singh S, Singh HB (2015) Microbial consortium mediated plant defense against phytopathogens: readdressing for enhancing efficacy. *Soil Biol Biochem* 87:25–33

Sharma, H. K., Singh, S., & Meher, H. C. (2007). Management of root-knot nematode, Meloidogyne incognita and wilt fungus, *Fusarium oxysporum* complex on okra. *Pesticide Research Journal*, 19(2), 176-179.

Sharma, S. B., Sayyed, R. Z., Trivedi, M. H., & Gobi, T. A. (2013). Phosphate solubilizing microbes: sustainable approach for managing phosphorus deficiency in agricultural soils. *SpringerPlus*, 2, 587.

Sharon, J. A., Hathwaik, L. T., Glenn, G. M., Imam, S. H., & Lee, C. C. (2016). Isolation of efficient phosphate solubilizing bacteria capable of enhancing tomato plant growth. Journal of soil science and plant nutrition, 16(2), 525-536.

Shen, J., Yuan, L., Zhang, J., Li H., Bai Z., Chen X., Zhang W., Zhang F. (2011). Phosphorus dynamics: from soil to plant. Plant Physiology 156, 997–1005

Shi, W., Xing, Y., Zhu, Y., Gao, Ying, Y. (2022) Diverse responses of pqqC- and phoD-harbouring bacterial communities to variation in soil properties of Moso bamboo forests. *Microbial Biotechnology,* 15, 2097–2111

Singh S (2019) Integrated approach for management of root-knot nematode (*Meloidogyne incognita*) in bitter gourd (*Momordica charantia*). *Ind J Agric Sci* 89:71–76

Singh, B. K. (2017). Creating new business, economic growth and regional prosperity through microbiome-based products in the agriculture industry. *Microbial Biotechnology*, 10(2), 224.

Singh, S., Balodi, R., Meena, P. N., & Singhal, S. (2021). Biocontrol activity of *Trichoderma harzianum, Bacillus subtilis* FBS07 and *Pseudomonas fluorescens* against *Meloidogyne incognita*, *Fusarium oxysporum* and *Rhizoctonia solani*. *Indian Phytopathology*, 74(3), 703-714.

Sleator, R. D., & Hill, C. (2002). Bacterial osmoadaptation: the role of compatible solutes. *Microbiology Reviews*, 26(1), 49-71.

Soliman, S. A., Abdelhameed, R. E., & Metwally, R. A. (2023). In vivo and In vitro evaluation of the antifungal activity of the PGPR *Bacillus amyloliquefaciens* RaSh1 (MZ945930) against *Alternaria alternata* with growth promotion influences on *Capsicum annuum* L. plants. *Microbial Cell Factories*, 22(1), 70.

Sporchia, F., & Caro, D. (2023). Exploring the potential of circular solutions to replace inorganic fertilizers in the European Union. *Science of the total environment*, 892, 164636.

Sudesh, K., Abe, H., & Doi, Y. (2000). Synthesis, structure and properties of olyhydroxyalkanoates: biological polyestrs. *Progress in polymer science*, 25(10), 1503-1555.

Tahir, H. A., Gu, Q., Wu, H., Raza, W., Hanif, A., Wu, L., ... & Gao, X. (2017). Plant growth promotion by volatile organic compounds produced by *Bacillus subtilis* SYST2. *Frontiers in microbiology*, 8, 171.

Tarafdar, J. C., Meenu Bareja, M. B., & Jitendra Panwar, J. P. (2003). Efficiency of some phosphatase producing soil-fungi. CABI digital library, 27-32.

Tejada, M., Benítez, C., Gómez, I., & Parrado, J. (2011). Use of biostimulants on soil restoration: Effects on soil biochemical properties and microbial community. *Applied soil ecology*, 49, 11-17.

Teng, Z., Shao, W., Zhang, K., Huo, Y., & Li, M. (2019). Characterization of phosphate solubilizing bacteria isolated from heavy metal contaminated soils and their potential for lead immobilization. *Journal of environmental management*, 231, 189-197.

Thakur, D., Kaushal, R., & Shyam, V. (2014). Phosphate solubilising microorganisms: role in phosphorus nutrition of crop plants-a review. *Agricultural Reviews*, 35(3), 159-171.

Traon, D., Amat, L., Zotz, F., & du Jardin, P. (2014). A Legal Framework for Plant Biostimulants and Agronomic Fertiliser Additives in the EU-Report to the European Commission, DG Enterprise & Industry.

Tsukanova, K. A., Meyer, J. J. M., & Bibikova, T. N. (2017). Effect of plant growth-promoting Rhizobacteria on plant hormone homeostasis. *South African journal of botany*, 113, 91-102.

Vacheron, J., Desbrosses, G., Bouffaud, M. L., Touraine, B., Moënne-Loccoz, Y., Muller, D., ... & Prigent-Combaret, C. (2013). Plant growth-promoting rhizobacteria and root system functioning. *Frontiers in plant science*, *4*, 356.

Vacheron, J., Renoud, S., Muller, D., Babalola, O.O., Prigent-Combaret, C. (2015). Alleviation of Abiotic and Biotic Stresses in Plants by *Azospirillum* . In: Cassán, F., Okon, Y., Creus, C. (eds) Handbook for *Azospirillum*. Springer, Cham.

Van Dijk, K. C., Lesschen, J. P., & Oenema, O. (2016). Phosphorus flows and balances of the European Union Member States. Science of the Total Environment, 542, 1078-1093.

Van Wees, S. C., Van der Ent, S., & Pieterse, C. M. (2008). Plant immune responses triggered by beneficial microbes. *Current opinion in plant biology*, 11(4), 443-448.

Vargas-Hernandez, M., Macias-Bobadilla, I., Guevara-Gonzalez, R. G., Romero-Gomez, S. D. J., Rico-Garcia, E., Ocampo-Velazquez, R. V., ... & Torres-Pacheco, I. (2017). Plant hormesis management with biostimulants of biotic origin in agriculture. *Frontiers in plant science*, 8, 1762.

Verma, P. P., Shelake, R. M., Das, S., Sharma, P., & Kim, J. Y. (2019). Plant growth-promoting rhizobacteria (PGPR) and fungi (PGPF): potential biological control agents of diseases and pests. *Microbial Interventions in Agriculture and Environment*: Volume 1: Research Trends, Priorities and Prospects, 281-311.

Versaw, W. K., & Harrison, M. J. (2002). A chloroplast phosphate transporter, PHT2; 1, influences allocation of phosphate within the plant and phosphate-starvation responses. *The Plant Cell*, 14(8), 1751-1766

Vessey, J. K. (2003). Plant growth promoting rhizobacteria as biofertilizers. *Plant and soil*, 255(2), 571-586.

Vinale, F., Salvatore, MM., Nicoletti, R., Staropoli, A., Manganiello, G., Venneri, T., Borrelli, F., Della Greca, M., Salvatore, F., Andolfi, A. (2020) Identification of the main metabolites of a marine-derived strain of *Penicillium brevicompactum* using LC and GC MS techniques. *Metabolites*, 10-55.

Vinale, F., Sivasithamparam, K., Ghisalberti, E. L., Marra, R., Woo, S. L., & Lorito, M. (2008). *Trichoderma*–plant–pathogen interactions. *Soil biology and Biochemistry*, 40(1), 1-10.

Violante, P. (1996). Chimica del suolo e della nutrizione delle piante. *Edagricole*. ISBN-88-506-4912-6

Vlot, A. C., Klessig, D. F., & Park, S. W. (2008). Systemic acquired resistance: the elusive signal (s). *Current opinion in plant biology*, 11(4), 436-442.

Von Uexkull, H. R., & Mutert, E. (1995). Global extent, development and economic impact of acid soils. *Plant Soil*, 171, 1-15.

Walpola, B. C., & Yoon, M. H. (2013). *In vitro* solubilization of inorganic phosphates by phosphate solubilizing microorganisms. *African Journal of Microbiology Research*, 7(27), 3534-3541.

Wang, R., Chen, D., Khan, R. A. A., Cui, J., Hou, J., & Liu, T. (2021). A novel *Trichoderma asperellum* strain DQ-1 promotes tomato growth and induces resistance to gray mold caused by Botrytis cinerea. *FEMS Microbiology Letters*, 368(20), fnab140.

Wang, W., Liu, D., Qin, M., Xie, Z., Chen, R., & Zhang, Y. (2021). Effects of supplemental lighting on potassium transport and fruit coloring of tomatoes grown in hydroponics. *International Journal of Molecular Sciences*, 22(5), 2687.

Wei, Y., Zhao, Y., Shi, M., Cao, Z., Lu, Q., Yang, T., ... & Wei, Z. (2018). Effect of organic acids production and bacterial community on the possible mechanism of phosphorus solubilization during composting with enriched phosphate-solubilizing bacteria inoculation. *Bioresource Technology*, 247, 190-199.

Whipps, J. M. (2001). Microbial interactions and biocontrol in the rhizosphere. *Journal of experimental Botany,* 52(suppl_1), 487-511.

Wilson, M. K., Abergel, R.J., Raymond, K.N, Arceneaux J.E.L, Byers B.R. (2006). Siderophores of *Bacillus anthracis, B. cereus, and B. thuringiensis*. *Journal of Bacteriology*, volume 348 (1), 320-325.

Wyciszkiewicz, M., Saeid, A., Chojnacka, K., & Górecki, H. (2015). Production of phosphate biofertilizers from bones by phosphate-solubilizing bacteria *Bacillus megaterium*. Open Chemistry, 13(1), 000010151520150123.

Yakhin, O. I., Lubyanov, A. A., Yakhin, I. A., & Brown, P. H. (2017). Biostimulants in plant science: a global perspective. *Frontiers in plant science*, 7, 2049.

Yasmin, H., Naeem, S., Bakhtawar, M., Jabeen, Z., Nosheen, A., Naz, R., Keyani, R., Mumtaz, S., Hassan, M.N. (2020). Halotolerant rhizobacteria *Pseudomonas pseudoalcaligenes* and *Bacillus subtilis* FBS07 mediate systemic tolerance in hydroponically grown soybean (Glycine max L.) against salinity stress. *Plos on,* 15 (4).

Yu, Y., Gui, Y., Li, Z., Jiang, C., Guo, J., & Niu, D. (2022). Induced systemic resistance for improving plant immunity by beneficial microbes. *Plants*, 11(3), 386.

Zabihi, H. R., Savaghebi, G. R., Khavazi, K., Ganjali, A., & Miransari, M. (2011). *Pseudomonas* bacteria and phosphorous fertilization, affecting wheat (*Triticum aestivum* L.)

yield and P uptake under greenhouse and field conditions. *Acta Physiologiae Plantarum*, 33(1), 145-152.

Zandonadi, D. B., Santos, M. P., Caixeta, L. S., Marinho, E. B., Peres, L. E. P., & Façanha, A. R. (2016). Plant proton pumps as markers of biostimulant action. *Scientia Agricola*, 73, 24-28.

Ringraziamenti

Desidero esprimere la mia più sincera gratitudine a tutte le persone che, in modi diversi, hanno contribuito alla realizzazione di questo lavoro e hanno accompagnato il mio percorso di dottorato, grazie per il sostegno e la fiducia.

I miei primi ringraziamenti vanno alla professoressa Roberta Marra e alla dottoressa Stefania Lanzuise per aver guidato questo lavoro con competenza e dedizione. La loro disponibilità al confronto, i preziosi suggerimenti e la fiducia che mi hanno dato nel corso di questi anni hanno contribuito alla realizzazione di questa tesi. Ringrazio la professoressa Vincenza Cozzolino e il dottore Francesco Scognamiglio per le analisi riguardanti la solubilizzazione del fosforo. Un ringraziamento sentito va al professore Zoina e al laboratorio fitopatologico della Regione Campania per la caratterizzazione metabolica dei cappi. Un ringraziamento all'azienda Fertilidea, per il materiale fornito in questi anni. Un ringraziamento va anche alla dottoressa Alessia Stipoli e alla dottoressa Giuseppina per la loro disponibilità e per il contribuito nelle analisi al GC-MS.

I miei sinceri ringraziamenti vanno a Carmen Scamardella, che mi ha accompagnata in questo percorso, aiutata e sostenuta, sia nell'ambito accademico che non, rendendo ogni giornata più leggera.

Un ringraziamento speciale va ad Annabella Pappalardo, collega e amica soprattutto, per aver contribuito ai folli esperimenti, dandomi la consapevolezza di non essere mai sola in qualsiasi progetto. Ricorderò tutte le giornate passate a studiare e pensare di avere grandi idee, consapevole che, con differenti argomenti, queste giornate non termineranno mai.

I miei ringraziamenti più sentiti vanno ai miei genitori, parte fondamentale di questi anni, hanno sempre sostenuto ogni scelta, e mi hanno sempre accompagnata in ogni giornata. Non esistono percorsi facili, ma la vera differenza la fa chi ti è accanto, e non esiste motivazione migliore di chi ti ricorda quanto vali e quanto, in ogni percorso, conta chi si decida di essere.

A mia sorella Antonella, grazie per aver sopportato ogni sfogo, per quanto distanti, non esistono chilometri che allontano due sorelle, e non esistono discorsi che un telefono possa rallentare.

A mio fratello Luigi, mia spalla comica da sempre, grazie per esserci stato sempre e aver alleggerito le giornate e avermi fatto compagnia durante le serate interminabili, insieme a Simona, dove ho sempre potuto trovare conforto e un confronto su tutto.

A mio marito Salvatore, questi anni non potevano essere più ricchi di così, posso dire con assoluta certezza di non essermi mai annoiata o passato un momento che io possa dimenticare, grazie per avermi ascoltata e aver creduto in me.

Grazie a mio figlio Vincenzo, che senza saperlo, mi ha fatto capire quali sono le cose importanti della vita, mi ha resa una persona migliore e mi ha fatto conoscere una parte di

me ancora nascosta. Che possa nella vita avere tutto ciò che desidera, senza dimenticare quanto è importante trovare se stessi e non rinnegarsi mai.

Grazie a chiunque mi è stato vicino, alle mie amiche, che tra una chiacchiera e un caffè mi hanno sempre sostenuta, in particolar modo Angela, che da veterana della stessa avventura, mi ha saputa sempre aiutare e consigliare.